NASA/TM-20250003756

Erosion Results of the MISSE 9-15 Polymers and Composites Experiment 1-4 (PCE 1-4)

Kim K. de Groh
Glenn Research Center, Cleveland, Ohio

Bruce A. Banks
Science Applications International Corporation, Cleveland, Ohio

May 2025

NASA STI Program Report Series

Since its founding, NASA has been dedicated to the advancement of aeronautics and space science. The NASA scientific and technical information (STI) program plays a key part in helping NASA maintain this important role.

The NASA STI program operates under the auspices of the Agency Chief Information Officer. It collects, organizes, provides for archiving, and disseminates NASA's STI. The NASA STI program provides access to the NTRS Registered and its public interface, the NASA Technical Reports Server, thus providing one of the largest collections of aeronautical and space science STI in the world. Results are published in both non-NASA channels and by NASA in the NASA STI Report Series, which includes the following report types:

- TECHNICAL PUBLICATION.
  Reports of completed research or a major significant phase of research that present the results of NASA programs and include extensive data or theoretical analysis. Includes compilations of significant scientific and technical data and information deemed to be of continuing reference value. NASA counterpart of peer-reviewed formal professional papers but has less stringent limitations on manuscript length and extent of graphic presentations.

- TECHNICAL MEMORANDUM.
  Scientific and technical findings that are preliminary or of specialized interest, e.g., quick release reports, working papers, and bibliographies that contain minimal annotation. Does not contain extensive analysis.

- CONTRACTOR REPORT.
  Scientific and technical findings by NASA-sponsored contractors and grantees.

- CONFERENCE PUBLICATION.
  Collected papers from scientific and technical conferences, symposia, seminars, or other meetings sponsored or cosponsored by NASA.

- SPECIAL PUBLICATION.
  Scientific, technical, or historical information from NASA programs, projects, and missions, often concerned with subjects having substantial public interest.

- TECHNICAL TRANSLATION.
  English-language translations of foreign scientific and technical material pertinent to NASA's mission.

Specialized services also include organizing and publishing research results, distributing specialized research announcements and feeds, providing information desk and personal search support, and enabling data exchange services.

For more information about the NASA STI program, see the following:

- Access the NASA STI program home page at http://www.sti.nasa.gov

NASA/TM-20250003756

Erosion Results of the MISSE 9-15 Polymers and Composites Experiment 1-4 (PCE 1-4)

Kim K. de Groh
Glenn Research Center, Cleveland, Ohio

Bruce A. Banks
Science Applications International Corporation, Cleveland, Ohio

National Aeronautics and
Space Administration

Glenn Research Center
Cleveland, Ohio 44135

May 2025

Acknowledgments

We are grateful to the NASA Flight Opportunities program, the International Space Station Program Office and Aegis Aerospace for making these flight opportunities possible. We would like to thank Diane Malarik, formerly of NASA Headquarters, along with Craig Robinson and Kelly Bailey of NASA Glenn Research Center for their long-term support of these MISSE-FF experiments. We would like to thank our many PCE 1-4 collaborators for providing flight and control samples for the MISSE-FF experiments. Finally, we would like to thank Sylvie Crowell, Pathways Intern at NASA Glenn Research Center, for helping with the FESEM imaging. This work is supported by NASA's Biological and Physical Sciences Division.

Level of Review: This material has been technically reviewed by technical management.

This report is available in electronic form at https://www.sti.nasa.gov/ and https://ntrs.nasa.gov/

NASA STI Program/Mail Stop 050
NASA Langley Research Center
Hampton, VA 23681-2199

Contents

Erosion Results of the MISSE 9-15 Polymers and Composites Experiment 1-4 (PCE 1-4)

Kim K. de Groh
National Aeronautics and Space Administration
Glenn Research Center
Cleveland, Ohio 44135

Bruce A. Banks
Science Applications International Corporation
Cleveland, Ohio 44135

Abstract

Polymers and other oxidizable materials on the exterior of spacecraft in the low Earth orbit (LEO) space environment can be eroded from reaction with atomic oxygen (AO). Therefore, in order to design durable spacecraft it is important to know the extent of erosion that will occur during a mission. This can be determined by knowing the LEO AO erosion yield, E_y (volume loss per incident oxygen atom), of materials susceptible to AO reaction. In addition, recent flight experiments have shown that the AO E_y can vary with the AO fluence and/or solar exposure. Therefore, obtaining AO E_y data for materials flown on various spaceflight missions is important. NASA Glenn Research Center has flown numerous experiments as part of the Materials International Space Station Experiment (MISSE) missions on the exterior of the International Space Station (ISS) to characterize the LEO E_y of polymers, composites, protective coatings, and other spacecraft materials. Recently, four Glenn experiments with 365 flight (F) samples were flown on ISS's MISSE-Flight Facility (MISSE-FF). These experiments are the Polymers and Composites Experiment-1 (PCE-1) flown as part of the MISSE-9 mission, the PCE-2 flown as part of the MISSE-10 mission, the PCE-3 flown as part of the MISSE-12 and MISSE-15 missions, and the PCE-4 flown as part of the MISSE-13 mission. Although each experiment had numerous sample objectives, the primary objective was to determine the LEO AO E_y of various spacecraft materials as a function of solar irradiation and AO fluence. This paper provides a summary of the erosion data for the PCE 1-4 AO E_y samples. The AO E_y for 150 samples flown in either the LEO ram, wake, zenith or nadir directions are provided. The AO ram fluence varied from 2.97×10^{20} atoms/cm^2 after 0.89 years of direct space exposure (with relatively high levels of Si contamination) on MISSE 12 to 3.93×10^{20} atoms/cm^2 after 1.17 years of direct space exposure on MISSE-10. The ram AO E_y values for uncoated polymers range from 3.81×10^{-25} cm^3/atom for polytetrafluoroethylene (M9R-C20 F) exposed to an AO fluence of 3.44×10^{20} atoms/cm^2 on MISSE-9 to 4.43×10^{-23} cm^3/atom for AO etched low density polyimide aerogel (M12R-C21 F) exposed to an AO fluence of 2.97×10^{21} atoms/cm^2 on MISSE-12. Because of the low AO fluence and relatively high Si contamination, a number of PCE-3 wake samples experienced mass gain. Thus, AO E_y values are not provided for these samples. Although there are calculated AO E_y values for the zenith, wake and nadir samples, the ram AO E_y for a particular material is a more reliable value in terms of AO exposure because the zenith, wake and nadir directions were exposed to either no or very little AO fluence and thus other space environmental factors (i.e. vacuum, thermal extremes and thermal cycling, and/or various types of radiation) are responsible for the mass loss.

Introduction

Materials used on the exterior of spacecraft are subjected to many environmental threats that can cause degradation. In low Earth orbit (LEO) these threats include visible light photon radiation, ultraviolet (UV) radiation, vacuum ultraviolet (VUV) radiation, x-rays, solar wind particle radiation (electrons, protons), cosmic rays, temperature extremes, thermal cycling, impacts from micrometeoroids and orbital debris (MMOD), on-orbit contamination, and atomic oxygen (AO). These environmental exposures can result in erosion, embrittlement and optical property degradation of susceptible materials threatening spacecraft performance and durability.

The spaceflight orientation highly affects the environmental exposure. Ram facing surfaces (facing the direction of travel) receive a high flux of directed AO (ram AO) and sweeping (moderate) solar exposure. Zenith facing surfaces (direction facing away from Earth) receive a low flux of grazing arrival AO and the highest solar exposure. Wake facing surfaces (facing away from the direction of travel) receive essentially no AO flux and moderate solar radiation (levels similar to ram experiments). And, nadir facing surfaces (direction facing towards Earth) receive a low flux of grazing arrival AO and minimal solar radiation (albedo sunlight). All surfaces receive charged particle and cosmic radiation, which are omnidirectional. Figure 1 provides a diagram of the ram, wake, zenith and nadir flight orientations on the International Space Station (ISS).

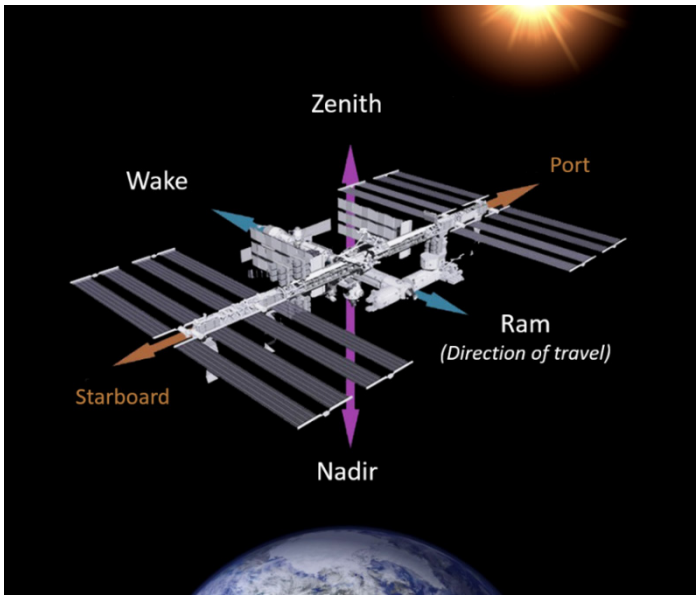

Figure 1. Diagram showing ram, wake, zenith, and nadir directions on the International Space Station.

Atomic oxygen is a particularly serious structural, thermal, and optical threat, especially to exterior oxidizable spacecraft components. Atomic oxygen is formed in the LEO environment through photodissociation of diatomic oxygen (O_2). Short-wavelength (< 243 nm) solar radiation has sufficient energy to break the 5.12-eV O_2 diatomic bond in an environment where the mean free path is sufficiently long (~10^8 m) so that the probability of re-association, or the formation of ozone (O_3), is small.[1,2] In LEO, between the altitudes of 180 and 650 km, AO is the most abundant species.[3] Atomic oxygen is also present in other planetary environments, such as low Mars orbit (LMO).

A number of processes can take place when an oxygen atom strikes a spacecraft surface as a result of its orbital velocity and the thermal velocity of the atoms. These include chemical reaction with surface molecules, elastic scattering, scattering with partial or full thermal accommodation, and recombination or excitation of ram species, which consists predominantly of ground-state $O(^3P)$ atomic oxygen atoms.[4] Atomic oxygen can react with polymers, carbon, and many metals to form oxygen bonds with atoms on the exposed surface. For most polymers, hydrogen abstraction, oxygen addition, or oxygen insertion can occur, with the oxygen interaction pathways eventually leading to volatile oxidation products.[5,6] This results in gradual erosion of hydrocarbon or halocarbon material, with the exception of silicone materials, which form a glassy silicate surface layer with AO exposure. Figure 2 shows AO erosion of Teflon™ fluorinated ethylene propylene (FEP) around a small protective particle after 5.8 years of space exposure on the Long Duration Exposure Facility (LDEF). An example of the complete loss of a Kapton® H thermal blanket insulation layer on the LDEF and degradation of other polymeric materials caused by AO erosion in LEO are provided in Figure 3.[2,7] AO scattering can cause oxidation of sensitive components not normally in direct line-of-site with AO, such as within a telescope body.

The most common approach to protecting susceptible spacecraft materials from AO erosion is to coat the material with a thin protective film, such as SiO_x (where x = 1.8 to 2). Even materials with AO protective coatings can be susceptible to AO erosion. This can occur when microscopic scratches, dust particles, or other imperfections in the substrate surface result in defects or pin windows in the protective coating.[8,9] These coating defects can provide pathways for AO exposure and undercutting erosion of the substrate can occur, even under directed ram AO exposure in LEO. One of the first examples of directed ram AO undercutting erosion in LEO was reported by de Groh and Banks for aluminized-Kapton insulation blankets from the LDEF.[8] Undercutting erosion can be a serious threat to component survivability. An example is shown in Figure 4, where AO undercutting erosion has severely degraded the P6 Truss port solar array wing two-surface aluminized-Kapton blanket box cover on the International Space Station (ISS) after 1 year of space exposure.[10]

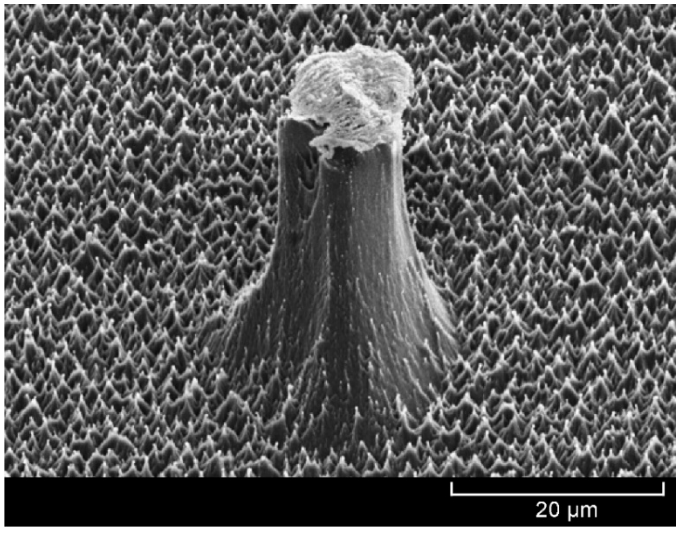

Figure 2. Atomic oxygen erosion of Teflon FEP after 5.8 years of space exposure.[2]

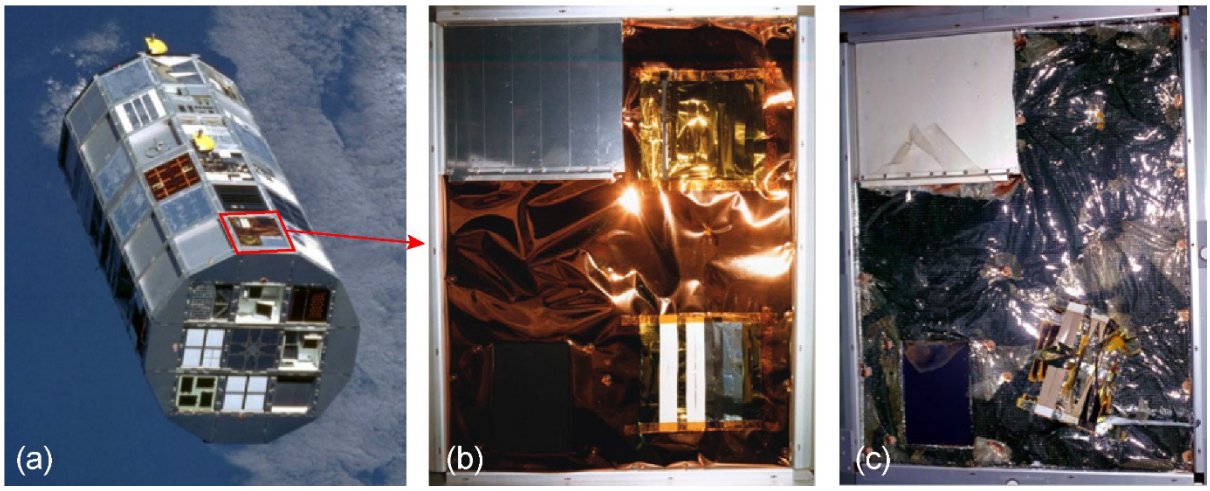

Figure 3. Atomic oxygen erosion of a Kapton insulation blanket from LDEF experiment Tray F-9, located on the leading edge and exposed to direct-ram AO for 5.8 years: a). LDEF, b). Tray F-9 pre-flight, and c). Tray F-9 post-flight.[2,7]

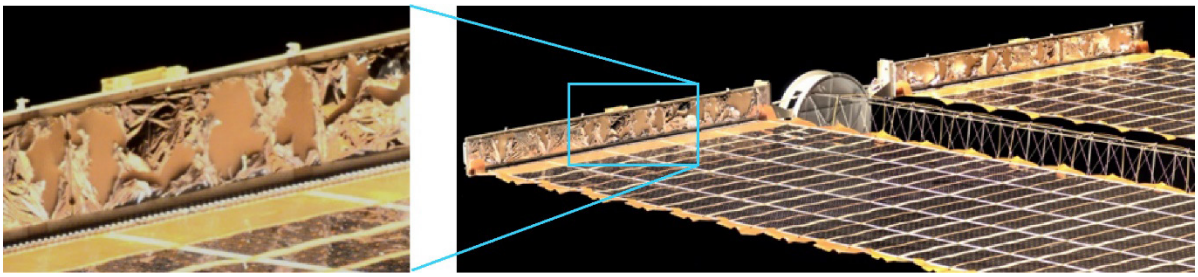

Figure 4. Atomic oxygen undercutting degradation of the P6 Truss solar array wing blanket box cover on the ISS after only 1 year of space exposure.[10]

In order to design durable high-performance spacecraft systems it is essential to understand the LEO AO erosion yield (E_y) of materials being considered for spacecraft applications along with AO scattering characteristics. The E_y is the volume of material that is removed (through oxidation) per incident oxygen atom and is measured in units of cm^3/atom. The E_y can be impacted by a variety of factors. Hydrocarbon or halocarbon polymers that contain metal oxide pigment particles, or ash, will have E_y values that are fluence dependent. This is because AO will erode the polymer content on the surface, leaving a proliferation of inorganic particles that tend to shield the underlying polymer from AO attack. As a result, the E_y of the polymer gradually reduces with fluence. In addition, for any particular ash-filled polymer, it is believed that the greater the volume fill of the ash particles, the greater the rate of reduction in the E_y with fluence.[11]

Another LEO threat to spacecraft materials is solar UV radiation, which can be considered to be in the 0.1 to 0.4 μm wavelength range as wavelengths shorter than approximately 120 nm represent a negligible portion of the solar spectrum.[6,12] Ultraviolet radiation is energetic enough to cause the breaking of organic bonds such as C=C, C=O, and C–H as well as bonds in other functional groups.[5] A molecule is raised to an excited state when an organic molecule absorbs a

photon of UV radiation, and bond dissociation can occur if the molecule acquires enough energy at the excited state. Depending on the temperature and physical properties of the materials, the dissociated radical species are reactive intermediates, with the capability of diffusing several atomic distances from their point of origin and can participate in further reactions.[5] Solar radiation often results in bond breakage in materials as well as threats to functionality and stability of the materials. Therefore, solar radiation can impact the erosion of some materials along with AO.

Because spaceflight materials exposure opportunities are rare, expensive, space-limited, and time-consuming, ground laboratory testing is most often relied upon for spacecraft material environmental durability prediction. However, differences exist between ground facilities and actual space exposures, which may result in differences in rates of oxidation that are material dependent. Therefore, actual spaceflight AO E_y data are ideal to best assess the durability of a material for spacecraft mission applicability. In addition, data from materials spaceflight experiments can be used to determine correlations between exposures in ground test facilities and space exposure, allowing for more accurate predictions of in-space materials performance based on ground facility testing. Materials spaceflight experiments for LEO E_y determination have been flown on the space shuttle, the LDEF, the Russian space station Mir, and other spacecraft.[13] More recently, experiments have been flown as a part of the Materials International Space Station Experiment (MISSE) missions flown on the exterior of the ISS.[13,14]

To increase our understanding of the AO erosion of spacecraft materials, NASA Glenn Research Center has developed and flown a series of experiments as part of the MISSE missions. NASA Glenn flew experiments as part of the MISSE 1-8 missions from 2001-2013.[2,15-20] More recently, Glenn flew four experiments with 365 flight samples on ISS's MISSE-Flight Facility (MISSE-FF).[21] These experiments are the Polymers and Composites Experiment-1 (PCE-1) flown as part of the MISSE-9 mission, the PCE-2 flown as part of the MISSE-10 mission, the PCE-3 flown as part of the MISSE-12 and MISSE-15 missions, and the PCE-4 flown as part of the MISSE-13 mission. Although each PCE 1-4 experiment has numerous sample objectives, the primary objective is to determine the LEO AO E_y of spacecraft materials as a function of solar irradiation and AO fluence.[21] This paper provides an overview of the MISSE-FF PCE 1-4 experiments and a summary of the LEO erosion data for the PCE 1-4 AO E_y samples.

Materials International Space Station Experiment-Flight Facility (MISSE-FF)

The MISSE-FF is operated by Aegis Aerospace, Inc (previously called Alpha Space).[22] It is a modular and robotically serviceable external facility that is located on ISS Express Logistics Carrier-2 (ELC-2) Site 3. Figure 5 provides an image showing the location of the MISSE-FF on ELC-2 Site 3. The MISSE-FF provides ram, wake, zenith, and nadir space exposures. The MISSE-FF supports both passive and active experiments, with downlink of data. It is designed to include active environmental sensors that provide environmental data over time in each flight orientation, including temperature, contamination and solar exposure (UV radiation). Arrangements can be made for sensors to be flown to provide AO fluence and total ionizing dose data. On-orbit facility cameras are scheduled to provide monthly sample images.

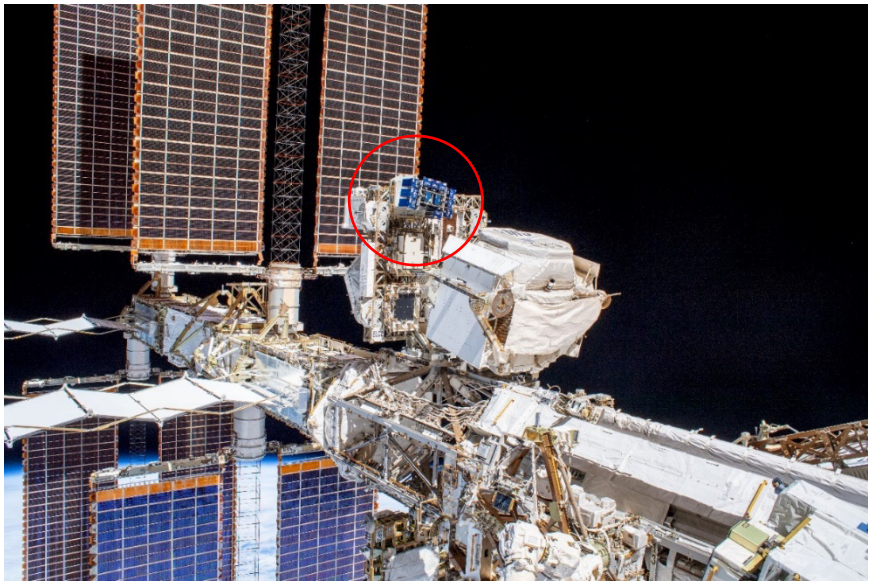

Figure 5. A view of the MISSE-FF on ELC-2 Site 3 as photographed during an EVA on November 15, 2019 (iss061e040917).

MISSE Sample Carriers (MSCs), also called MISSE Science Carriers, house the material flight experiments. Each MSC has two sides, a mount-side (MS) and a swing-side (SS), with a central hinge. Materials and spacecraft components can be flown on either the MS or SS decks for direct space exposure, or they can be mounted on the underdecks. The MSCs are launched closed as pressurized cargo on either the Northrup Grumman Cygnus or SpaceX Dragon spacecraft, and then stored inside ISS. They are moved outside the ISS through the Kibo Japanese Experiment Module (JEM) Airlock on the MISSE Transfer Tray (MTT) and then installed on the MISSE-FF structure via ISS's Special Purpose Dexterous Manipulator (SPDM) robotic arm. The SS decks are remotely opened to expose the experiments to space. The MSCs are closed during ship dockings to prevent contamination and minimize AO exposure of wake surfaces. The MSCs are typically closed during local EVAs and for on-demand images. Figure 6a provides a drawing of the MISSE-FF with MSCs closed. This image also lists the exposure direction and the MSC positions are labeled (R1, R2, R3, etc.). Figure 6b provides a drawing of the MISSE-FF with MSCs open. The MISSE-FF is rotated 8° "pitch up" such that the zenith direction is 8° away from ram and the nadir direction is 8° towards ram. Thus, the nadir samples will get slightly more grazing AO fluence and the zenith samples will get slightly less grazing AO fluence during the MISSE-FF missions. And, the ram surface is offset 8° from true ram. This rotation "offset" can be seen in Figures 6a and 6b.

The MSCs get initial space vacuum exposure when the JEM airlock is put under vacuum and opened to space. Figure 7 shows astronauts Drew Morgan and Jessica Meir preparing MSCs for transfer through the JEM Airlock on the MTT. It can take several days to robotically move the MTT with the MSCs to ELC-2 and install the MSCs in the MISSE-FF. Figure 8 shows a close-up image of the robotic arm moving two of the MSCs (MSC 5 and MSC 19) during Expedition 69.

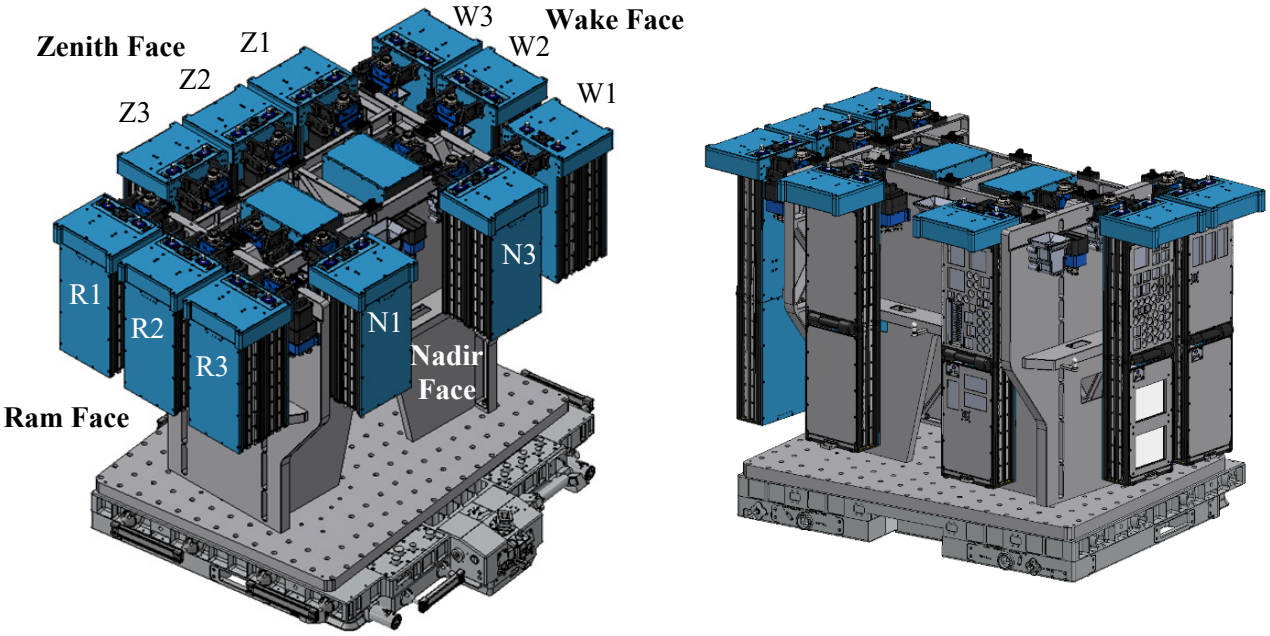

a. b.

Figure 6. Drawings of MISSE-FF with MSCs: a). MSCs closed and the MSC positions labeled, and b). MSC's open. The MISSE-FF 8° rotation can be seen in both of these images (Aegis Aerospace image).

Figure 7. Astronauts Drew Morgan and Jessica Meir preparing MSCs for transfer through the Japanese Experiment Module (JEM) Airlock using the MISSE Transfer Tray (MTT) on the ORU Transfer Interface (JOTI) in March 2020 (iss062e090043).

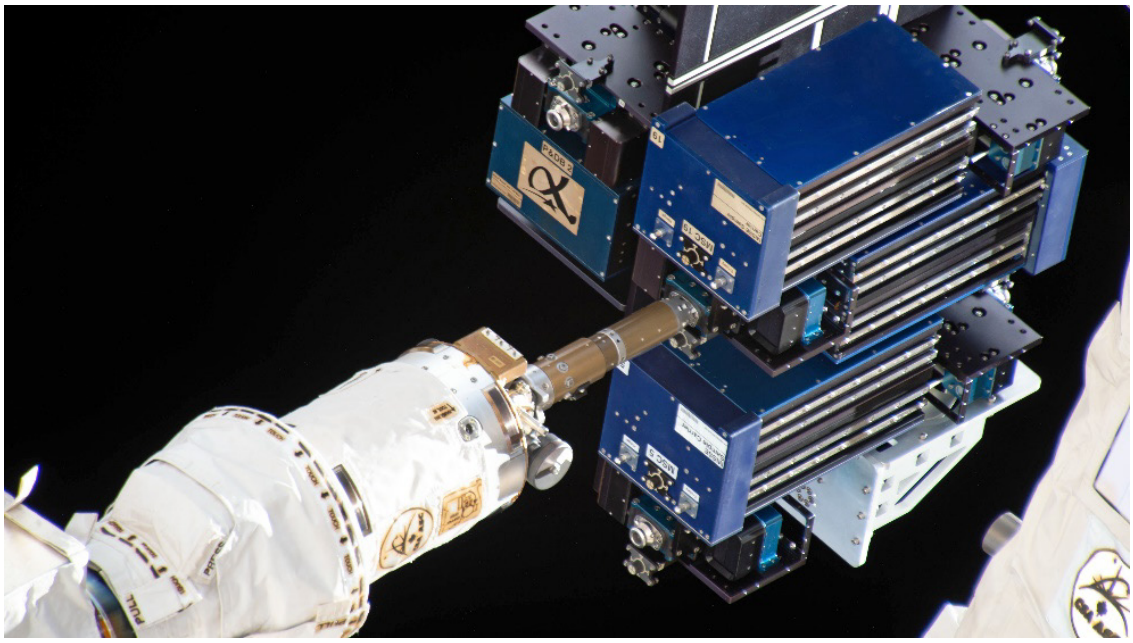

Figure 8. Close-up image of the robotic arm moving MSC 5 and MSC 19 during Expedition 69 (iss069e000575).

After insertion into the MISSE-FF, the MSC is then remotely "deployed" or opened to the space environment for the first time. As mentioned above, the MSCs are typically closed and re-opened numerous times during a mission. The MSCs are then closed for a final time, robotically retrieved from the MISSE-FF and placed back on the MTT, and the MTT is robotically moved back into the JEM airlock and re-pressurized. Thus, with respect to exposure durations, the space vacuum exposure is longest, then the duration installed on the MISSE-FF, then the "deployed duration" (first time opened to final time closed), and finally the actual time samples are directly exposed to space (accumulated open durations).

Polymers and Composites Experiments 1-4 (PCE 1-4)

MISSE-9 Polymers and Composites Experiment-1 (PCE-1)

The Polymers and Composites Experiment-1 (PCE-1) was flown as part of the MISSE-9 inaugural mission of MISSE-FF. The MISSE-9 PCE-1 was a passive experiment with 138 flight samples that were flown in ram (39 samples), wake (52 samples) and zenith (47 samples) orientations. The primary objective of the PCE-1 was to determine the LEO AO E_y of spacecraft polymers, composites, and coated samples as a function of solar irradiation and AO fluence. Samples were also included to determine the mission AO fluence and on-orbit molecular contamination in each flight direction. In addition, thin film polymer tensile samples were flown in the wake and zenith directions for studying space radiation induced embrittlement. A complete list of the PCE-1 samples is provided by de Groh in Reference 21 along with additional experiment objectives and pre-flight photos of select PCE-1 experiment samples.

Figure 9 shows a pre-flight photograph of the PCE-1 samples loaded into the MISSE-9 ram, wake and zenith flight mount-side (MS) decks. Each of these decks includes samples from two experiments, the PCE-1 and NASA Langley Research Center's Polymeric Materials Experiment.

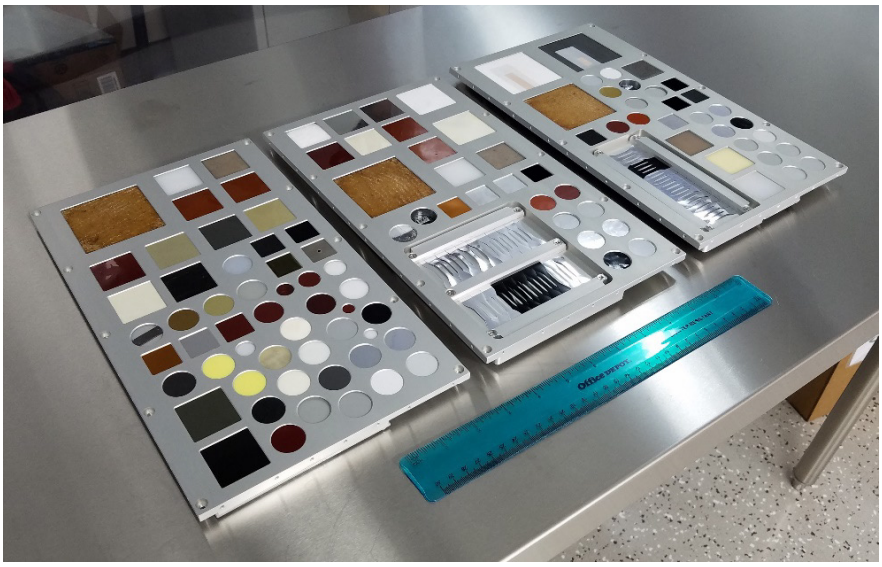

Figure 9. Pre-flight photograph of the MISSE-9 PCE-1 samples loaded into the MSC MS flight decks, from left to right: R2 MSC 3 (ram), W3 MSC 8 (wake), and Z3 MSC 5 (zenith).

Kapton® H (E. I. du Pont de Nemours and Company) was used for the AO fluence witness samples for the PCE-1 and also for the PCE 2-4 experiments. Numerous PCE 1-4 materials, such as Kapton® HN, Teflon fluorinated ethylene propylene (FEP), polytetrafluoroethylene (PTFE), white Tedlar® (crystalline polyvinyl fluoride with white pigment), polyethylene (PE), Upilex-S®, and other polymers were also flown as part of Glenn's MISSE 2-8 experiments. The manufacturing information for these materials are provided in Reference 16. All PCE 1-4 flight samples were heated at 60 °C for 24 hours under vacuum as part of Aegis Aerospace's flight hardware pre-flight testing. The control samples were not thermal vacuum exposed.

During hand delivery of the PCE-1 flight and back-up samples to Aegis Aerospace in Houston, TX for flight hardware integration, and post-flight for return of the flight samples to Cleveland, OH, arrangements were made for the samples to be exempt from airport x-ray screening to avoid non-space x-ray exposure. The back-up (control) samples were stored at NASA Glenn Research Center at ambient conditions (i.e. room temperature, 1 atm, etc.). The PCE 2-4 flight samples were also exempt from x-ray screening and the control samples were stored in ambient conditions at NASA Glenn during the flight mission.

MISSE-10 Polymers and Composites Experiment-2 (PCE-2)

The MISSE-10 PCE-2 was a passive experiment with 43 samples that were flown in ram (21 samples), zenith (10 samples), and nadir (12 samples) directions. The objectives of the PCE-2 were similar to the PCE-1. The primary objective was to determine the LEO AO E_y of polymers, composites, and coated samples as a function of solar irradiation and AO fluence. Also like the PCE-1, samples were flown to determine the AO fluence for the mission and characterize molecular contamination in each flight direction. A complete list of the PCE-2 samples is provided in Reference 21 along with additional experiment objectives and pre-flight photos of select PCE-2 experiment samples. A pre-flight photograph of the PCE-2 samples loaded into the MISSE-10 ram (R1 MSC 11), zenith (Z2 MSC 10), and nadir (N3 MSC 13) MS decks is shown in Figure 10.

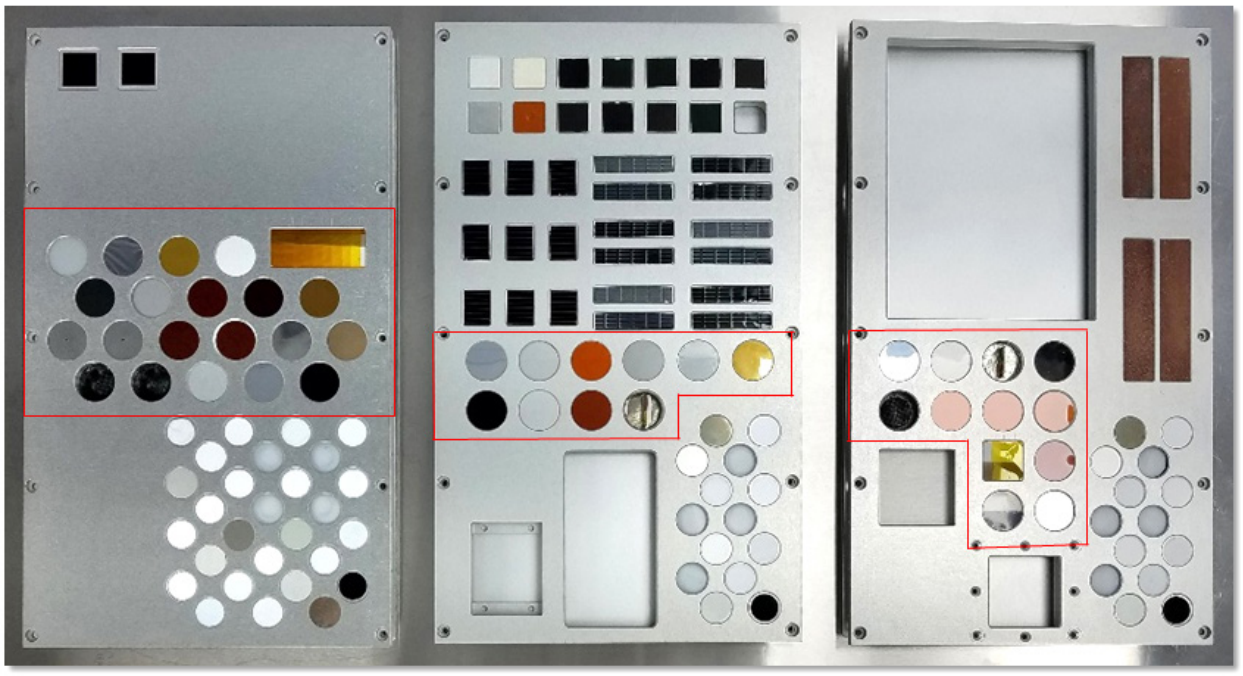

Figure 10. Pre-flight photograph of the MISSE-10 PCE-2 samples loaded into the MSC MS flight decks, from left to right: R1 MSC 11 (ram), Z2 MSC 10 (zenith), and N3 MSC 13 (wake). The PCE-2 samples are shown outlined in red.

MISSE-12 and MISSE-15 Polymers and Composites Experiment-3 (PCE-3)

The MISSE-12 PCE-3 was a passive experiment with 86 samples that was flown in ram (30 samples), wake (42 samples) and zenith (14 samples) directions. The primary objective was to determine the LEO AO E_y of polymers, composites, and coated samples as a function of solar irradiation and AO fluence. Like the PCE 1-2, samples in the PCE-3 were included to determine the AO fluence for the mission and characterize any molecular contamination in each flight direction. The objectives of the PCE-3 are similar to the PCE-1 and PCE-2. A complete list of the PCE-3 samples is provided in Reference 21 along with additional experiment objectives and pre-flight photos of select PCE-3 experiment samples.

A pre-flight photograph of the PCE-3 samples loaded into the MISSE-12 ram (R2 MSC 4 SS), zenith (Z1 MSC 18 MS), and wake (W3 MSC 6 MS) decks is shown in Figure 11. It should be noted that six wake samples and four zenith samples were moved to different MSC deck locations after the photograph in Figure 11 was taken during sample integration. These 10 samples have two red boxes around them in Figure 11. The final flight positions are provided in the zenith and wake deck photos in Figure 12, with two red boxes around the samples in their new positions. The large yellow sample in Z1 MSC 18 MS shown in Figures 11 and 12 is not part of the PCE-3.

As discussed later, the MISSE-12 wake samples were not exposed to space environment during the MISSE-12 mission. Thus, the 42 wake samples were reflown (in the same deck sample holders) during the MISSE-15 mission in the wake direction. A pre-flight photograph of the PCE-3 wake samples in the MISSE-15 MSC deck is provided in Figure 12c.

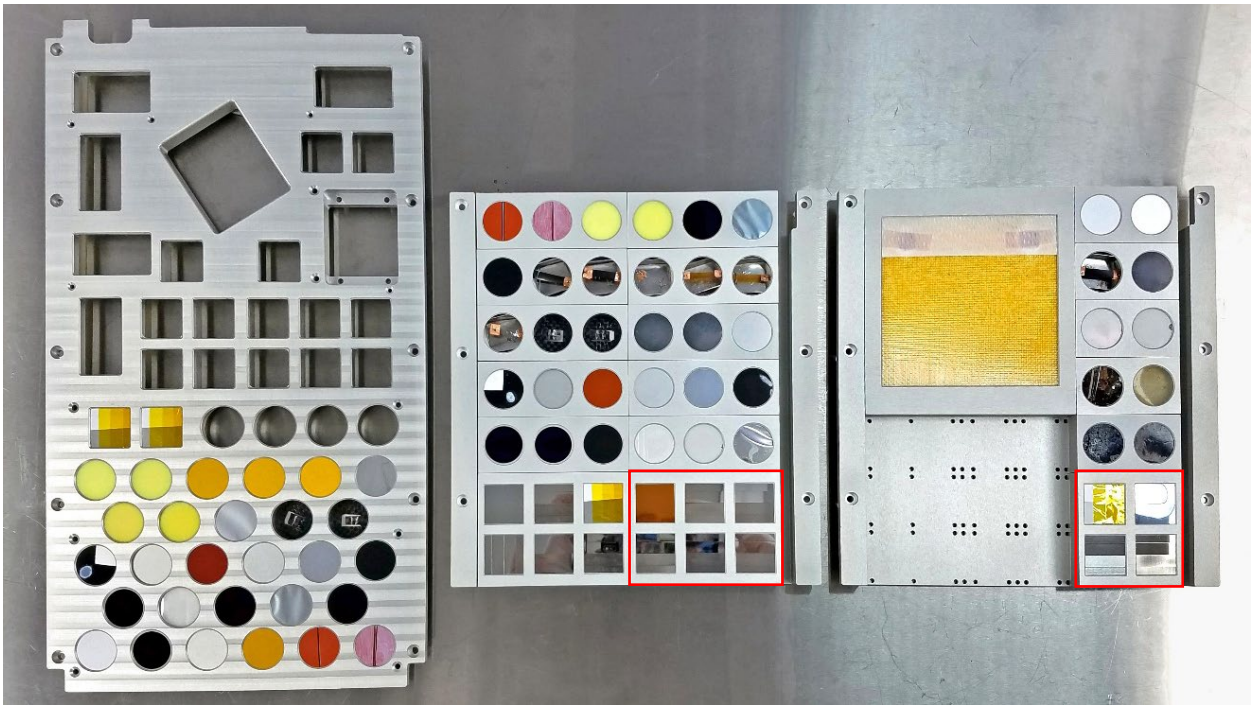

Figure 11. Pre-flight photograph of the MISSE-12 PCE-3 samples loaded into the MSC flight decks, from left to right: R2 MSC 4 SS (ram), W3 MSC 6 MS (wake), and Z1 MSC 18 MS (zenith). Samples in red boxes were moved to a different location on the deck prior to flight.

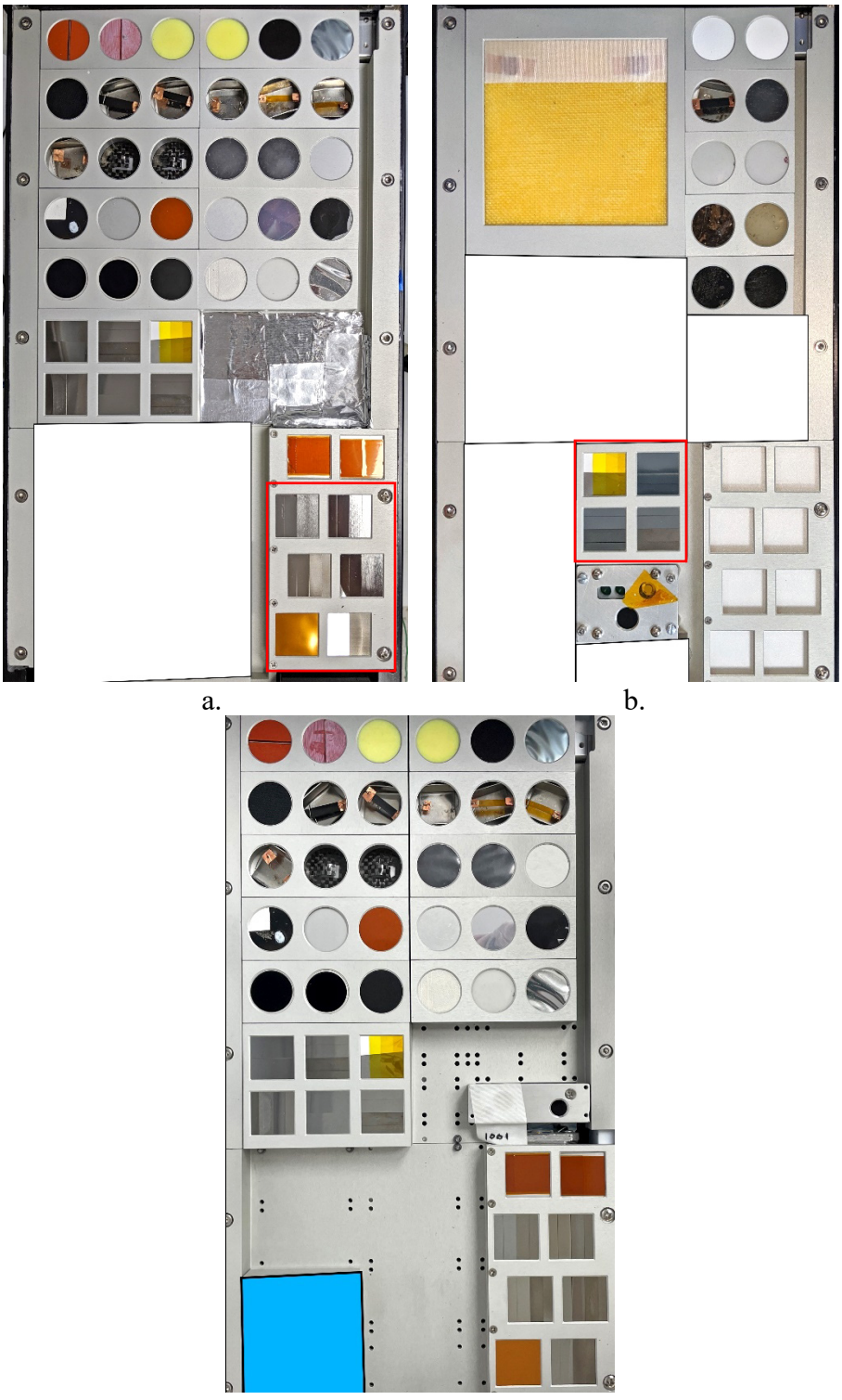

Figure 12. Final pre-flight deck configurations of the MISSE-12 wake and zenith and MISSE-15 wake MSC flight decks: a). MISSE-12 W3 MSC 6 MS (wake), b). MISSE-12 Z1 MSC 18 MS (zenith), and c). MISSE-15 W1 MSC 10 MS (wake). The moved samples are in the red-box areas in 12a and 12b (Aegis Aerospace image).

MISSE-13 Polymers and Composites Experiment-4 (PCE-4)

The MISSE-13 PCE-4 was a passive experiment with 98 samples that was flown in the wake (65 samples) and zenith (33 samples) directions. The primary objectives of the PCE-4 were to determine optical and mechanical property degradation of spacecraft materials, and to assess the functionality of shape memory alloys, shape memory polymer composites, melanin-based composites and elastomer seal samples after radiation exposure in LEO. Samples were also flown for AO erosion determination, and like the PCE 1-3, samples were included to determine the AO fluence in each mission orientation. Teflon FEP samples were used for contamination studies. A complete list of the PCE-4 samples is provided in Reference 21 along with additional experiment objectives and pre-flight photos of select PCE-4 experiment samples. It should be noted that sample M13W-C21 has been corrected from synthetic melanin powders infused into PLA with polyvinyl chloride (PVC) backing layer (PLA-SynMel/PVC), as listed in Reference 21, to animal melanin (octopus ink) infused into PLA with polyvinyl chloride (PVC) backing layer (PLA-AniMel/PVC).

A pre-flight photograph of the PCE-4 samples loaded into the MISSE-13 zenith (Z2 MSC 19 MS), wake mount side (W1 MSC 5 MS) and wake swing side (W1 MSC 5 SS) decks is shown in Figure 13. The PCE-4 samples in the wake MS deck are outlined in red. The large white and metallized square samples in MSC 5 MS were not part of the PCE-4.

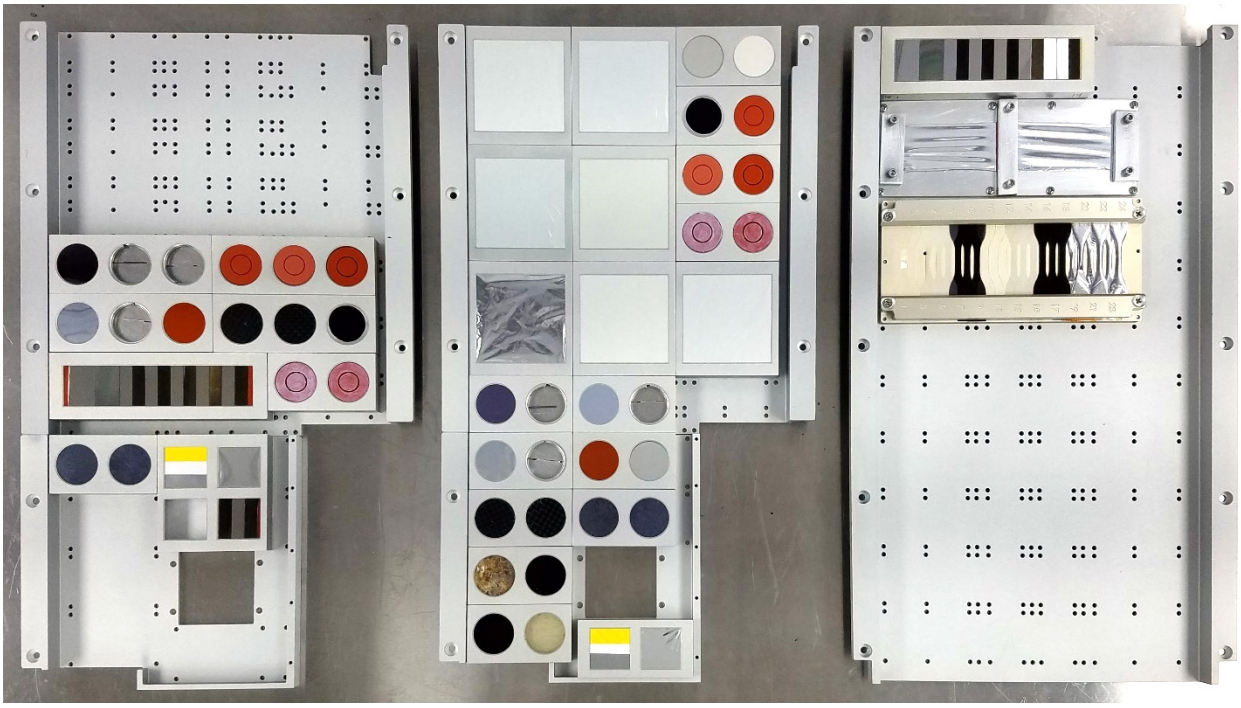

Figure 13. Pre-flight photograph of the MISSE-13 PCE-4 samples loaded into the MSC flight decks, from left to right: Z2 MSC 19 MS (zenith), W1 MSC 5 MS (wake) and W1 MSC 5 SS (wake). The seven large square samples in the wake MS deck are not a part of the PCE-1.

PCE 1-4 MISSE-Flight Facility Missions

The MISSE-FF and the inaugural set of experiments, called MISSE-9, were launched aboard the SpaceX Commercial Resupply Services-14 (CRS-14) Dragon, also called SpaceX-14, on April 2, 2018. The MISSE-FF was robotically installed on ELC-2 Site 3 on April 8, 2018. The MISSE-9 MSCs were installed in the MISSE-FF April 18-19, and the MISSE-9 PCE-1 samples were deployed on April 19, 2018 for a 1-year space exposure mission.

The PCE 1-4 flight experiments were flown as part of the MISSE-9, MISSE-10, MISSE-12, MISSE-13 and MISSE-15 missions. The last flown PCE 1-4 MSC (MISSE-15 wake) was closed for the final time on July 18, 2022 and retrieved from the MISSE-FF on August 2, 2022. The MISSE-15 MSCs were returned in the SpaceX-25 Dragon capsule on August 20, 2022. Thus, the PCE 1-4 experiments were flown on the MISSE-FF from April 2018 to August 2022. Additional details of the mission exposures for each MSC are provided by de Groh in References 21 and 23.

Figure 14 provides an on-orbit photograph of the MISSE-FF with the MISSE-9 and MISSE-10 MSCs installed. As seen from this top perspective, the ram MSCs are on the left (partial hidden in this image), the zenith MSCs are at the top, the wake MSCs are on the right and the nadir MSCs (two) are at the bottom. The MSC numbers (i.e., R1, R2, and R3) are in numerical order going counter-clockwise (i.e., R1 is near the zenith direction (top ram MSC in Figure 14) and R3 is near the nadir direction (bottom ram MSC in Figure 14). Figures 15 and 16 provide on-orbit images of the MISSE-FF with the MISSE-10 PCE-2 and MISSE-12 PCE-3 MSCs installed.

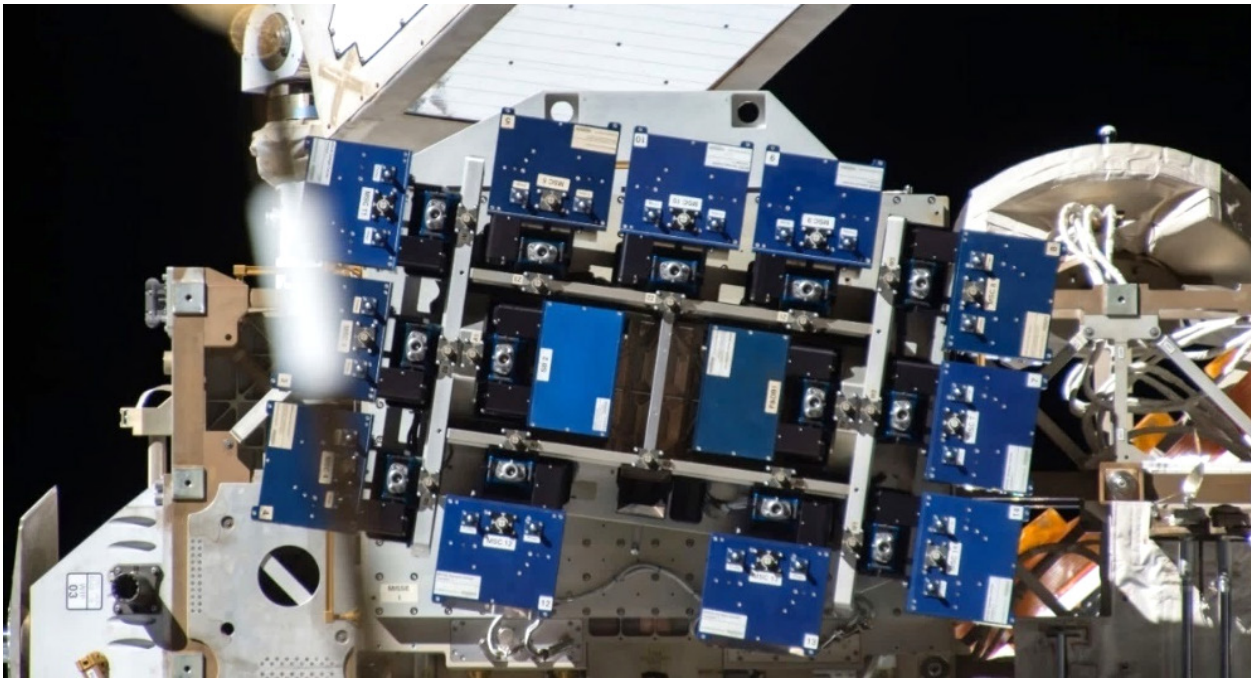

Figure 14. An on-orbit image taken on January 16, 2019 showing the top of the MISSE-FF with the MISSE-9 and MISSE-10 MSCs installed (iss058e003972).

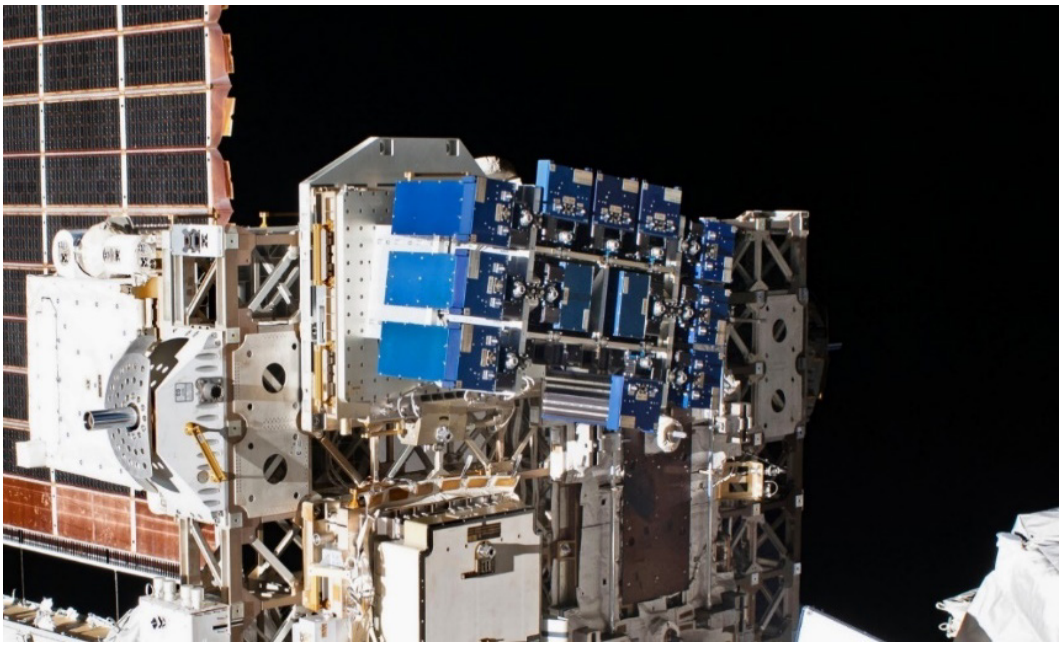

Figure 15. Close-up image of the MISSE-FF with the MISSE-10 PCE-2 and MISSE-12 PCE-3 MSCs as photographed during an EVA on January 25, 2020. The front surface of the blue ram MSCs can be seen in the closed position (iss061e142772).

Figure 16. The wake side of the MISSE-FF with the MISSE-10 PCE-2 and MISSE-12 PCE-3 MSCs as photographed on January 25, 2020 during an EVA. The MSCs are closed, except for the central wake MSC which is open (iss061e143021).

It should be noted that while MSCs are installed on the MISSE-FF and are closed, the samples on those MSCs are exposed to the vacuum of space, thermal cycling (different levels than when the MSCs are open) and energetic radiation, such as galactic cosmic rays. But, when the MSCs are closed the samples are not exposed to visible, UV and VUV radiation, x-rays, solar wind particle radiation (electrons, protons), impacts from MMOD and atomic oxygen (AO). For these experiments, "space exposure" means the MSCs are open and the samples are directly exposed to the space environment.

PCE 1-4 Space Environmental Exposure

Two types of passive samples were flown as part of the PCE 1-4 experiments for AO fluence determination: 1-inch diameter Kapton H samples and Photographic AO Fluence Monitors. The Kapton H AO fluence witness samples were flown in most mission flight orientations for mass loss based fluence computation. Multi-layered Photographic AO Fluence Monitors (also called AO Photo Monitors) were flown as part of the MISSE-10 PCE-2, MISSE-12 PCE-3 and MISSE-13 PCE-4 experiments. These unique samples were designed to determine incremental AO fluence versus mission time based on on-orbit images. In addition, a thin carbon coated white Tedlar sample (M10Z-C2 F) was flown as part of the MISSE-10 PCE-2 experiment in the zenith direction for visual AO fluence determination. Details about these samples and the corresponding post-flight AO fluence computations are provided in Reference 23.

Table 1 provides the mission environmental exposure summary table for the PCE 1-4 experiment samples as provided by de Groh in Reference 23. The table provides the MISSE mission, specific experiment, on-orbit flight direction (or flight orientation), MSC details including mount or swing side deck, launch and return missions, and the dates of MSC installation onto the MISSE-FF along with the MSC retrieval dates from the MISSE-FF. The table also provides for each MSC the direct space vacuum duration, direct space exposure duration (total time the MSC was open and exposed to the space environment), the computed AO fluence and the solar exposure provided as total mission Equivalent Sun Hours (ESH). The PCE 1-4 mission ESH are estimated values based on MISSE-8 ESH/year.[23] As stated in Reference 23, the MISSE-8-based ESH values are the best ESH estimates available for the PCE 1-4 missions. But it should be kept in mind that these values are lower than rough theoretical values for the wake orientations (≈18% lower) and higher than rough theoretical values for the zenith (≈21% higher) and nadir orientations.[23]

As discussed in Reference 23, the AO fluence reported for each MSC was computed from Kapton H AO Fluence Witness sample dehydrated mass loss, except for MISSE-12 zenith where the AO fluence was based on the erosion morphology of a Photographic AO Fluence Monitor (M12Z-S1). References 21 and 23 provide specific details on the PCE 1-4 mission exposures and includes MSC deploy and final closure dates. Minor updates have been made to the mission duration table published by de Groh in Reference 21. The MISSE-12 zenith direct space exposure duration has been updated from 0.44 to 0.45 years, and the MISSE-13 wake swing and mount-side sample decks have been corrected (39 samples were flown in SS (not MS) and 26 samples were flown in MS (not SS)).

Each of the MISSE-FF MSCs are equipped with temperature sensors that measure the anodized aluminum deck on-orbit. Under ideal circumstances, the MSC temperature was measured daily at one second intervals. A significant amount of temperature data is available for the MISSE-9 MSCs, the MISSE-10 ram and nadir MSCs, the MISSE-12 ram and zenith MSCs, and the MISSE-15 wake MSC. Limited data is available for the other MSCs. No data is available for the MISSE-12 wake MSC. Typical temperature ranges for the MISSE-FF MSCs were provided by Aegis Aerospace and are listed below.[26] The temperatures can vary during each mission depending on the Sun's Beta angle and ISS orientation.

- Ram: -30 °C to 45 °C
- Zenith: -20 °C to 50 °C
- Wake: -26 °C to 45 °C
- Nadir: -7 °C to 40 °C

As previously noted, all MSC decks loaded with flight samples underwent a pre-flight thermal vacuum bake-out at Aegis Aerospace. The thermal vacuum bake-out was conducted at 60 °C for 24 hours while under vacuum (approximately 3×10^{-5} torr).

The PCE 1-4 experiments included passive contamination witness samples in each flight direction for post-flight molecular contamination analyses. A total of 13 contamination flight samples were flown.[27] The majority of the contamination samples were alumina (Al_2O_3, sapphire) slides as alumina does not erode with AO exposure and silicone contamination can be easily detected. One of two binary NiTi SMA samples was used for XPS analyses for the MISSE-12 zenith direction. Back-surface aluminized-Teflon FEP samples (FEP/Al) were used for contamination detection for the MISSE-13 mission due to the low E_y of FEP and the easy detection of Si. The post-flight analyses of the PCE 1-4 contamination samples included X-ray Photoelectron Spectroscopy (XPS) analyses (surface and ion sputter depth analyses), optical properties (total reflectance, total transmittance and solar absorptance) and UV light imaging. Details on the PCE 1-4 contamination samples and the corresponding post-flight analyses are reported by de Groh in Reference 27.

Although the PCE 1-4 contamination flight samples experienced minimal optical property changes, the UV (365 nm) light images showed significant changes in numerous flight samples in the space exposed regions.[27] The XPS analyses indicated varying levels of molecular contamination with Si atomic concentrations from 1.5 to 15.5 at.%. The MISSE-12 ram and MISSE-12/MISSE-15 wake samples experienced the highest levels of silicone contamination at 15.1 at.%.[27] The Si atomic concentrations, which could impact the AO E_y values, are provided in Table 2.

Table 1. Polymers and Composites Experiment 1-4 (PCE 1-4) Mission Exposure Summary.[23]

MISSE Mission and Experiment	Flight Direction	MISSE Sample Carrier (MSC)	Launch Mission	Installed on MISSE-FF	Retrieved from MISSE-FF	Return Mission	Space Vacuum Duration (Years)	Time on MISSE-FF (Years)	Direct Space Exposure Duration (Years)	Atomic Oxygen Fluence (atoms/cm^2)^	Mission Equivalent Sun Hours (ESH)^^
MISSE-9 PCE-1	Ram	R2 (MSC 3) MS	SpaceX-14 April 2, 2018	April 18, 2018	Nov. 11, 2019	SpaceX-19 Jan. 7, 2020	1.59	1.57	0.77	3.44E+20	1232
	Wake	W3 (MSC 8) MS		April 18, 2018	April 26, 2019	SpaceX-17 June 3, 2019	1.07	1.02	0.54	4.46E+16	720
	Zenith	Z3 (MSC 5) MS		April 19, 2018			1.07	1.02	0.54	3.19E+18	1539
MISSE-10 PCE-2	Ram	R1 (MSC 11) MS	NG-10 Nov. 17, 2018	Jan. 4, 2019	Nov. 25, 2020	SpaceX-21 Jan. 13, 2021*	1.93	1.90	1.17	3.93E+20	1872
	Zenith	Z2 (MSC 10) MS			March 18, 2020	SpaceX-20 April 7, 2020	1.25	1.20	0.69	4.84E+18	1967
	Nadir	N3 (MSC 13) MS					1.25	1.20	0.48	6.94E+18	179
MISSE-12 PCE-3	Ram	R2 (MSC 4) SS	NG-12 Nov. 2, 2019	Nov. 11, 2019	Nov. 25, 2020	SpaceX-21 Jan. 13, 2021*	1.07	1.04	0.89	2.97E+20	1424
	Wake	W3 (MSC 6) MS			Nov. 27, 2020		1.07	1.05	0**	0	0
	Zenith	Z1 (MSC 18) MS			Nov. 26, 2020		1.07	1.05	0.45	*≈1.67E+18*	1283
MISSE-13 PCE-4	Wake	W1 (MSC 5) MS/SS	SpaceX-20 March 6, 2020	March 18, 2020	Nov. 27, 2020	SpaceX-21 Jan. 13, 2021*	0.72	0.70	0.44	2.65E+18	587
	Zenith	Z2 (MSC 19) MS			Nov. 26, 2020		0.72	0.70	0.46	2.24E+18	1311
MISSE-15 PCE-3 Wake Re-flight**	Wake	W1 (MSC 10) MS	SpaceX-23 Aug. 29, 2021	Dec. 28, 2021	Aug. 2, 2022	SpaceX-25 Aug. 20, 2022	0.71	0.60	0.44	4.77E+18	587

MS: Mount side deck; SS: Swing side deck

*January 13, 2021 EST (January 14, 2021 UTC)

**The PCE-3 wake samples were re-flown as part of the MISSE-15 mission

^AO fluence was computed from dehydrated Kapton H mass loss, except for MISSE-12 zenith which was based on erosion morphology of the M12Z-S1 Photographic AO Fluence Monitor

^^Mission Equivalent Sun Hours (ESH) estimates based on MISSE-8 ESH/year

Table 2. PCE 1-4 Contamination Samples Si Atomic Concentrations.[27]

MISSE-FF Flight Sample ID	Flight Orientation	Material	Time on MISSE-FF (Years)	Direct Space Exposure Duration (Years)	Si Atomic Concentration (at.%)	Si Atomic Concentration per Year (at.%/Year)
MISSE-9						
M9R-C6 F	Ram	Al_2O_3	1.57	0.77	**6.0**	7.8
M9R-C27 F	Ram	MgF_2	1.57	0.77	**4.4**	5.7
M9W-C3 F	Wake	Al_2O_3	1.02	0.54	**1.7**	3.1
M9Z-C3 F	Zenith	Al_2O_3	1.02	0.54	**1.5**	2.8
M9Z-C18 F	Zenith	MgF_2	1.02	0.54	**1.8**	3.3
MISSE-10						
M10R-C4 F	Ram	Al_2O_3	1.9	1.17	**8.4**	7.2
M10N-C5 F	Nadir	Al_2O_3	1.2	0.48	**8.1**	**16.9**
M10Z-C5 F	Zenith	Al_2O_3	1.2	0.69	**6.6**	9.6
MISSE-12						
M12R-C3 F	Ram	Al_2O_3	1.04	0.89	**15.1**	**17.0**
M12W-C3 F	Wake	Al_2O_3	1.05	0**	**N/A**	N/A
M12Z-S2 F	Zenith	SMA NiTi	1.05	0.45	**6.2**	**13.8**
MISSE-13						
M13W-C4 F	Wake	FEP/Al	0.7	0.44	**1.6**	3.6
M13Z-C4 F	Zenith	FEP/Al	0.7	0.46	**2.2**	4.8
MISSE-12 & MISSE-15 Re-flight**						
M12W-C3 F	Wake	Al_2O_3	1.04 + 0.6	0.44	**15.1**	**34.3**

Experimental Procedures

Mass-Based Atomic Oxygen Erosion Yield

The sensitivity of a hydrocarbon material to reaction with AO is quantified by the AO E_y of the material. As previously mentioned, the AO E_y is the volume of a material that is removed (through oxidation) per incident oxygen atom and is measured in units of cm^3/atom. The AO E_y has been referred to as the recession rate, AO Reactivity and AO Reaction Efficiency (R_e) but the units of erosion (cm^3/atom) are the same.

A common technique for determining the E_y of flight materials is based on mass loss and should be calculated using dehydrated mass measurements because many polymers are hygroscopic (absorbing up to 2 percent of their weight in moisture) and can fluctuate in mass with humidity and temperature.[28] The E_y of the sample is determined through the following equation:

$$E_y = \frac{\Delta M_S}{\left(A_S \rho_S F\right)} \tag{1}$$

where

E_y = *erosion yield of flight sample (cm^3/atom)*
ΔM_S = *mass loss of the flight sample (g)*
A_S = *surface area of the flight sample exposed to AO (cm^2)*
ρ_S = *density of flight sample (g/cm^3)*
F = *low Earth orbit AO fluence (atoms/cm^2)*

The LEO AO fluence (F) of a spaceflight mission can be determined through the mass loss of a Kapton® H witness sample because Kapton H has a well characterized erosion yield, E_K (3.0×10^{-24} cm^3/atom) in the LEO environment. de Groh provides an overview of Kapton H E_K values as reported for various flight missions and their corresponding spaceflight mission altitudes in Reference 23. The values from various Shuttle missions and the Long Duration Exposure Facility (LDEF) range from $2.8\text{-}3.05\times10^{-24}$ cm^3/atom for altitudes ranging from 225 km to 470 km.[29-35] Silverman states in his contract report "Space Environmental Effects on Spacecraft: LEO Materials Selection Guide" that the Kapton E_K of 3.0×10^{-24} cm^3/atom should be used for spacecraft design considerations.[34]

The mass loss based AO fluence can be calculated using the following equation:

$$F = \frac{\Delta M_K}{\left(A_K \rho_K E_K\right)} \tag{2}$$

where

F = *low Earth orbit AO fluence (atoms/cm^2)*
ΔM_K = *mass loss of Kapton H witness sample (g)*
A_K = *surface area of Kapton H witness sample exposed to AO (cm^2)*
ρ_K = *density of Kapton H witness sample ($1.4273\ g/cm^3$)*[2,15]
E_K = *erosion yield of Kapton H witness sample (3.0×10^{-24} cm^3/atom)*[29-31,34]

Like E_y computation, it is important to calculate the AO fluence using dehydrated mass measurements before and after flight because Kapton is very hygroscopic and can fluctuate in mass with humidity and temperature.[28] The AO fluence can also be determined using recession measurements.

Recession-Depth-Based Erosion Yield

Recession measurements can be used for AO E_y determination based on erosion depth step-heights. The erosion or recession depth (D) can be measured from a protected surface using profilometry, scanning electron microscopy (SEM), optical interferometry, or atomic force microscopy for low-fluence exposures.[36] The recession based E_y can be calculated through the following equation:

$$E_y = \frac{D}{F} \tag{3}$$

where

E_y = *erosion yield of flight sample (cm^3/atom)*
D = *erosion depth of flight sample (cm)*
F = *low Earth orbit AO fluence (atoms/cm^2)*

The recession depth technique used for some of the Glenn MISSE flight samples involved pre-flight protection of the sample surface using isolated small salt (NaCl) particles that are in intimate contact with the sample.[36,37] The salt particles are applied to the sample substrate by spraying a saturated salt solution using an atomizer. This results in isolated, protective particles that typically remain in contact on the surface during flight and retrieval. The particles are then removed post-flight by washing off the salt with distilled water followed by drying with nitrogen gas.[36,37] The recession depth can then be determined using SEM.

Using SEM, images are obtained at a high tilt angle such as 45° and D is determined using the following equation:

$$D = \frac{d}{\sin\theta} \tag{4}$$

where

D = *erosion depth of flight sample (cm)*
d = *erosion depth measured from SEM image obtained at θ tile angle (cm)*
θ = *SEM tilt angle (degrees)*

The SEM-image-based erosion depth (d) is measured from the top of the protected surface to the mid-length of the remaining erosion cones.

Mass Measurements

Because many of the PCE 1-4 polymer and composites materials are hygroscopic, the samples were fully dehydrated immediately prior to measuring the mass both pre-flight and post-flight. The PCE 1-4 AO E_y samples were dehydrated at room temperature in a vacuum desiccator maintained at a pressure of 5.3 to 13.3 Pa (40 to 100 mtorr) with a mechanical roughing pump. Typically, ten samples were placed in a vacuum desiccator, in a particular order (i.e. order of weighing), and left under vacuum for 72-96 hours. Once a sample was removed for weighing, the vacuum desiccator was immediately put back under vacuum to keep the other samples under vacuum. Previous tests showed that the mass of a dehydrated sample was not adversely affected if the desiccator was opened and quickly closed again and pumped back down to approximately 20 Pa (150 mtorr) prior to that sample being weighed. This process allows multiple samples to be dehydrated together. The time at which the sample was first exposed to air was recorded along with the times at which it was weighed. A total of three mass readings were obtained and averaged. The total time it took to obtain the three readings, starting from the time air was let into the desiccator, was typically 5 minutes. The samples were weighed pre-flight using a Sartorius ME5 Microbalance (±0.005 mg sensitivity). Heavier samples were measured using a Sartorius Balance R160P (±0.00001 g sensitivity). Records of the following were kept: the sequence of sample weighing, the number of samples in each set, the time under vacuum prior to weighing, the temperature and humidity in the

room, the time air was let into the desiccator, and the time a sample was taken out of the desiccator, the time of each weighing and the mass. The same procedure and sequence was repeated as best as possible with the samples post-flight.

Several of the PCE 1-4 ram samples were flown as "stacked" samples with multiple thin film layers stacked together in case the AO fluence was high enough to erode through a single layer of material. For these samples, the top space exposed sample layer (called Part A) was typically weighed separately from the remaining layers (called Part B).

Density

The densities of the majority of the samples were based on density gradient column measurements of polymers made for the MISSE 2 Polymer Erosion and Contamination Experiment (PEACE) Polymers experiment.[2,15] The density gradient columns were created in 50-mL burets either with solvents of cesium chloride (CsCl, density $\rho \approx 2$ g/cm^3) and water (H_2O, $\rho = 1.0$ g/cm^3) for less dense polymers such as Kapton H or with solvents of carbon tetrachloride (CCl_4, $\rho = 1.594$ g/cm^3) and bromoform ($CHBr_3$, $\rho = 2.899$ g/cm^3) for more dense polymers such as fluoropolymers.[2,15] A quadratic calibration curve was developed for each column based on the equilibrium vertical position of three to four standards of known density (±0.0001 g/cm^3).[2,15] Subsequently, density values of samples were calculated based on the vertical positions of small (<2 mm) pieces placed into the column and allowed to settle for 2 hours.[2,15] Where possible, the same batch of material was used for all the Glenn MISSE polymers experiments. The densities of polymers, composites and coatings not included in the MISSE 2 PEACE Polymers experiment were obtained from the sample collaborator or material manufacturer.

Exposed Surface Area

The exposed surface area for each flight sample was determined by measuring the MSC deck tray opening using digital calipers. For the 1-in. circular openings, each specific tray opening was measured at six different diameter orientations to determine an average diameter. For the 1-inch square sample openings, three measurements were taken in one direction and averaged, and three measurements were taken in the other direction and averaged. The 1-inch square MSC sample deck holder openings have 0.032 inch (0.08128 cm) rounded corners, so an area of 0.00567 cm^2 was subtracted from the measured area of each 1-inch exposed sample.

The exposed surface area of the few unusually shaped samples, such as the MISSE-9 ram rectangular highly oriented pyrolytic graphite (HOPG) sample (M9R-C22) was determined using AutoCAD® (Autodesk, Inc.) computer design software to trace the exposed border of the sample on a sample photograph. The sample photograph was taken, along with a scale bar, with a Canon EOS Rebel SL1 digital camera on a Polaroid Land camera stand. The surface area was computed using AutoCAD® based on the traced area as well as measurements of the scale bar. For the M9R-C22 HOPG sample, the rectangular sample was flown in a 1-inch circular holder.

Pre- and Post-Flight Images

Pre-flight and post-flight photographs of the flight and control samples were taken with either a Fujifilm Finepix S1500 or more often with a Canon EOS Rebel SL1 with a 60 mm EF-S macro lens on a Land Camera stand. Both pre- and post-flight photographs were also taken of the flight

samples loaded in the MSC flight decks during integration and de-integration in Aegis Aerospace's cleanroom. The cleanroom images were taken with either a Samsung S10 Plus or a Sony RX-100 IV camera. In addition to taking post-flight visible light images, post-flight photographs were also taken of the flight and control samples with a 365 nm wavelength UV light source (UV Beast flashlight) to see changes in fluorescence due to space exposure. Because of the large number of flight samples for AO E_y determination, and hence large number of pre- and post-flight images, only a select number of sample images are provided in this paper.

MISSE 9-15 PCE 1-4 Erosion Data

MISSE-9 Polymers and Composites Experiment-1 (PCE-1)

MISSE-9 PCE-1 Ram Samples

Figure 17 shows pre- and post-flight photographs of the MISSE-9 ram MS deck (R2 MSC 3) section containing the 39 PCE-1 ram samples. Figure 18 provides a sample map showing the specific location of the PCE-1 ram samples. The four larger square samples in the upper and lower left indicated with an "X" in Figure 17a are not part of the PCE-1 experiment. As can be seen by comparing the two images in Figure 17, the 0.77-year LEO ram space exposure resulted in significant discoloration of the anodized aluminum deck and of several PCE-1 samples. It should be noted that some of the highly reflective samples, such as the metallized Teflon FEP samples (M9R-C16 and M9R-C17), can appear different based on image reflections and not necessarily on space exposure changes. This would be true for other highly reflective PCE 1-4 samples.

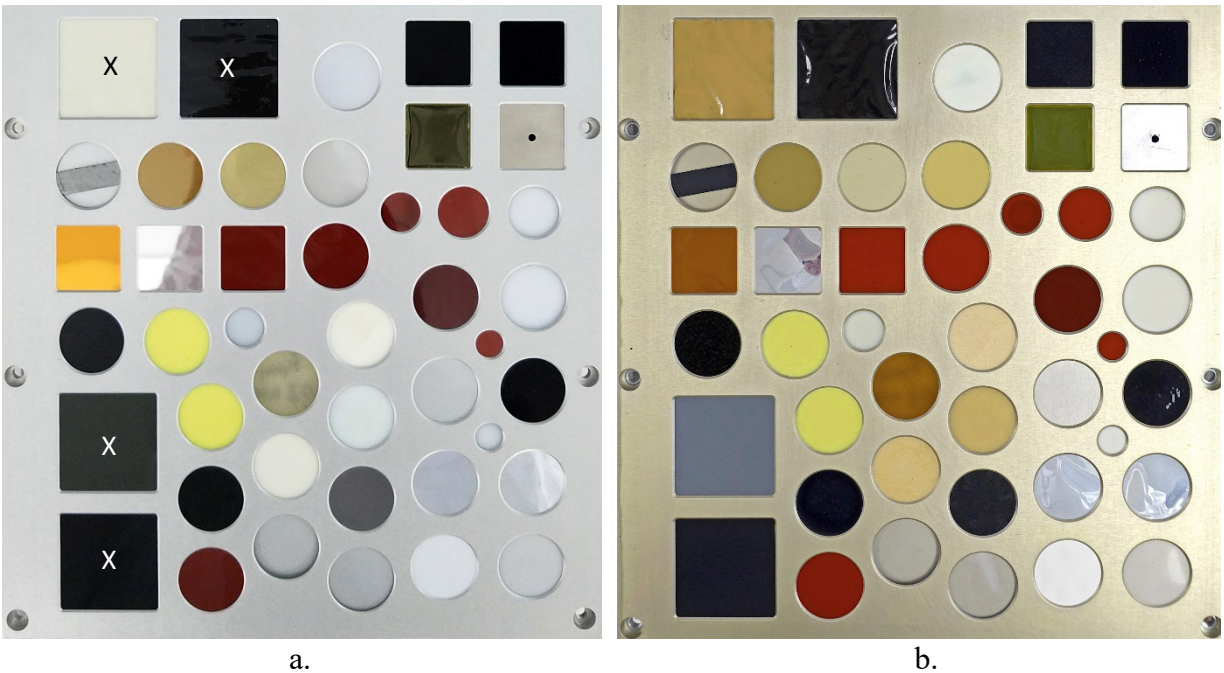

a. b.

Figure 17. Photographs of the MISSE-9 PCE-1 ram MS deck (R2 MSC 3): a). Pre-flight with the PCE-1 ram samples (the four large square samples with "X" are not part of the PCE-1), and b). Post-flight showing discoloration of the deck and numerous samples.

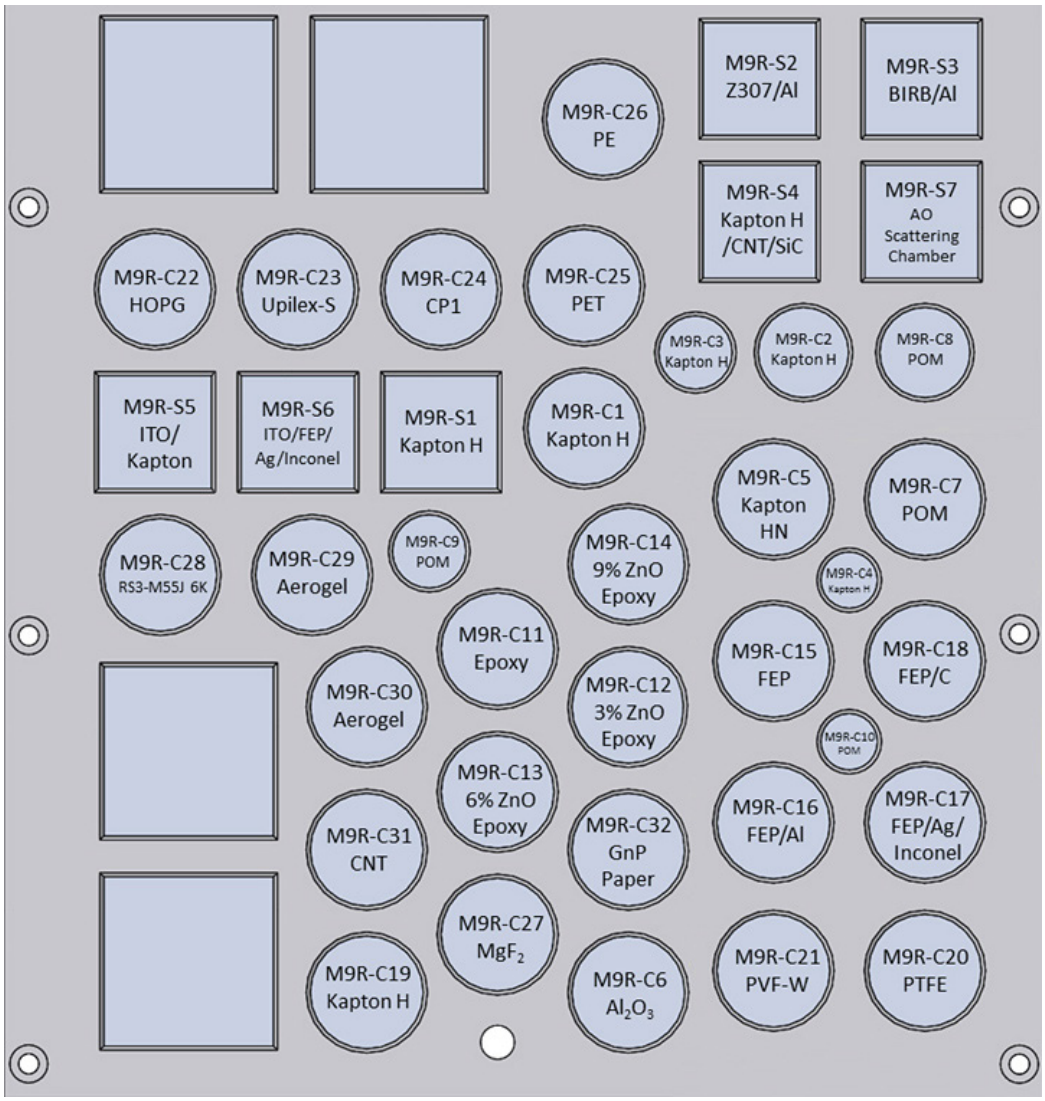

Figure 18. The MISSE-9 PCE-1 R2 ram sample map.

For PCE 1-4 experiments, the sample ID provides the MISSE mission number (M#), the flight orientation (ram (R), wake (W), nadir (N) or zenith (Z)), the sample's shape (circular (C), square (S) or rectangular (R)), the ID number and the pre-flight sample designation of Flight (F) or Back-up (B). So for example, M9R-C1 F was a circular sample (#1) flown on the MISSE-9 mission in the ram direction and was designated as the flight sample. Occasionally, a sample designated as the back-up sample (B) was flown instead of the flight sample (F). For example, the back-up sample of Z307 coated aluminum (M9R-S2 B) was flown because the sample designated as the flight sample (F) did not fit in the flight deck during integration. Thus, in this case, the "F" sample became the control sample. As stated previously, for the two-layered ram samples, the layer labeled 'Part A' was the space exposed top layer, and the 'Part B' layer(s) was stacked underneath Part A. The Part A and Part B layers were weighed separately pre-flight. Because the AO fluence was relatively low for the MISSE-9 mission, only the top layer of the multilayered ram samples was eroded. Therefore, only the top layer was weighed post-flight and compared with the top layer pre-flight mass for determining the sample mass loss, unless stated otherwise.

The MISSE-9 ram AO fluence was determined to be 3.44×10^{20} atoms/cm^2 based on dehydrated mass loss of two 1-inch (2.54 cm) circular Kapton H AO fluence witness samples (M9R-C1 F and M9R-C19 F).[23] A post-flight photograph of the top layer (Part A) of the MISSE-9 ram Kapton H AO fluence witness sample (M9R-C1 F) and corresponding non-flown control sample (M9R-C1 B) is provided in Figure 19. As can be seen, the flight sample appears textured in the space exposed area as the surface appears diffuse and substantially brighter as compared to the protected area on the control sample. Table 3 provides the MISSE-9 LEO AO E_y values for the PCE-1 ram samples. Included in Table 3 is the MISSE-9 ram sample ID, material, material abbreviation, sample layer thickness, number of sample layers flown, sample size, dehydrated mass loss, exposed surface area, density, and the MISSE-9 ram AO fluence. It should be noted that the AO E_y value for the PCE-1 coated samples, such as the MISSE-9 ITO/Kapton HN/Al and ITO/FEP/Ag/Inconel samples, is an overall E_y value for the entire sample and not just the surface coating. Thus, erosion of ITO coated samples is likely including AO erosion of the polymer substrate at coating defect sites. This is true for all the PCE 1-4 coated samples.

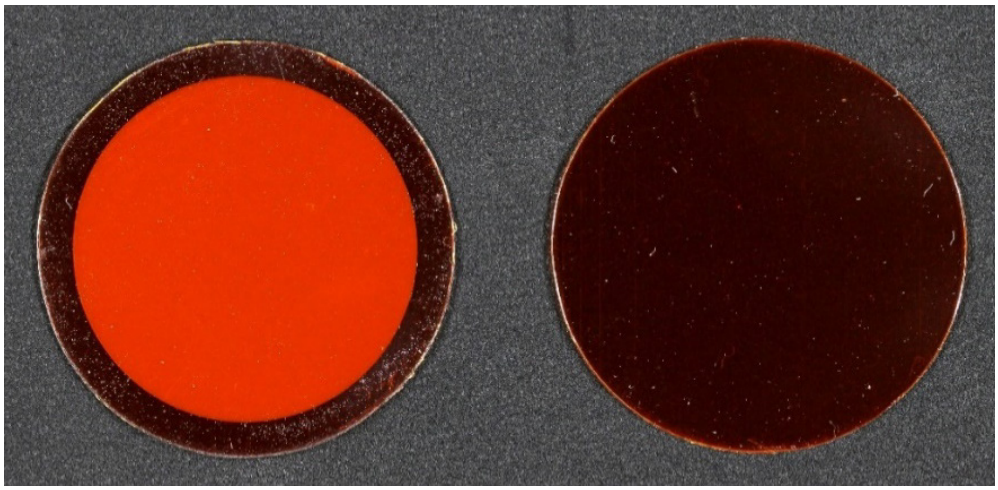

Figure 19. The top layer (Part A) of the MISSE-9 ram Kapton H AO fluence witness sample (M9R-C1 F, on the left) and control sample (M9R-C1 B, on the right).

Table 3. Erosion Data for the MISSE-9 PCE-1 Ram Flight Samples.

MISSE-9 Ram ID	Material (Trade Name)	Abbreviation	Thickness (mils) (# Layers Flown)	Size (inch)	Mass Loss (g)	Exposed Surface Area (cm^2)	Density (g/cm^3)[15]	MISSE-9 Ram AO Fluence ($atoms/cm^2$)[23]	MISSE-9 Ram AO E_y ($cm^3/atom$)
M9R-C1 F	Polyimide (PMDA) (Kapton H)	Kapton H	5 (2)	1	0.005265	3.569	1.4273	**3.445E+20**	***3.00E-24***
M9R-C19 F	Polyimide (PMDA) (Kapton H)	Kapton H	5 (2)	1	0.005350	3.646	1.4273	**3.427E+20**	***3.00E-24***
M9R-C2 F	Polyimide (PMDA) (Kapton H)	Kapton H	5 (2)	0.8	0.003155	2.169	1.4273	3.44E+20	2.97E-24
M9R-C3 F	Polyimide (PMDA) (Kapton H)	Kapton H	5 (2)	0.65	0.001870	1.290	1.4273	3.44E+20	2.96E-24
M9R-C4 F	Polyimide (PMDA) (Kapton H)	Kapton H	5 (2)	0.5	0.000923	0.636	1.4273	3.44E+20	2.96E-24
M9R-C5 F	Polyimide (PMDA) (Kapton HN)	Kapton HN	5 (2)	1	0.005318	3.556	1.4346	3.44E+20	3.03E-24
M9R-C7 F	Polyoxymethylene (Delrin acetal)	POM	10 (2)	1	0.040970	3.548	1.3984	3.44E+20	2.40E-23
M9R-C8 F	Polyoxymethylene (Delrin acetal)	POM	10 (2)	0.8	0.026818	2.164	1.3984	3.44E+20	2.58E-23
M9R-C9 F	Polyoxymethylene (Delrin acetal)	POM	10 (2)	0.65	0.010320	1.299	1.3984	3.44E+20	1.65E-23
M9R-C10 F	Polyoxymethylene (Delrin acetal)	POM	10 (2)	0.5	0.010559	0.636	1.3984	3.44E+20	3.45E-23
M9R-C15 F	Fluorinated ethylene propylene (Teflon FEP)	FEP	5 (1)	1	0.001386	3.560	2.1443	3.44E+20	5.28E-25
M9R-C16 F	Aluminized-Teflon (FEP/Al)*	FEP/Al	5 (1)	1	0.001385	3.572	2.1443	3.44E+20	5.26E-25
M9R-C17 F	Silver-Teflon (FEP/Ag/Inconel)*	FEP/Ag/Inconel	5 (1)	1	0.001359	3.556	2.1443	3.44E+20	5.19E-25
M9R-C18 F	Carbon painted (India Ink) Teflon (FEP/C/FEP)*	FEP/C/FEP	14 (1)	1	0.002696	3.555	2.1443	3.44E+20	1.03E-24
M9R-C20 F	Polytetrafluoroethylene (Chemfilm DF 100)	PTFE	5 (1)	1	0.001007	3.574	2.1503	3.44E+20	3.81E-25
M9R-C21 F	Crystalline polyvinyl fluoride w/white pigment (white Tedlar)	PVF-W	2 (1)	1	0.001363	3.567	1.6241	3.44E+20	6.85E-25
M9R-C22 F	Highly Oriented Pyrolytic Graphite	HOPG	41 (1)	1"×0.3"	0.001181	1.688	2.245^	3.44E+20	9.07E-25
M9R-C23 F	Polyimide (BPDA) (Upilex-S)	Upilex-S	1 (2)	1	0.004157	3.573	1.3866	3.44E+20	2.44E-24
M9R-C24 F	Polyimide (CP1)	CP1	3 (2)	1	0.003445	3.576	1.4193	3.44E+20	1.98E-24
M9R-C25 F	Polyethylene terephthalate (Mylar)	PET	2 (4)	1	0.006827	3.577	1.3925	3.44E+20	3.99E-24
M9R-C26 F	Polyethylene	PE	2 (5)	1	0.003290	3.569	0.918	3.44E+20	2.92E-24
M9R-C27 F	Magnesium Fluoride	MgF_2	108 (1)	1	0.000016	3.626	3.15^^	3.44E+20	3.99E-27
M9R-C28 F	Cyanate ester graphite fiber composite (RS3-M55J 6K)	RS3-M55J 6K	62 (1)	1	0.004012	3.557	1.623**	3.44E+20	2.02E-24
M9R-C29 F	Polyimide aerogel	Polyimide Aerogel	125 (1)	1	0.001790	3.583	0.15**	3.44E+20	9.69E-24
M9R-C30 F	Polyimide aerogel	Polyimide Aerogel	125 (1)	1	0.002080	3.580	0.15**	3.44E+20	1.13E-23
M9R-C31 F	Carbon nanotube (CNT) paper	Buckypaper	1.6 (3)	1	0.000488	3.617	0.553**	3.44E+20	7.11E-25
M9R-C32 F	Graphene nanoplatelets (GnP) paper	GnP paper	10 (1)	1	0.001037	3.606	2.000*	3.44E+20	4.19E-25

Table 3. Erosion Data for the MISSE-9 PCE-1 Ram Flight Samples.

MISSE-9 Ram ID	Material (Trade Name)	Abbreviation	Thickness (mils) (# Layers Flown)	Size (inch)	Mass Loss (g)	Exposed Surface Area (cm^2)	Density (g/cm^3)[15]	MISSE-9 Ram AO Fluence ($atoms/cm^2$)[23]	MISSE-9 Ram AO E_y ($cm^3/atom$)
M9R-S1 F	Polyimide (PMDA) (Kapton H)	Kapton H	5 (2)	1	0.006569	4.437	1.4273	3.44E+20	3.02E-24
M9R-S2 B	Z307 (black paint)/aluminum (Al)	Z307/Al	35 (1)	1	0.002283	4.424	0.205**	3.44E+20	7.33E-24
M9R-S3 F	Ball Infrared Black (BIRB) paint/Al	BIRB/Al	100 (1)	1	0.003683	4.412	0.423**	3.44E+20	5.74E-24
M9R-S5 F	Indium tin oxide coated Kapton HN/Al	ITO/Kapton HN/Al	2 (1)	1	0.000069	4.414	6.8[#]	3.44E+20	6.72E-27
M9R-S6 F	Indium tin oxide coated silver-Teflon	ITO/FEP/Ag/Inconel	5 (1)	1	0.000009	4.420	6.8[#]	3.44E+20	9.04E-28

*Teflon FEP layer is space facing
^ http://www.optigraph.eu/basics.html
^^https://www.matweb.com/index.aspx
**Sample Collaborator[21]
[#]J Vac Sci Tech A 19:5(2043-7); 2001

Atomic oxygen has a certain probability of reaction with an impacted surface, which is material dependent. For example, the probability of reaction with an anodized surface is negligible, thus AO can scatter off a spacecraft surface in LEO. This can result in AO erosion problems, such as AO scattering within a telescope body or AO undercutting of protective coatings with defect sites. Typically, MISSE sample holders have 45° chamfered edges which result in focused AO erosion near the chamfer edge of the flight sample due to scattering effects. Examples of focused AO erosion of MISSE 2 flight samples are provided by Banks et al. in Reference 38. The PCE-1 included eight samples flown to characterize MISSE flight hardware AO focusing effects on the AO E_y value. The PCE-1 samples included four different size samples (0.5-inch, 0.65-inch, 0.8-inch, and 1-inch diameter samples) of both Kapton® H and polyoxymethylene (POM) to determine the effect of chamfered holder sample size on E_y. Ideally, this type of data would allow one to more accurately extrapolate the LEO E_y which would occur on large area spacecraft surfaces from small test samples.

A Kapton HN sample (M9R-C5 F) was flown as part of the MISSE-9 PCE-1 ram samples. The AO E_y for M9R-C5 F was 3.03×10^{-24} cm^3/atom. This is slightly higher than for the assumed LEO AO E_y for Kapton H. Kapton HN was also flown as part of the MISSE 2 PEACE Polymers experiment, which was exposed to LEO ram AO for 4 years and had a high AO fluence of 8.43×10^{21} atoms/cm^2.[15] The MISSE 2 AO E_y for Kapton HN was found to be 2.81×10^{-24} cm^3/atom. [15] Kapton HN has a small amount of AO durable filler (i.e. ash) and thus, the AO E_y decreases with increasing AO fluence as more protective particles populate the surface during the erosion process.

Included in the PCE-1 ram samples were two 1-inch Kapton H samples (M9R-C1 F and M9R-C19 F) flown to determine the AO fluence for the ram tray, as previously discussed. Thus, the E_y for these samples was assumed to be 3.0×10^{-24} cm^3/atom based on prior flight data. The other Kapton H samples were: M9R-C2 F (0.8-inch diameter), M9R-C3 F (0.65-inch diameter) and M9R-C4 F (0.5-inch diameter). The AO E_y for M9R-C2 F was 2.97×10^{-24} cm^3/atom. The AO E_y for M9R-C3 F was 2.96×10^{-24} cm^3/atom, and the AO E_y for M9R-C4 F was 2.96×10^{-24} cm^3/atom. Thus, the smaller samples had a slightly lower E_y than the 1-inch diameter samples, which is opposite to the expected result. But, the AO fluence for the MISSE-9 ram samples may have been too low to show significant effects of AO scattering (i.e. focusing more AO arrival at the chamfered sample's holder edge and increasing the total AO fluence).

POM was selected as another material to analyze chamfer focusing affects because of its high E_y. The AO E_y for M9R-C7 F (1-inch diameter) was 2.40×10^{-23} cm^3/atom, which is an order of magnitude higher than Kapton H. The AO E_y for M9R-C8 F (0.8-inch diameter) was 2.58×10^{-23} cm^3/atom. The AO E_y for M9R-C9 F (0.65-inch diameter) was 1.65×10^{-23} cm^3/atom. And, the AO E_y for M9R-C10 F was 3.45×10^{-23} cm^3/atom. Thus, there was not a consistent trend of increasing or decreasing E_y for the four different sized POM samples. After the AO E_y values were determined, an attempt was made to re-weigh the flight samples, but two of the flight samples (M9R-C7 F and M9R-C10 F) had fallen apart near the chamfer edge and would not produce reliable mass data. Post-flight POM sample images are provided in Figure 20. Although there was not a consistent trend for AO E_y with sample diameter for the POM samples, the chamfer scattering effect appears have impacted degradation of the M9R-C7 F and M9R-C10 F flight samples at the chamfered sample holder perimeter. The POM flight samples also discolored, as seen in Figure 20.

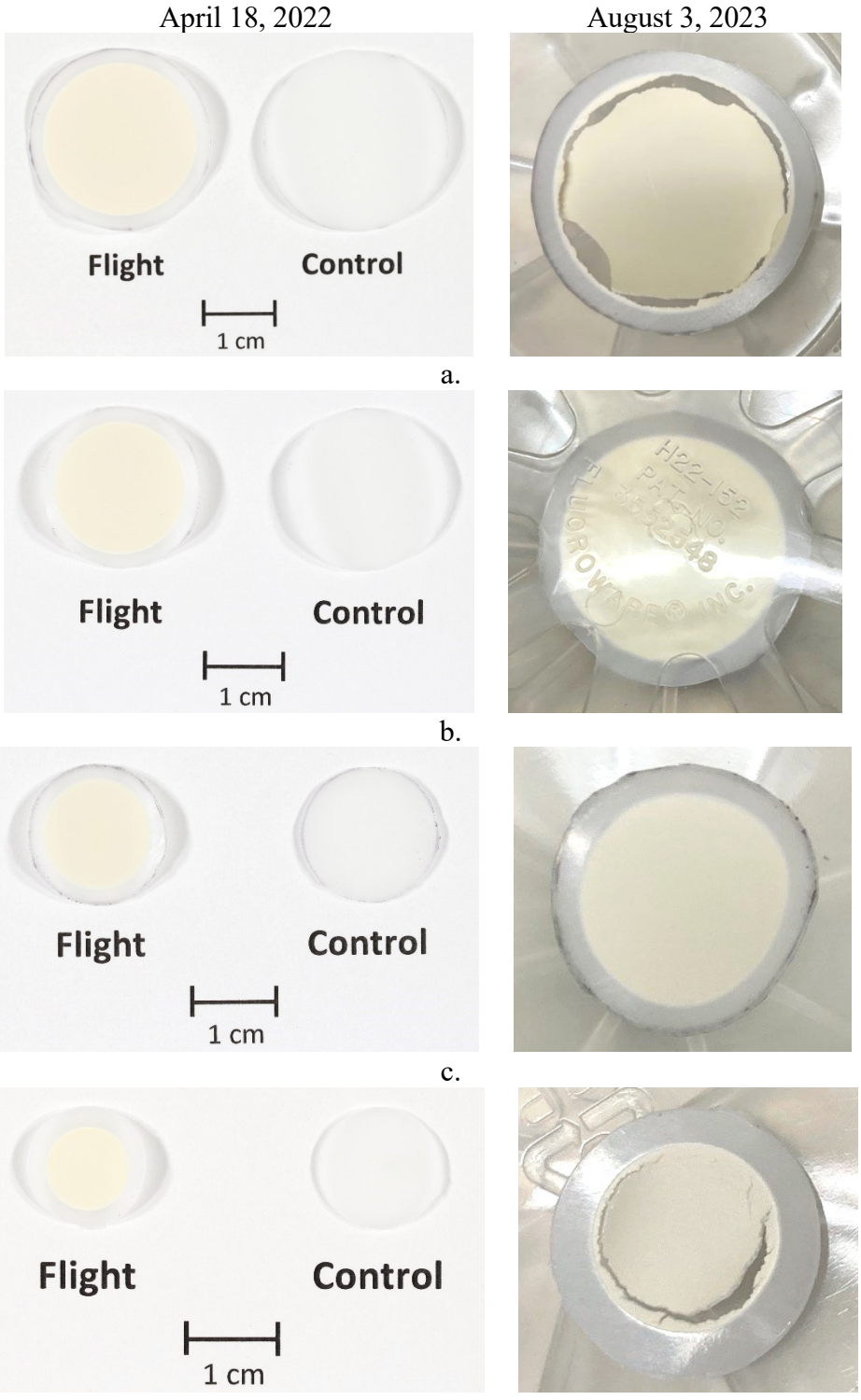

Figure 20. Post-flight photographs of the MISSE-9 ram POM F and B samples taken April 18, 2022 (left) and F samples taken August 3, 2023 (right): a). M9R-C7, b). M9R-C8 (2023 photo taken under fluoroware spider), c). M9R-C9, and d). M9R-C10.

Teflon FEP is a common spacecraft insulation material. Metallized-Teflon FEP is often used as the outer most layer of multilayer insulation (MLI) blankets, such as those on the Hubble Space Telescope (HST).[39,40] Past flight experiments and retrieved HST MLI blanket analyses indicated that the erosion of Teflon FEP is highly dependent on the solar and thermal exposure on-oribt.[16,40] To further understand the effect of solar exposure on the AO E_y of Teflon FEP, samples of clear Teflon FEP, back-surface aluminized Teflon (FEP/Al), silver-Teflon (FEP/Ag/Inconel) were flown on most of the PCE experiments in various flight orientations. In addition, back-surface carbon painted-Teflon FEP (FEP/C/FEP) or back-surface carbon coated-Teflon FEP (FEP/C) samples were also flown to provide passive heating during the mission to see the effect of heating on the AO E_y of Teflon FEP. As can be seen in Table 3, the AO E_y for the MISSE-9 ram FEP (M9R-C15 F), FEP/Al (M9R-C16 F) and FEP/Ag/Inconel (M9R-C17 F) samples were all similar at 5.28×10^{-25}, 5.26×10^{-25} and 5.19×10^{-25} cm^3/atom, respectively. However, the carbon back-surface painted Teflon FEP sample (M9R-C18 F) had a 2X higher AO E_y of 1.03×10^{-24} cm^3/atom. Thus, it appears that a higher level of on-orbit heating may have resulted in an increase in the erosion of Teflon FEP. It would be ideal to confirm the higher erosion for the carbon back-surface painted Teflon FEP based on temperature by repeating the experiment with thermocouple instrumentation to measure the temperature difference.

As mentioned previously, the MISSE-9 ram HOPG flight sample (M9R-C22 F) was an irregular shaped sample. Thus, the exposed surface area was determined using AutoCAD® software to trace the exposed border of the sample in the post-flight photograph, as shown in Figure 21. The resulting exposure area was determined to be 1.688 cm^2. The AO E_y of the MISSE-9 ram HOPG flight sample (M9R-C22 F) was determined using both dehydrated mass loss and recession depth measurements. The recession depth measurements were made using Hitachi S-4700 II field emission scanning electron microscope (FESEM) images of protected buttes imaged at a 45° title angle. Three buttes were imaged, and the depth measurement locations are shown in Figure 22. The corresponding recession depth (i.e., erosion depth) measurements and computed AO E_y values are provided in Table 4. The average AO E_y for the HOPG flight sample (M9R-C22 F) based on recession depth of the three buttes was determined to be 7.44×10^{-25} cm^3/atom. The mass loss-based AO E_y, provided in Table 3, was 9.07×10^{-25} cm^3/atom. This value is close to, but a little higher, than the recession depth-based value. There is some error in selecting the recession depth on the SEM images and the recession depth technique only averages data for local areas (i.e., select buttes). Thus, the mass loss-based E_y value is believed to be more accurate as it averages the entire erosion surface.

Figure 21. Post-flight photograph of MISSE-9 ram HOPG flight sample (M9R-C22 F) with the AutoCAD® red line trace used to determine the exposed surface area.

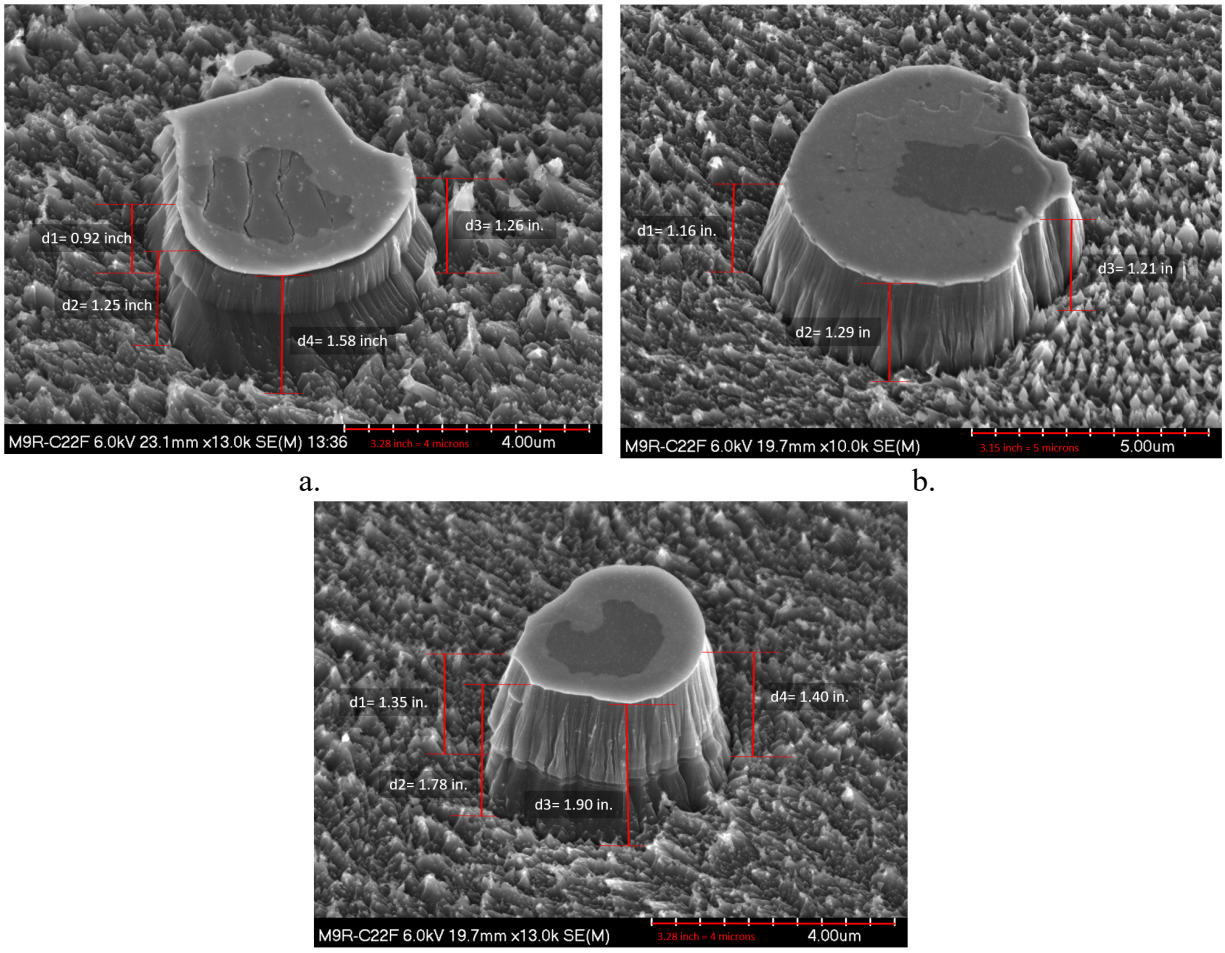

Figure 22. FESEM images of MISSE-9 ram HOPG flight sample (M9R-C22 F) at protected buttes taken at 45° tilt angles: a). Butte P28, b). Butte P35, and c). Butte P39.

Table 4. Recession Depth Based Erosion Data for HOPG (M9R-C22 F).

Measurement #	d (inch)	Sin 45	D on Image (inch)	Image conversion	Depth (microns)	Depth (cm)	AO F	Recession based E_y (cm^3/atom)	Average E_y (cm^3/atom)
P28 d1	0.92	0.7071	1.30	1.220	1.59	0.000159	3.44E+20	4.62E-25	
P28 d2	1.25	0.7071	1.77	1.220	2.16	0.000216	3.44E+20	6.27E-25	**6.29E-25**
P28 d3	1.26	0.7071	1.78	1.220	2.17	0.000217	3.44E+20	6.32E-25	
P28 d4	1.58	0.7071	2.23	1.220	2.72	0.000272	3.44E+20	7.93E-25	
P35 d1	1.16	0.7071	1.64	1.587	2.60	0.000260	3.44E+20	7.58E-25	
P35 d2	1.29	0.7071	1.82	1.587	2.90	0.000290	3.44E+20	8.43E-25	**7.97E-25**
P35 d3	1.21	0.7071	1.71	1.587	2.72	0.000272	3.44E+20	7.91E-25	
P39 d1	1.35	0.7071	1.91	1.220	2.33	0.000233	3.44E+20	6.78E-25	
P39 d2	1.78	0.7071	2.52	1.220	3.07	0.000307	3.44E+20	8.93E-25	**8.07E-25**
P39 d3	1.9	0.7071	2.69	1.220	3.28	0.000328	3.44E+20	9.54E-25	
P39 d4	1.4	0.7071	1.98	1.220	2.41	0.000241	3.44E+20	7.03E-25	

While searching for protected buttes, several interesting micrometeoroid and orbital debris (MMOD) impact sites were found on the HOPG flight sample. An example is provided in Figure 23. HOPG is a highly ordered form of high-purity pyrolytic graphite, a graphite material with a high degree of preferred crystallographic orientation. The space exposed surface was the basal plane. Thus, the MMOD impacted the top "space exposed" graphite layer (i.e. a basal plane layer). The resulting impact did not produce a typical impact crater lip, but instead produced an "impact flower" where various basal plane layers are peeled back with underlying basal plane layers opened up. Also, interesting is that the outer "petals" appear to have shielded the underlying area from AO erosion, as shown in Figure 23b, thus, this impact likely occurred relatively early in the mission.

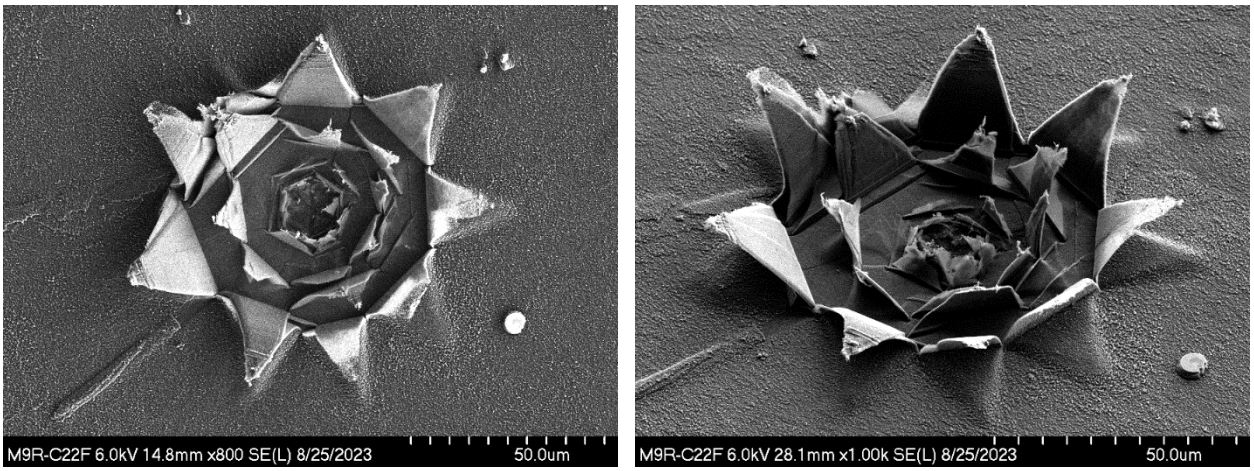

a. b.

Figure 23. FESEM images of an impact site in the MISSE-9 ram HOPG flight sample (M9R-C22 F): a). Image taken at 800X and 0° tilt, and b). Image taken at 1kX and 45° tilt.

Epoxy samples with various percentages of zinc oxide powder were flown as part of the PCE-1 in the ram direction (M9R-C11 F to M9R-C14 F).[21] Unfortunately, there appears to be errors in the pre-flight mass data and further analyses are needed for these samples. A sample of carbon nanotube (CNT) coated SiC was flown with a 0.5 mil Kapton H cover on it (M9R-S4 F) to minimize the amount of AO exposure.[21] The Kapton H cover did not completely erode away during the mission, and so the sample's dehydrated mass was not obtained post-flight. An alumina slide (M9R-C6R F) was flown for post-flight contamination analyses.[21,27] The pre-flight and post-flight mass of the alumina sample was not obtained. Thus, AO E_y values for these samples are not reported here. XPS analyses of the alumina sample indicated the presence of 6 at.% Si, as listed in Table 2. Detailed contamination results for the alumina sample are provided in Reference 27.

Additional post-flight analyses can be found for the following PCE-1 ram flight samples:

- Polyimide aerogel (M9R-C29 F and M9R-C30 F): References 41 and 42
- Z307 (black paint) coated Al (M9R-S2 B) and cyanate ester graphite fiber composite (RS3-M55J 6K) (M9R-C28 F): Reference 43
- Indium tin oxide (ITO) coated Kapton HN/Al (M9R-S5 F) and ITO coated silver-Teflon (M9R-S6 F): Reference 44

MISSE-9 PCE-1 Wake Samples

Figure 24 shows pre- and post-flight photographs of the MISSE-9 wake MS deck (W3 MSC 8) section containing the 52 PCE-1 wake samples. Figure 25 provides a sample map showing the specific location of the PCE-1 wake samples. An aluminum block with "RBF" ("remove before flight") written on it shown in the pre-flight photograph in Figure 24a (sample M9W-C10, circled in blue) was removed before flight. As can be seen by comparing the images in Figure 24, the 0.54 year LEO wake space exposure resulted in discoloration of the anodized aluminum deck and several PCE-1 wake samples. The anodized deck discoloration was not as discolored as the PCE-1 ram deck. The lower right wake sample (M9W-C8, polyvinylchloride (PVC)) became extremely discolored with the LEO wake exposure.

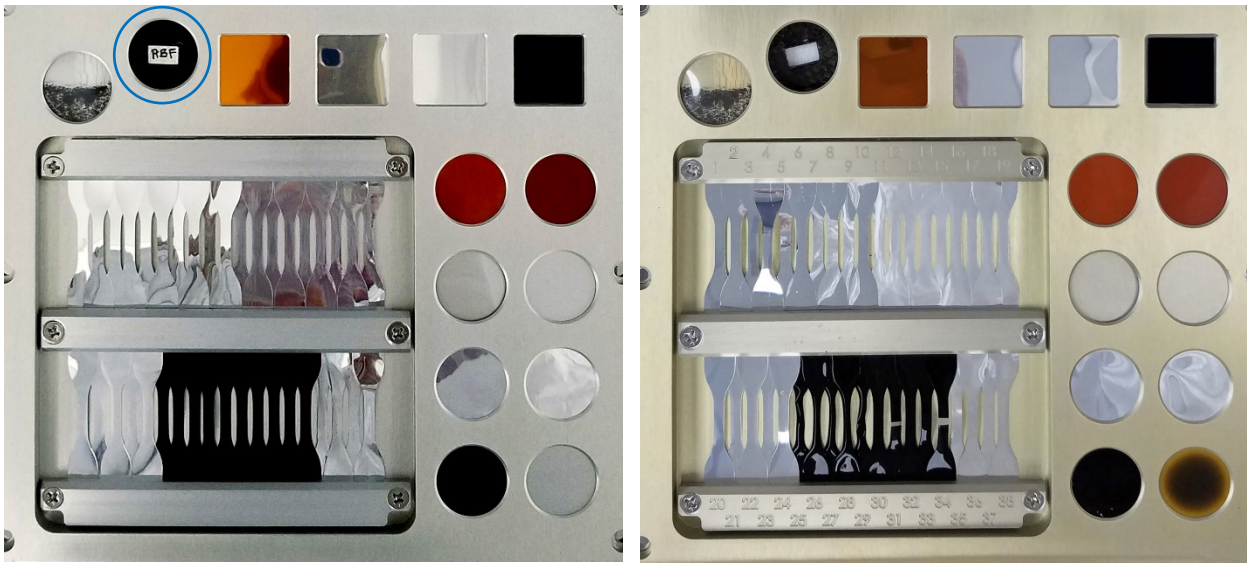

a. b.

Figure 24. Photographs of the MISSE-9 PCE-1 wake MS deck (W3 MSC 8): a). Pre-flight with the PCE-1 wake samples, and b). Post-flight showing discoloration of the deck and numerous samples.

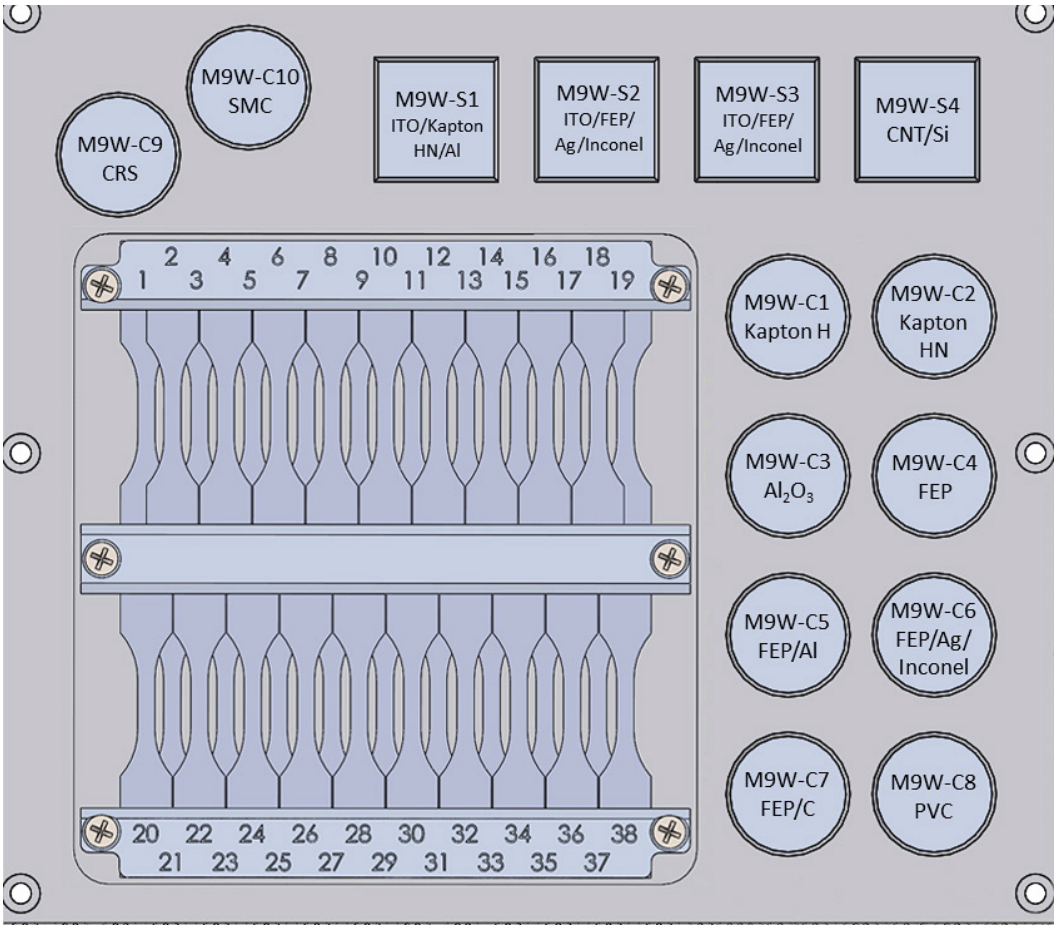

Figure 25. The MISSE-9 PCE-1 W3 wake sample map.

The MISSE-9 wake AO fluence was determined to be 4.46×10^{16} atoms/cm^2 based on dehydrated mass loss of the Kapton H AO fluence witness sample (M9W-C1 F).[23] Table 5 provides the MISSE-9 LEO AO E_y values for the PCE-1 wake samples. Included in Table 5 is the MISSE-9 wake sample ID, material, material abbreviation, sample layer thickness, dehydrated mass loss, exposed surface area, density, and the MISSE-9 wake AO fluence. Only one sample layer was flown and all samples were 1-inch (2.54 cm) in size (circular or square). It is noted that the AO fluence, and corresponding AO E_y values, are based on Kapton H mass loss of **0.001 mg**. This is within experimental error and the wake samples received essentially no AO exposure during the MISSE-9 wake mission. Any mass loss that occurred for the MISSE-9 wake flight samples, and hence the calculated "AO E_y" would be due to space radiation, thermal and/or vacuum exposure. The sample mass loss is more meaningful than the reported AO E_y value.

Table 5. Erosion Data for the MISSE-9 PCE-1 Wake Flight Samples.

MISSE-9 Wake ID	Material	Abbreviation	Thickness (mils)	Mass Loss (g)	Exposed Surface Area (cm_2)	Density (g/cm^3)[1] [5]	MISSE-9 Wake AO Fluence ($atoms/cm^2$) [23]	MISSE-9 Wake AO E_y ($cm^3/atom$)
M9W-C1 F	Polyimide (PMDA) (Kapton H)	Kapton H	5	*0.000001*[+]	3.488	1.4273	**4.46E+16**	***3.00E-24***
M9W-C2 F	Polyimide (PMDA) (Kapton HN)	Kapton HN	5	-0.000005[+]	3.484	1.4346	4.46E+16	*N/A*
M9W-C4 F	Fluorinated ethylene propylene (Teflon FEP)	FEP	5	0.000182	3.502	2.1443	4.46E+16	5.42E-22
M9W-C5 F	Aluminized-Teflon (FEP/Al)*	FEP/Al	5	0.000207	3.484	2.1443	4.46E+16	6.22E-22
M9W-C6 F	Silver-Teflon (FEP/Ag/Inconel)*	FEP/Ag/Inconel	5	0.000175	3.470	2.1443	4.46E+16	5.26E-22
M9W-C7 F	Carbon painted (India Ink) Teflon (FEP/C/FEP)*	FEP/C/FEP	15	0.000926	3.462	2.1443	4.46E+16	2.79E-21
M9W-C8 F	Polyvinyl chloride	PVC	5	0.000358	3.498	1.34^	4.46E+16	1.71E-21
M9W-C9 F	Cosmic ray shielding	CRS	39	0.000590	3.457	0.907**	4.46E+16	4.22E-21
M9W-C10 F	Shape memory composite	SMC	236	-0.000748	2.914	1.18**	4.46E+16	N/A
M9W-S1 F	Indium tin oxide coated Kapton HN/Al	ITO/Kapton HN/Al	2	0.000043	4.406	6.8[#]	4.46E+16	3.19E-23
M9W-S2 F	Indium tin oxide coated silver-Teflon	ITO/FEP/Ag/Inconel	5	*0.000003*[+]	4.387	6.8[#]	4.46E+16	*2.00E-24*
M9W-S3 F	Indium tin oxide coated silver-Teflon	ITO/FEP/Ag/Inconel	5	*0.000002*[+]	4.416	6.8[#]	4.46E+16	*1.74E-24*
M9W-S4 F	Vertically aligned carbon nanotube (CNT) coated SiC	CNT/SiC	130	-0.000587	4.422	2.000	4.46E+16	N/A

*Teflon FEP layer is space facing
^MISSE-7[18]
**Sample Collaborator[21]
[#]J Vac Sci Tech A 19:5(2043-7); 2001
[+]*Within balance error*

Samples of clear Teflon FEP, back-surface metallized FEP (FEP/Al and FEP/Ag/Inconel), and back-surface carbon painted-Teflon FEP (FEP/C/FEP) were flown in the wake direction of MISSE-9. As can be seen in Table 5, the mass loss and thus corresponding AO E_y for the MISSE-9 wake FEP (M9W-C4 F), FEP/Al (M9W-C5 F) and FEP/Ag/Inconel (M9W-C6 F) samples were all similar at 5.42×10^{-22}, 6.22×10^{-22} and 5.26×10^{-22} cm^3/atom, respectively. However, the carbon back-surface painted Teflon FEP sample (M9W-C7 F) had ≈5X higher mass loss and AO E_y of 2.79×10^{-21} cm^3/atom. Therefore, the MISSE-9 wake samples, like the MISSE-9 ram samples, showed increased erosion of Teflon FEP due to the increased on-orbit heating. It should be noted that erosion of Teflon FEP in the wake direction (and other polymers) must be due to other environmental factors such as radiation and thermal exposure because there was essentially no AO. Interestingly, it was observed that the clear and back-surface metallized Teflon FEP flight samples had a different UV fluorescence in the space exposure area as compared to the control sample. An example for the clear FEP (M9W-C4 F) sample is provided in Figure 26. As can be seen in Figure 26a, the flight and control samples look similar under visible light. The flight sample does not appear eroded or discolored. However, as can be seen in Figure 26b, the flight sample (sample on the left) glows in the space exposed area indicating some type of chemical change has occurred likely due to the solar or charged particle radiation exposure. The MISSE-9 clear and back-surface metallized Teflon FEP ram samples exhibited a similar fluorescence as the wake samples.

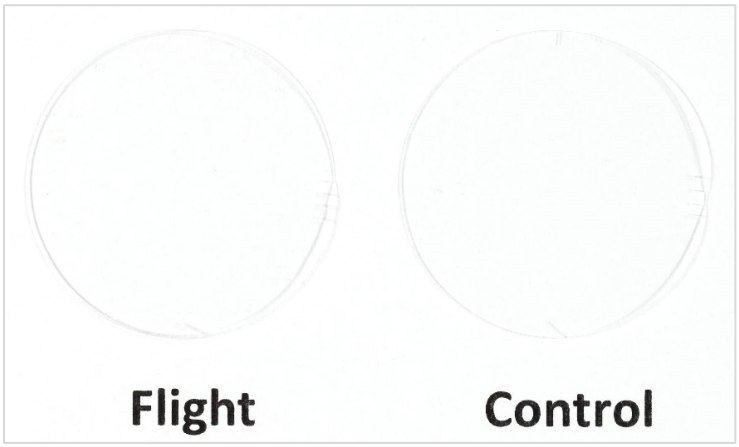

a.

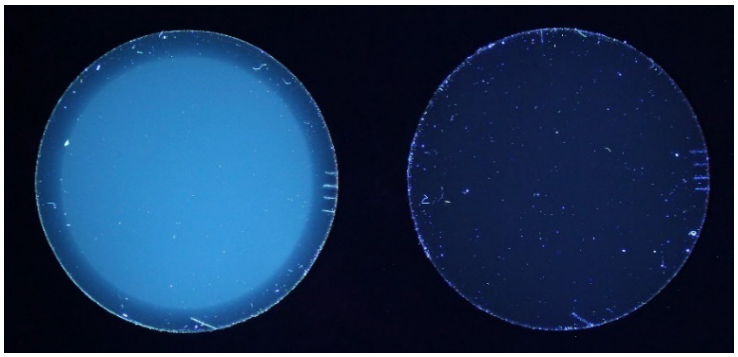

b.

Figure 26. Post-flight photographs of clear Teflon flight (M9W-C4 F) and control (M9W-C4 B) samples: a). Visible light image, and b). Image taken with 365 nm UV light (flight on left and control on right).

As mentioned above, the PVC flight sample (M9W-C8 F) became extremely discolored with the LEO wake exposure. Post-flight photographs of the PVC flight and control samples are provided in Figure 27. Figure 27a and 27b are visible light images and Figure 27c is a UV light image. In addition to getting very dark, the sample also became embrittled and had surface cracks, as seen in Figure 27b.

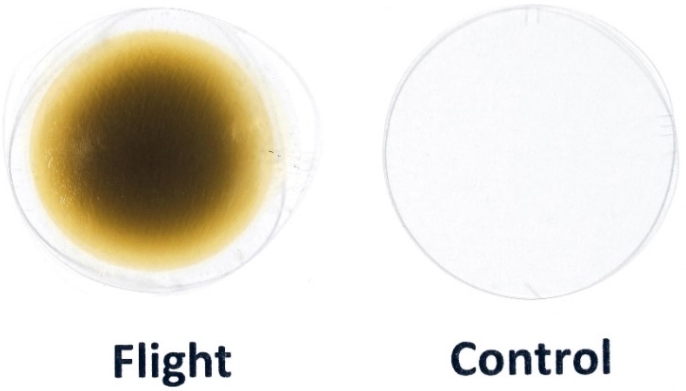

a.

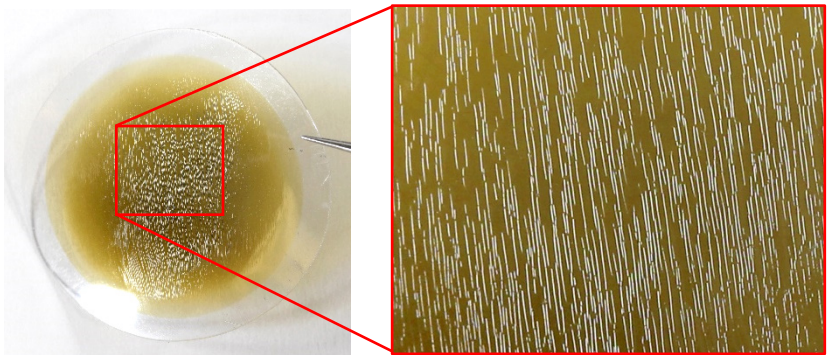

b.

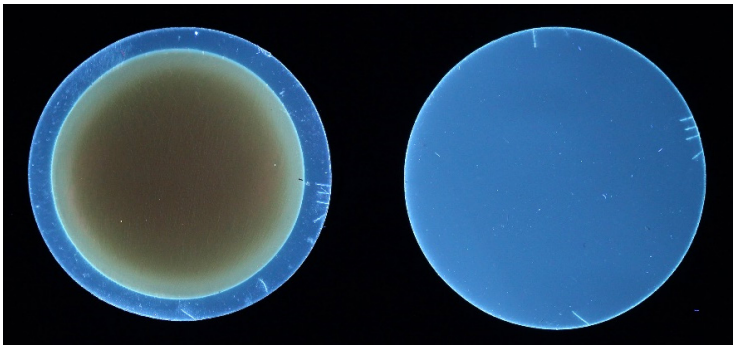

c.

Figure 27. Post-flight photographs of PVC flight (M9W-C8 F) and control (M9W-C8 B) samples: a). Visible light image, b). Close-up of the flight sample showing surface cracks, and c). Image taken with 365 nm UV light (flight on left and control on right).

Numerous samples had mass loss or gain that was within experimental error for the Sartorius ME5 Microbalance (±0.005 mg sensitivity). In addition to the Kapton H AO fluence witness sample (M9W-C1), these samples include Kapton HN (M9W-C2 F) and two indium tin oxide (ITO) coated samples (M9W-S2 F and M9W-S3 F). The shape memory polymer sample (M9W-C10 F) gained mass quickly during mass measurement rehydration and resulted in mass gain (0.748 mg). The vertically aligned carbon nanotube (CNT) coated SiC (M9W-S4 F) also had mass gain. No AO E_y is reported for the samples with mass gain. And, an alumina slide (M9W-C3 F) was flown for post-flight contamination analyses.[21,27] The pre-flight and post-flight mass of the alumina sample was not obtained. Thus, AO E_y for the alumina sample is also not provided. But, XPS analyses of the MISSE-9 wake alumina sample indicated the presence of 1.7 at.% Si, as listed in Table 2, which is lower than for the ram alumina sample. Detailed contamination results for the alumina sample are provided in Reference 27.

Additional post-flight analyses can be found for the following PCE-1 wake flight samples:

- Cosmic ray shielding (CRS, M9W-C9 F): References 45 and 46
- Shape memory composite (SMC, M9W-C10 F): References 45, 47 and 48
- ITO coated Kapton HN/Al (M9W-S1 F) and ITO coated silver-Teflon (M9W-S2 F and M9W-S3 F): Reference 44

MISSE-9 PCE-1 Zenith Samples

Figure 28 shows pre- and post-flight photographs of the MISSE-9 zenith MS deck (Z3 MSC 5) section containing the 47 PCE-1 zenith samples. Figure 29 provides a sample map showing the specific location of the PCE-1 zenith samples. An aluminum block with “RBF” (“remove before flight”) written on it shown in the pre-flight photograph in Figure 28a (sample M9Z-C17, circled in blue) was removed before flight. As can be seen by comparing the images in Figure 28, the 0.54-year LEO zenith space exposure resulted in discoloration of the anodized aluminum deck and numerous PCE-1 zenith samples.

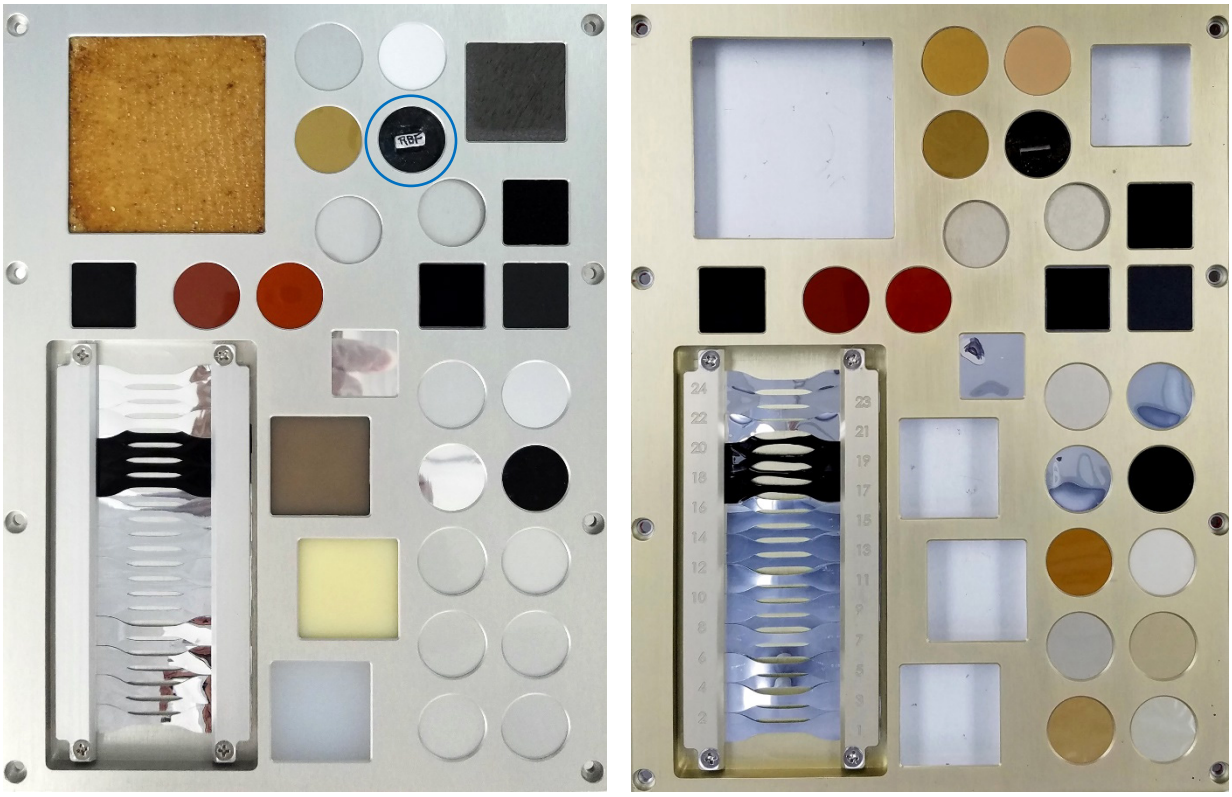

a. b.

Figure 28. Photographs of the MISSE-9 PCE-1 zenith MS deck (Z3 MSC 5): a). Pre-flight with the PCE-1 zenith samples (the five larger square samples are not part of the PCE-1), and b). Post-flight showing discoloration of the deck and numerous samples.

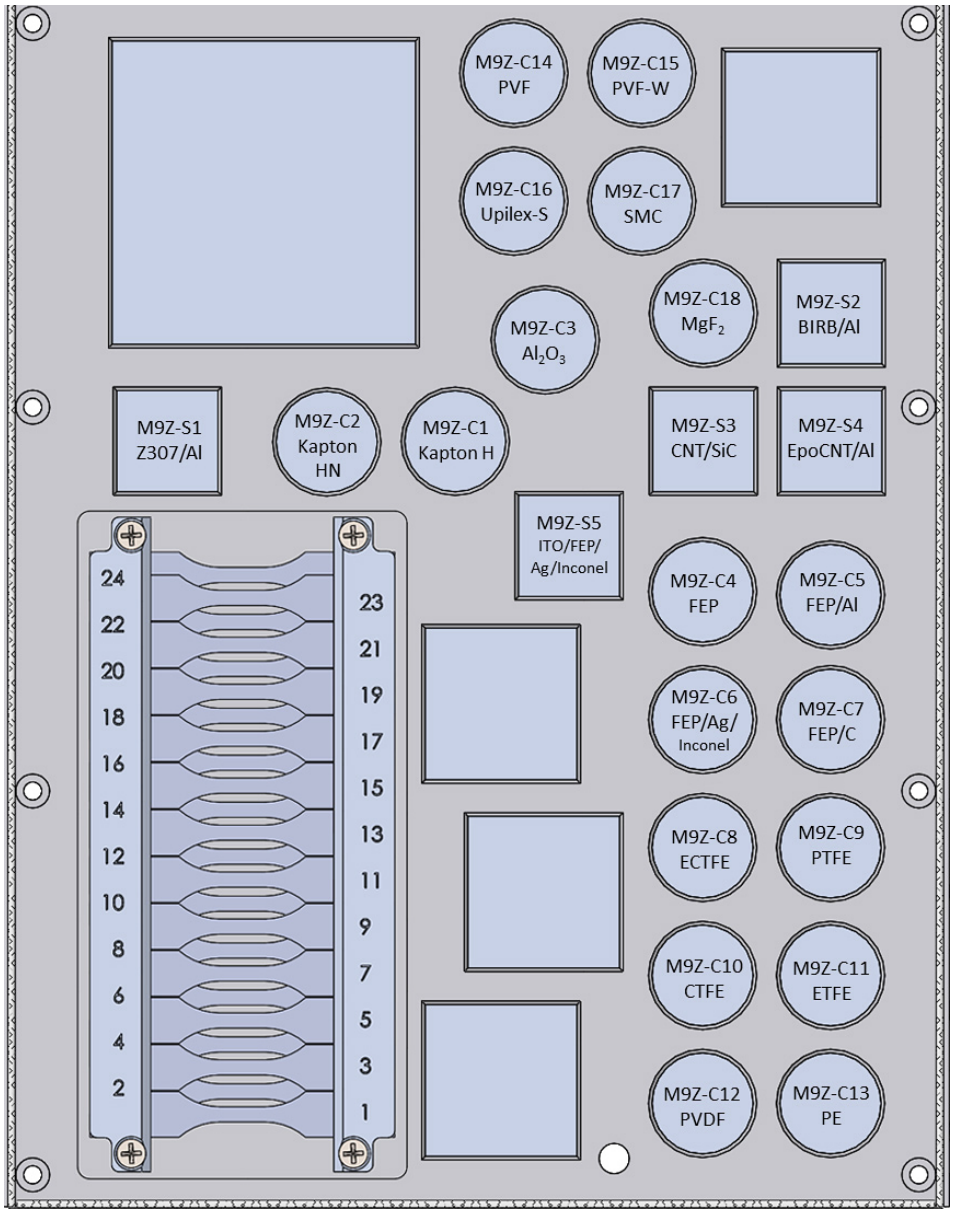

Figure 29. The MISSE-9 PCE-1 Z3 zenith sample map.

The MISSE-9 zenith AO fluence was determined to be 3.19×10^{18} atoms/cm^2 based on dehydrated mass loss of the Kapton H AO fluence witness sample (M9Z-C1 F).[23] Table 6 provides the MISSE-9 LEO AO E_y values for the PEC-1 zenith samples. Included in Table 6 is the MISSE-9 zenith sample ID, material, material abbreviation, sample layer thickness, dehydrated mass loss, exposed surface area, density, and the MISSE-9 zenith AO fluence. Only one sample layer was flown and all samples were 1-inch (2.54 cm) in size (circular or square). The AO fluence, and corresponding AO E_y values, are based on Kapton H mass loss of only 0.049 mg. Like the MISSE-9 wake samples, with the very low AO fluence for the zenith samples, mass loss and other analysis techniques that are more sensitive to smaller levels of change (optical, surface chemistry, etc.) would be better indicators of durability than the reported AO E_y value.

Table 6. Erosion Data for the MISSE-9 PCE-1 Zenith Flight Samples.

MISSE-9 Zenith ID	Material	Abbreviation	Thickness (mils)	Mass Loss (g)	Exposed Surface Area (cm^2)	Density (g/cm^3)[15]	MISSE-9 Zenith AO Fluence ($atoms/cm^2$)[23]	MISSE 9 Zenith AO E_y (cm^3/atom)
M9Z-C1 F	Polyimide (PMDA) (Kapton H)	Kapton H	5	0.000049	3.612	1.4273	**3.19E+18**	***3.00E-24***
M9Z-C2 F	Polyimide (PMDA) (Kapton HN)	Kapton HN	5	0.000063	3.650	1.4346	3.19E+18	3.79E-24
M9Z-C4 F	Fluorinated ethylene propylene (Teflon FEP)	FEP	5	0.000313	3.551	2.1443	3.19E+18	1.29E-23
M9Z-C5 F	Aluminized-Teflon (FEP/Al)*	FEP/Al	5	0.000350	3.543	2.1443	3.19E+18	1.44E-23
M9Z-C6 F	Silver-Teflon (FEP/Ag/Inconel)*	FEP/Ag/Inconel	5	0.000326	3.575	2.1443	3.19E+18	1.33E-23
M9Z-C7 F	Carbon painted (India Ink) Teflon (FEP/C/FEP)*	FEP/C/FEP	15	0.001309	3.540	2.1443	3.19E+18	5.41E-23
M9Z-C8 F	Ethylene-chlorotrifluoroethylene (Halar)	ECTFE	3	0.000393	3.548	1.6761	3.19E+18	2.07E-23
M9Z-C9 F	Polytetrafluoroethylene (Teflon PTFE)	PTFE	5	0.000218	3.534	2.1503	3.19E+18	8.98E-24
M9Z-C10 F	Chlorotrifluoroethylene (Kel-F)	CTFE	5	0.000400	3.590	2.1327	3.19E+18	1.64E-23
M9Z-C11 F	Ethylene-tetrafluoroethylene (Tefzel ZM)	ETFE	3	0.000079	3.525	1.7397	3.19E+18	4.04E-24
M9Z-C12 F	Polyvinylidene fluoride (Kynar)	PVDF	3	0.000133	3.549	1.7623	3.19E+18	6.68E-24
M9Z-C13 F	Polyethylene	PE	2	0.000111	3.558	0.918	3.19E+18	1.06E-23
M9Z-C14 F	Polyvinyl fluoride (clear Tedlar)	PVF	1	0.000105	3.673	1.3792	3.19E+18	6.48E-24
M9Z-C15 F	Crystalline polyvinyl fluoride w/white pigment (white Tedlar)	PVF-W	2	0.000090	3.649	1.6241	3.19E+18	4.74E-24
M9Z-C16 F	Polyimide (BPDA) (Upilex-S)	Upilex-S	1	0.000011	3.669	1.3866	3.19E+18	6.57E-25
M9Z-C17 F	Shape memory composite	SMC	236	0.000459	3.455	1.18**	3.19E+18	3.53E-23
M9Z-C18 F	Magnesium Fluoride	MgF2	108	0.000013	3.630	3.15^^	3.19E+18	3.66E-25
M9Z-S1 F	Z307 (black paint)/Al	Z307/Al	35	0.000235	4.499	0.205**	3.19E+18	7.98E-23
M9Z-S2 F	Ball Infrared Black (BIRB) paint/Al	BIRB/Al	100	0.000386	4.453	0.423**	3.19E+18	6.42E-23
M9Z-S3 F	Vertically aligned carbon nanotube (CNT) coated SiC	CNT/SiC	130	-0.000013	4.520	2.0	3.19E+18	N/A
M9Z-S4 F	EpoCNT (carbon nanotube in epoxy matrix)/Al	EpoCNT/Al	64	0.000229	4.441	1.12**	3.19E+18	1.44E-23
M9Z-S5 F	Indium tin oxide coated silver-Teflon	ITO/FEP/Ag/Inconel	5	*0.000001*[+]	4.501	6.8[#]	3.19E+18	*6.83E-27*

*Teflon FEP layer is space facing
**Sample Collaborator[21]
^^https://www.matweb.com/index.aspx
[#]J Vac Sci Tech A 19:5(2043-7); 2001
[+]*Within balance error*

Samples of clear Teflon FEP, back-surface metallized FEP, and back-surface carbon painted-FEP were flown in the zenith direction of MISSE-9. As can be seen in Table 6, the mass loss and thus corresponding AO E_y for the MISSE-9 zenith FEP (M9Z-C4 F), FEP/Al (M9Z-C5 F) and FEP/Ag/Inconel (M9Z-C6 F) samples were all similar at 1.29×10^{-23}, 1.44×10^{-23} and 1.33×10^{-23} cm^3/atom, respectively. But, the carbon back-surface painted Teflon FEP sample (M9Z-C7 F) had ≈4X higher mass loss and AO E_y of 5.41×10^{-23} cm^3/atom. So for the MISSE-9 zenith samples, like the MISSE-9 ram and wake samples, the increased on-orbit heating clearly impacted the erosion of the Teflon FEP. The zenith clear and back-surface metallized Teflon FEP samples exhibited UV fluorescence in the space exposure area, similar to the ram and wake samples.

As mentioned, numerous samples darkened during the MISSE-9 zenith exposure. Four polymer flight samples are provided as examples of varying degrees of darkening in Figure 30.

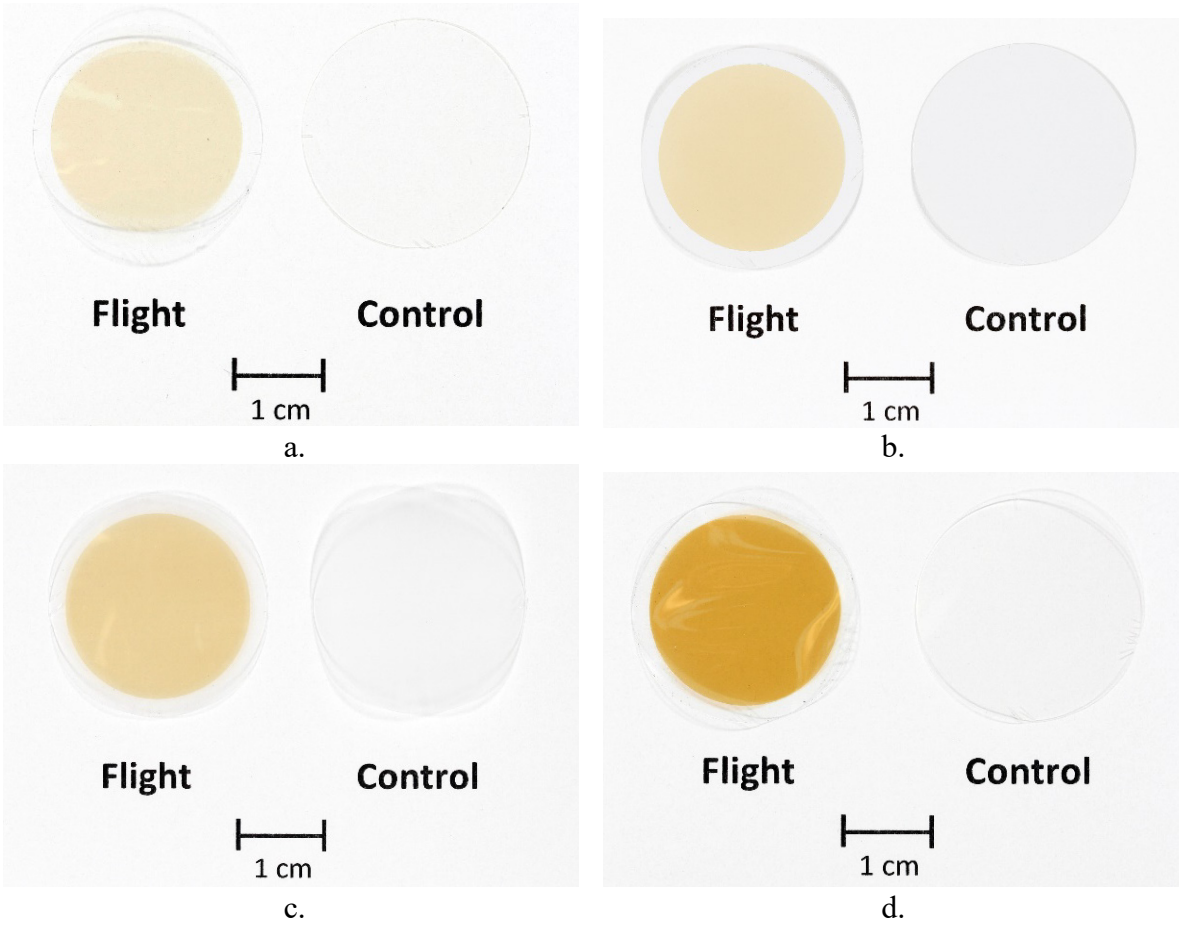

Figure 30. Post-flight photographs of MISSE-9 zenith flight and control samples: a). Ethylene-tetrafluoroethylene (ETFE, M9Z-C11 F and B), b). Crystalline polyvinyl fluoride with white pigment (PVF-W, M9Z-C15 F and B), c). Polyvinylidene fluoride (PVDF, M9Z-C12 F and B), and d). Ethylene-chlorotrifluoroethylene (ECTFE, M9Z-C8 F and B).

The ITO coated silver-Teflon sample (M9Z-S5 F) had mass loss (0.001 mg) that was within experimental error for the Sartorius ME5 Microbalance (±0.005 mg sensitivity). The vertically aligned carbon nanotube (CNT) coated SiC (M9Z-S3 F) had mass gain, similar to the wake sample. No AO E_y is reported for the CNT coated SiC sample. And, an alumina slide (M9Z-C3 F) was flown for post-flight contamination analyses.[21,27] The pre-flight and post-flight mass of the alumina sample was not obtained. Thus, AO E_y for the alumina sample is also not provided. But, XPS analyses of the MISSE-9 zenith alumina sample indicated the presence of 1.5 at.% Si, as listed in Table 2, which is lower than for the ram alumina sample and similar to the MISSE-9 wake sample. Detailed contamination results for the alumina sample are provided in Reference 27.

Additional post-flight analyses can be found for the following PCE-1 zenith flight samples:

- SMC (M9Z-C17 F): References 45, 47 and 48
- Z307 coated Al (M9Z-S1 F): Reference 43
- ITO coated silver-Teflon (M9Z-S5 F): Reference 44

MISSE-10 Polymers and Composites Experiment-2 (PCE-2)

MISSE-10 PCE-2 Ram Samples

Figure 30 shows pre- and post-flight photographs of the MISSE-10 ram MS deck (R1 MSC 11) section containing the 21 PCE-2 ram samples. Figure 31 provides a sample map showing the specific location of the PCE-2 ram samples. As can be seen by comparing the images in Figure 30, the 1.17 year LEO ram space exposure resulted in discoloration of several PCE-2 samples. The anodized aluminum deck was slightly discolored, but not as much as the MISSE-9 ram deck.

The MISSE-10 ram AO fluence was determined to be 3.93×10^{20} atoms/cm^2 based on dehydrated mass loss of the ram Kapton H AO fluence witness sample (M10R-C1 F).[23] Table 7 provides the MISSE-10 LEO AO E_y values for the PEC-2 ram samples. Included in Table 7 is the MISSE-10 ram sample ID, material, material abbreviation, sample layer thickness, number of sample layers flown, dehydrated mass loss, exposed surface area, density, and the MISSE-10 ram AO fluence. All samples for AO E_y were 1-inch (2.54 cm) circular in size. A rectangular AO Photo Monitor was also flown (M10R-R1) as part of the sample set.[21,23] Similar to the MISSE-9 ram samples, the MISSE-10 ram AO fluence was relatively low and only the top layer (Part A) of the multilayered ram samples was eroded. Therefore, only Part A was weighed post-flight and compared with the Part A pre-flight mass for determining sample mass loss.

As mentioned, a rectangular multi-layered Photographic AO Fluence Monitor sample (M10R-R1) was flown along with the MISSE-10 ram samples. This sample can be seen in the photographs in Figure 30. Post-flight visible erosion of the individual layers indicated an AO fluence of between 3.2 to 6.39×10^{20} atoms/cm^2, which is consistent with the AO fluence determined based on dehydrated mass loss of the 1-inch diameter Kapton H sample (M10R-C1 F).[23]

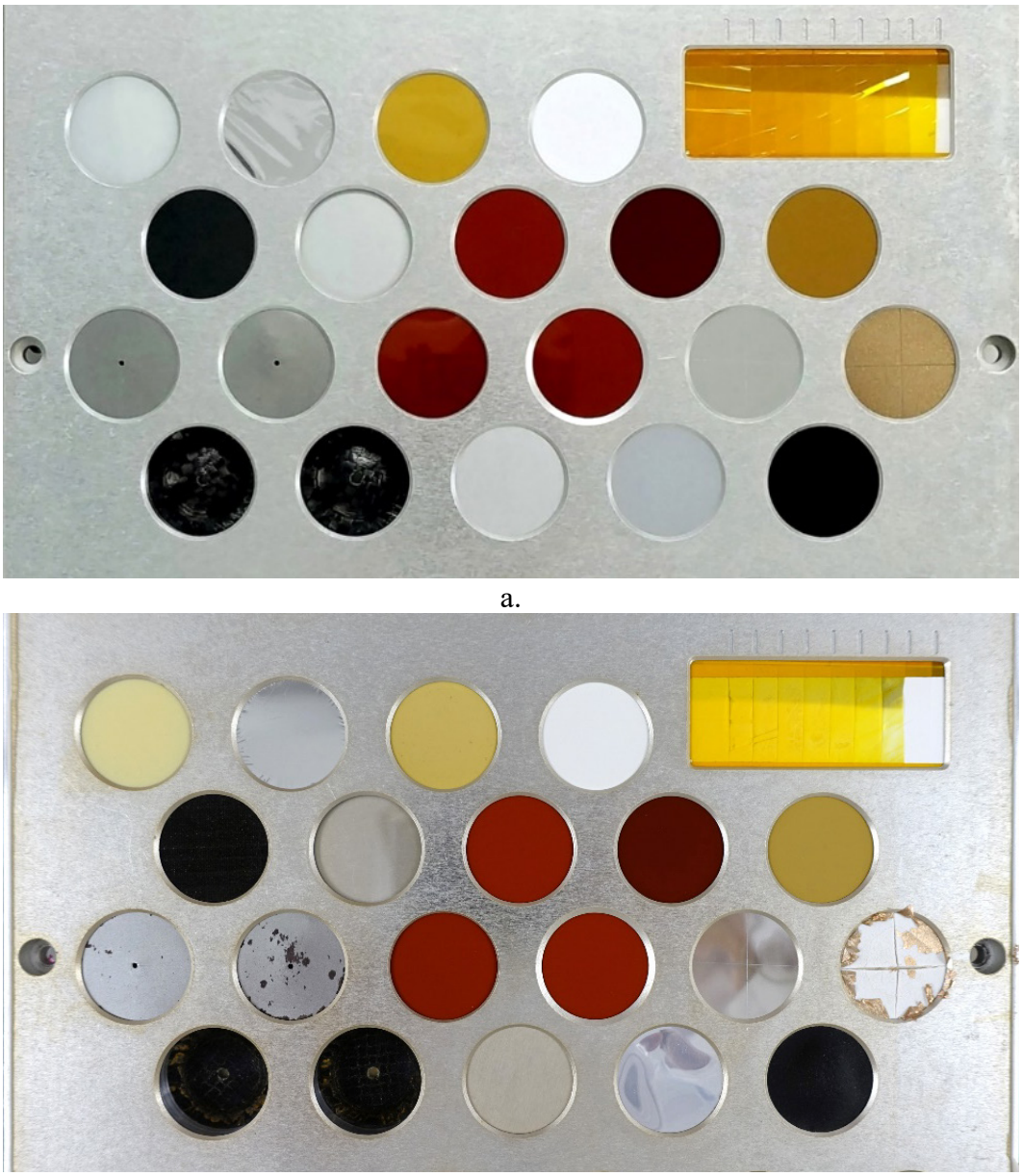

a.

b.

Figure 30. Photographs of the MISSE-10 PCE-2 ram MS deck (R1 MSC 11): a). Pre-flight with the PCE-2 ram samples, and b) Post-flight showing discoloration of numerous samples.

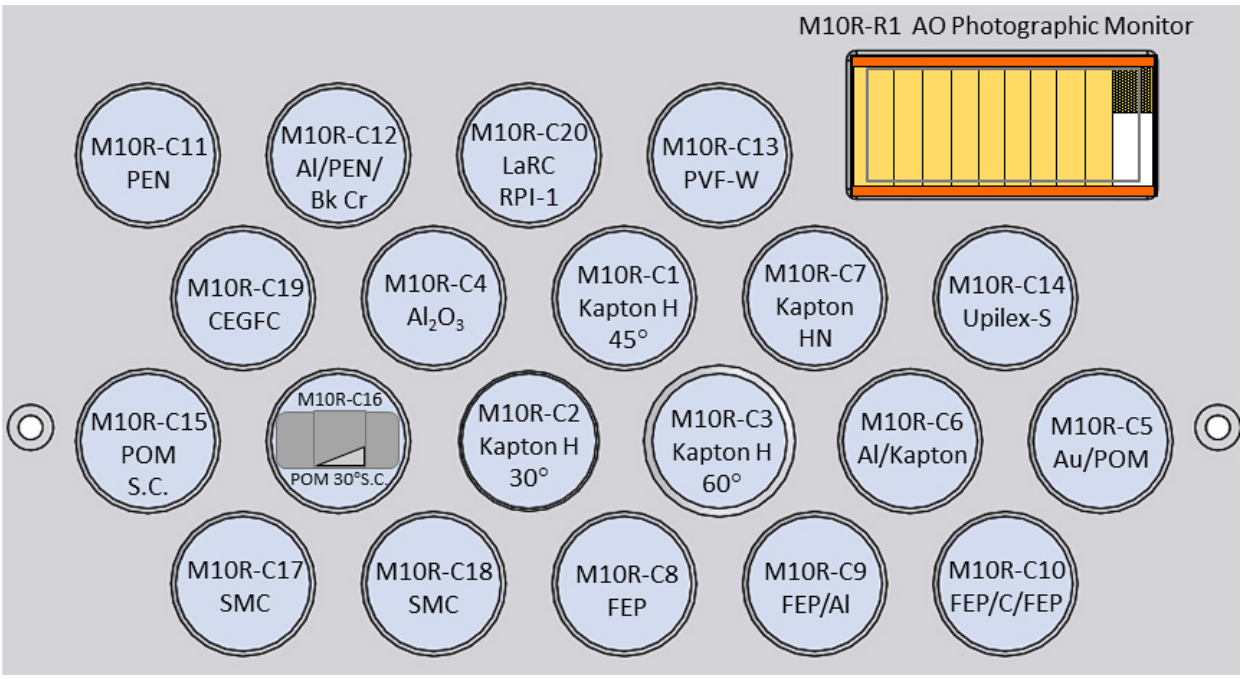

Figure 31. The MISSE-10 PCE-2 R1 ram sample map.

Three Kapton H samples were flown as part of the PCE-2 MISSE-10 ram (and MISSE-10 nadir) samples to determine the effect of the sample holder chamfer angle on the AO E_y. The MISSE-10 ram samples included Kapton H flown in MSC decks with 30° (M10R-C2 F), 45° (M10R-C1 F), and 60° (M10R-C3 F) chamber angles (θ). The standard MISSE sample holder (see Figure 32) has a 45° chamfer and a 0.030 inch thick lip. The AO E_y of the Kapton H in the standard 45° chamfer holder was assumed to be 3.00×10^{-24} cm^3/atom, as this sample was used as the Kapton H AO fluence witness sample.[23] The AO E_y of the Kapton H samples in both the 30° and 60° chamfer holders were 2.99×10^{-24} cm^3/atom. Thus, there was not a significant difference in the AO E_y for the varying chamfer angles for the MISSE-10 ram AO fluence of 3.93×10^{20} atoms/cm^2. Perhaps this is due to the relatively low area affected by the chamfer as compared to the exposed area.

Table 7. Erosion Data for the MISSE-10 PCE-2 Ram Flight Samples.

MISSE-10 Ram ID	Material	Abbreviation	Thickness (mils) (# Layers Flown)	Mass Loss (g)	Exposed Surface Area (cm^2)	Density (g/cm^3)[15]	MISSE-10 Ram AO Fluence ($atoms/cm^2$)[23]	MISSE 10 AO E_y ($cm^3/atom$)
M10R-C1 F	Polyimide (PMDA) (Kapton H) 45° chamfer (standard)	Kapton H	5 (2)	0.005964	3.540	1.4273	**3.93E+20**	***3.00E-24***
M10R-C2 F	Polyimide (PMDA) (Kapton H) 30° chamfer edge	Kapton H	5 (2)	0.005932	3.528	1.4273	3.93E+20	2.99E-24
M10R-C3 F	Polyimide (PMDA) (Kapton H) 60° chamfer edge	Kapton H	5 (2)	0.005940	3.537	1.4273	3.93E+20	2.99E-24
M10R-C4 F	Alumina slide	Al_2O_3	63 (1)	0.000021	3.534	3.987^	3.93E+20	3.85E-27
M10R-C7 F	Polyimide (PMDA) (Kapton HN)	Kapton HN	5 (2)	0.005894	3.543	1.4346	3.93E+20	2.95E-24
M10R-C8 F	Fluorinated ethylene propylene (Teflon FEP)	FEP	5 (1)	0.001909	3.534	2.1443	3.93E+20	6.40E-25
M10R-C9 F	Aluminized-Teflon (FEP/Al)*	FEP/Al	5 (1)	0.001945	3.537	2.1443	3.93E+20	6.52E-25
M10R-C10 F	Teflon FEP clad carbon paint (India Ink) (FEP/C/FEP)*	FEP/C/FEP	14 (1)	0.004471	3.542	2.1443	3.93E+20	1.50E-24
M10R-C11 F	Polyethylene naphthalate (PEN)	PEN	2.95 (2)	0.006229	3.526	1.36^^	3.93E+20	3.30E-24
M10R-C12 F	Metallized Polyethylene naphthalate (PEN) film (Al (100 nm)/PEN (2 micron)/black Cr (15 nm)) with Kapton ring	Al/PEN/Bk Cr (M-PEN)	0.083 (2)	*-0.000003*[+]	3.532	1.36^^	3.93E+20	*N/A*
M10R-C13 F	Crystalline polyvinyl fluoride w/white pigment (white Tedlar)	PVF-W	2 (1)	0.001454	3.536	1.6241	3.93E+20	6.44E-25
M10R-C14 F	Polyimide (BPDA) (Upilex-S)	Upilex-S	1 (2)	0.004653	3.537	1.3866	3.93E+20	2.41E-24
M10R-C17 F	Shape memory composite	SMC	275 (1)	0.005534	3.483	1.18**	3.93E+20	3.42E-24
M10R-C18 F	Shape memory composite	SMC	275 (1)	0.005544	3.482	1.18**	3.93E+20	3.43E-24
M10R-C19 F	Cyanate ester graphite fiber composite (CE3-M55J)	CEGFC	72.5 (1)	0.003417	3.531	1.623**	3.93E+20	1.52E-24
M10R-C20 F	LaRC SI (soluble imide) based polyimide/inorganic nanoparticle composite (radiation resistant polyimide (RPI))	LaRC RPI-2	1 (3)	0.002084	3.537	1.52**	3.93E+20	9.85E-25

*Teflon FEP is space facing
^https://www.matweb.com/index.aspx
^^https://usa.dupontteijinfilms.com/wp-content/uploads/2017/01/Q51-Datasheet.pdf
**Sample Collaborator[21]
[+]*Within balance error*

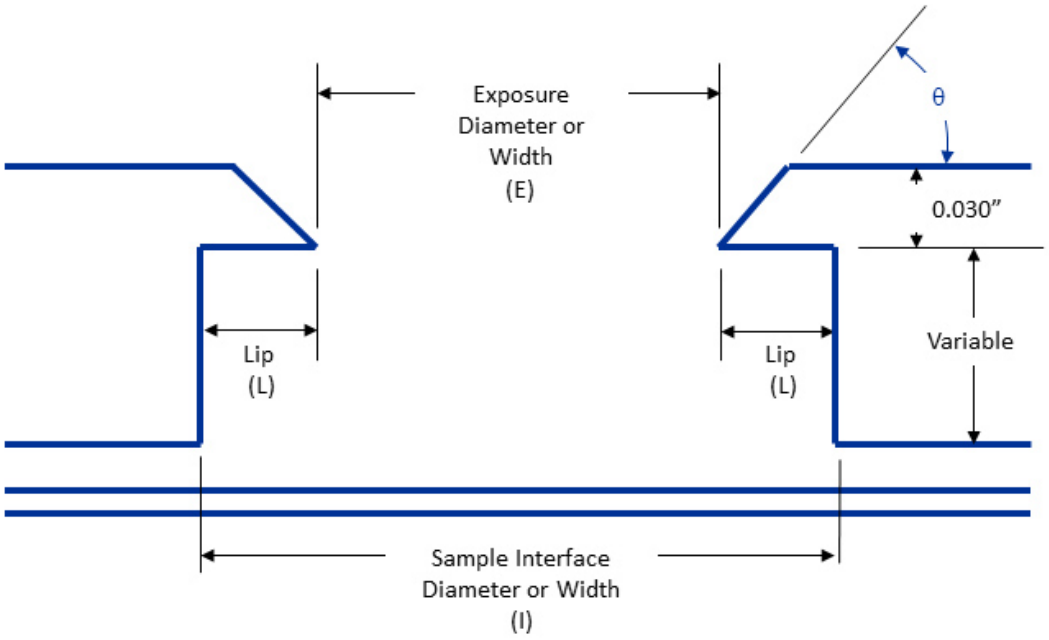

Figure 32. Standard MISSE sample holder.

Samples of clear Teflon FEP, back-surface metallized FEP, and back-surface carbon painted-FEP were flown in the ram direction of MISSE-10. As can be seen in Table 7, the mass loss and thus corresponding AO E_y for the MISSE-10 ram FEP (M10R-C8 F) and FEP/Al (M10R-C9 F) samples were similar at 6.40×10^{-25} and 6.52×10^{-25} cm^3/atom, respectively. But, the carbon back-surface painted Teflon FEP sample (M10R-C10 F) had ≈2X higher mass loss and AO E_y of 1.50×10^{-24} cm^3/atom. So for the MISSE-10 ram samples, like the MISSE-9 samples, the increased on-orbit heating impacted the erosion of the Teflon FEP. The clear and back-surface metallized Teflon FEP samples exhibited UV fluorescence in the space exposure area, similar to MISSE-9 samples.

As previously mentioned, alumina samples were flown in each MISSE-10 flight direction for post-flight contamination analyses. The dehydrated mass of the MISSE-10 alumina samples was measured. Although alumina is not expected to erode with AO exposure, the MISSE-10 ram sample (M10R-C4 F) had a very small mass loss of 0.021 mg, perhaps due to some hydrocarbon loss. XPS analyses of the sample indicated the presence of 8.4 at.% Si, as listed in Table 2. This is higher than for the MISSE-9 ram sample (6.0 at.%), and fairly significant. Detailed contamination results for M10R-C4 F are provided in Reference 27.

A Kapton HN sample (M10R-C7 F) was flown as part of the MISSE-10 PCE-2 ram samples. The AO E_y for M10R-C7 F was 2.95×10^{-24} cm^3/atom, which is slightly lower than for the assumed LEO AO E_y for Kapton H. Samples of polyethylene naphthalate (PEN, M10R-C11 F) and metallized PEN (M-PEN, M10R-C12 F) were flown. The uncoated PEN had a mass loss of 6.229 mg and a corresponding AO E_y of 3.30×10^{-24} cm^3/atom. While the metallized coating protected the M-PEN sample, which had mass loss within experimental error (-0.003 mg), and thus no AO E_y is reported. The AO E_y for white Tedlar (PVF-W, M10R-C13 F, AO E_y of 6.22×10^{-25} cm^3/atom), Upilex-S (M10R-C14F, AO E_y of 2.41×10^{-24} cm^3/atom) and cyanate ester graphite fiber composite (CEGFC, M10R-C19 F, AO E_y of 1.52×10^{-24} cm^3/atom) are also provided in Table 7.

Aluminum coated Kapton H (M10R-C6 F) and Au coated POM (M10R-C5 B) samples with scratches in the protective coatings were flown to evaluate the AO undercutting profile at the defect site. The Au coated POM sample was highly degraded, as can be seen in the post-flight deck photograph in Figure 30b, likely due to the high AO E_y for POM. And, two AO Scattering Chambers with salt-sprayed POM lids were flown to analyze scattered AO characteristics inside the AO Scattering Chamber: one with a normal (90°) Al base ((M10R-C15 F) and one that had a 30° angled Al base (M10R-C16 F). The AO E_y for these samples was not determined.

Additional post-flight analyses can be found for the following PCE-2 ram flight samples:

- Cyanate ester graphite fiber composite (M10R-C19 F): Reference 43
- SMC (M10R-C17 F and M10R-C18 F): References 45 and 47
- PEN (M10R-C11 F) and M-PEN (M10R-C12 F): Reference 49

MISSE-10 PCE-2 Zenith Samples

Figure 33 shows pre- and post-flight photographs of the MISSE-10 zenith MS deck (Z2 MSC 10) section containing the 10 PCE-2 zenith samples. Figure 34 provides a sample map showing the specific location of the PCE-2 ram samples. As can be seen by comparing the images in Figure 33, the 0.69 year LEO zenith space exposure resulted in discoloration of the anodized aluminum deck and the epoxy base of M10Z-C4.

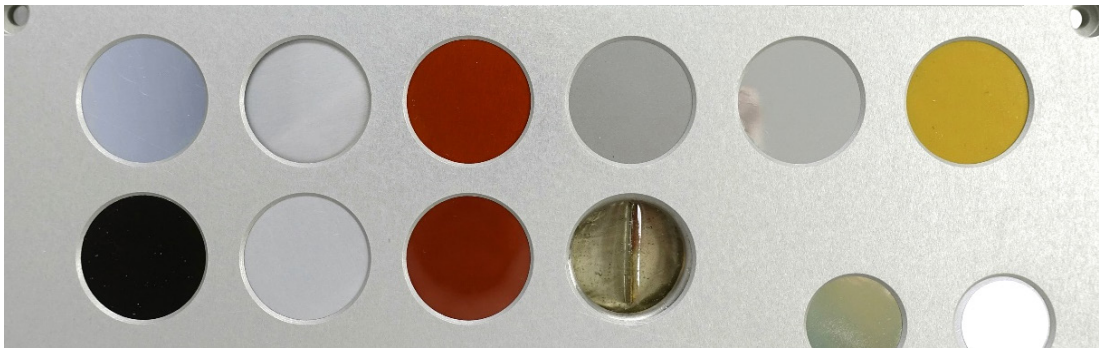

a.

b.

Figure 33. Photographs of the MISSE-10 PCE-2 zenith MS deck (Z2 MSC 10): a). Pre-flight with the PCE-2 zenith samples, and b). Post-flight showing discoloration of the MSC deck and the M10Z-C4 epoxy base.

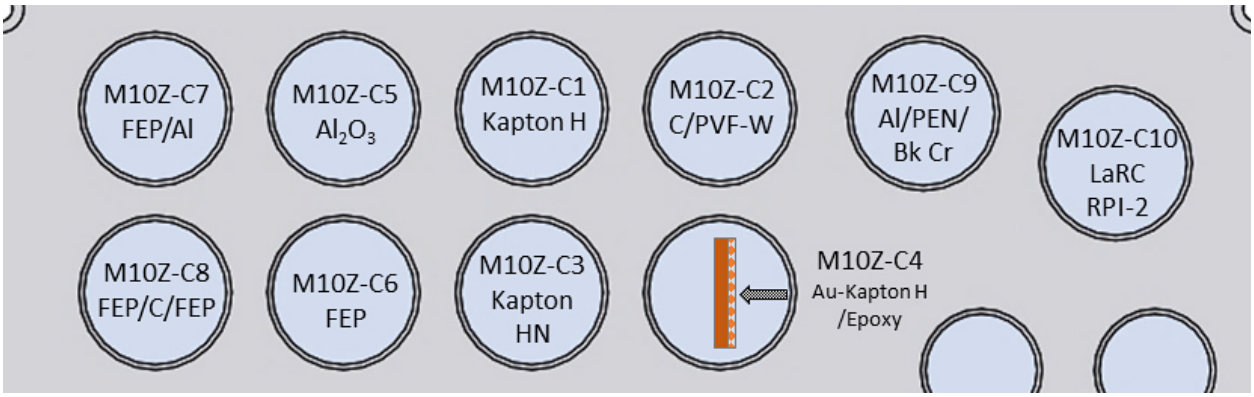

Figure 34. The MISSE-10 PCE-2 Z2 zenith sample map.

The MISSE-10 zenith AO fluence was determined to be 4.84×10^{18} atoms/cm^2 based on dehydrated mass loss of the zenith Kapton H AO fluence witness sample (M10Z-C1 F).[23] Table 8 provides the MISSE-10 LEO AO E_y values for the PEC-2 zenith samples. Included in Table 8 is the MISSE-10 zenith sample ID, material, material abbreviation, sample layer thickness, number of sample layers flown, dehydrated mass loss, exposed surface area, density, and the MISSE-10 ram AO fluence. All samples were 1-inch (2.54 cm) circular in size. Only the top layer (Part A) of the two multilayered zenith samples (M10Z-C9 F and M10Z-C10 F) was weighed post-flight and compared with the Part A pre-flight mass for determining sample mass loss. The AO fluence, and corresponding AO E_y values, are based on Kapton H mass loss of only 0.075 mg.

Samples of clear Teflon FEP, back-surface metallized FEP, and back-surface carbon painted-FEP were flown in the zenith direction of MISSE-10. As can be seen in Table 8, the mass loss and thus corresponding AO E_y for the MISSE-10 zenith FEP (M10Z-C6 F) and FEP/Al (M10Z-C7 F) samples were very similar at 1.14×10^{-23} and 1.15×10^{-23} cm^3/atom, respectively. But the carbon back-surface painted Teflon FEP sample (M10Z-C8 F) had ≈5X higher mass loss and an AO E_y of 5.41×10^{-23} cm^3/atom. Once again, the increased on-orbit heating impacted the erosion of the Teflon FEP and the clear and back-surface metallized Teflon FEP samples exhibited UV fluorescence in the space exposed area.

An alumina sample was flown in the zenith direction (M10Z-C5 F) for contamination analyses and had mass loss within error of the balance (0.004 mg). XPS analyses of the sample indicated the presence of 6.6 at.% Si, as listed in Table 2. Detailed contamination results for M10Z-C5 F are provided in Reference 27.

Table 8. Erosion Data for the MISSE-10 PCE-2 Zenith Flight Samples.

MISSE-10 Zenith ID	Material	Abbreviation	Thickness (mils) (# Layers Flown)	Mass Loss (g)	Exposed Surface Area (cm^2)	Density (g/cm^3)[15]	MISSE-10 Zenith AO Fluence ($atoms/cm^2$)[23]	MISSE-10 Zenith AO E_y ($cm^3/atom$)
M10Z-C1 F	Polyimide (PMDA) (Kapton H)	Kapton H	5 (1)	0.000075	3.602	1.4273	**4.84E+18**	***3.00E-24***
M10Z-C3 F	Polyimide (PMDA) (Kapton HN)	Kapton HN	5 (1)	0.000028	3.605	1.4346	4.84E+18	1.10E-24
M10Z-C5 F	Alumina slide	Al_2O_3	63 (1)	*0.000004*[+]	3.602	3.987^	4.84E+18	*5.27E-26*
M10Z-C6 F	Fluorinated ethylene propylene (Teflon FEP)	FEP	5 (1)	0.000427	3.597	2.1443	4.84E+18	1.14E-23
M10Z-C7 F	Aluminized-Teflon (FEP/Al)*	FEP/Al	5 (1)	0.000429	3.604	2.1443	4.84E+18	1.15E-23
M10Z-C8 F	Teflon FEP clad carbon paint (India Ink) (FEP/C/FEP)*	FEP/C/FEP	14 (1)	0.002018	3.592	2.1443	4.84E+18	5.41E-23
M10Z-C9 F	Metallized polyethylene naphthalate (PEN) film (aluminum (100 nm)/ PEN (2 micron)/black chromium (15 nm)) with Kapton ring	Al/PEN/Bk Cr (M-PEN)	0.083 (2)	0.000025	3.587	1.36^^	4.84E+18	1.04E-24
M10Z-C10 F	LaRC SI (soluble imide) based polyimide/inorganic nanoparticle composite (radiation resistant polyimide (RPI))	LaRC RPI-2	0.9 (3)	0.000035	3.576	1.52**	4.84E+18	1.32E-24

*Teflon FEP is space facing
^https://www.matweb.com/index.aspx
^^https://usa.dupontteijinfilms.com/wp-content/uploads/2017/01/Q51-Datasheet.pdf
**Sample Collaborator[21]
[+]*Within balance error*

A Kapton HN sample (M10Z-C3 F) was flown as part of the MISSE-10 PCE-2 zenith samples. The AO E_y for M10Z-C3 F was 1.10×10^{-24} cm^3/atom, which is 3X lower than for the assumed LEO AO E_y for Kapton H. Metallized PEN (M-PEN, M10Z-C9 F) and LaRC radiation resistant polyimide (LaRC RPI, M10Z-C10 F) were flown. The M-PEN had an AO E_y of 1.04×10^{-24} cm^3/atom, while the LaRC RPI had an AO E_y of 1.32×10^{-24} cm^3/atom.

Two additional samples were flown: 1) A carbon coated white Tedlar sample (C/PVF-W, M10Z-C2 F), and 2) A unique sample of Au coated Kapton H (½ Au coated and scratched and ½ NaCl sprayed) mounted 90° in epoxy facing the ram direction (Au-Kapton H/Epoxy, M10Z-C10 F). The C/PVF-W sample is discussed in Reference 27. The Au-Kapton H/Epoxy flight sample, shown in Figure 35, was flown to study the AO fluence and undercutting at 90° to ram. This sample has not been analyzed yet, but the epoxy substrate darkened significantly, as shown in Figure 35b. Additional post-flight analyses can be found for the following PCE-2 zenith M-PEN (M10Z-C9 F) flight samples in Reference 49.

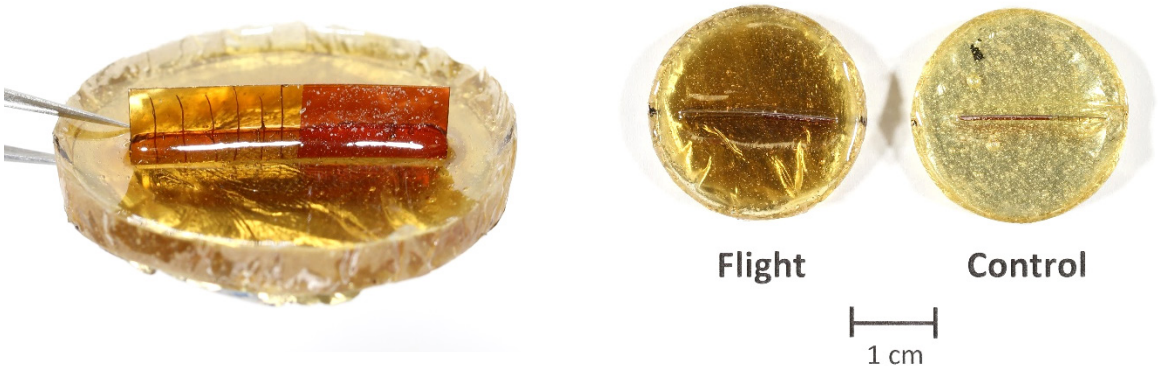

a. b.

Figure 35. Post-flight photographs of the Au-Kapton H/Epoxy sample (M10Z-C10 F): a). Image of the flight sample showing the ½ scratched Au coated surface and the ½ NaCl sprayed surface, and b). Visible light image of the flight (F) and control (B) samples.

MISSE-10 PCE-2 Nadir Samples

Figure 36 shows pre- and post-flight photographs of the MISSE-10 nadir MS deck (N3 MSC 13) section containing the 10 PCE-2 nadir samples. Figure 37 provides a sample map showing the specific location of the PCE-2 nadir samples. As can be seen by comparing the images in Figure 36, the 0.48 year LEO nadir space exposure resulted in minimal visual changes in the flight samples or the MSC deck color. The carbon film of the M10N-S1 AO Photo Monitor sample is lightened in the exposed area, but the thin carbon layer is not completed eroded, and the epoxy base of M10N-C4 F has darkened. Minimal changes are not surprising as nadir facing surfaces are exposed to the lowest level of solar radiation (albedo reflected) and grazing AO.

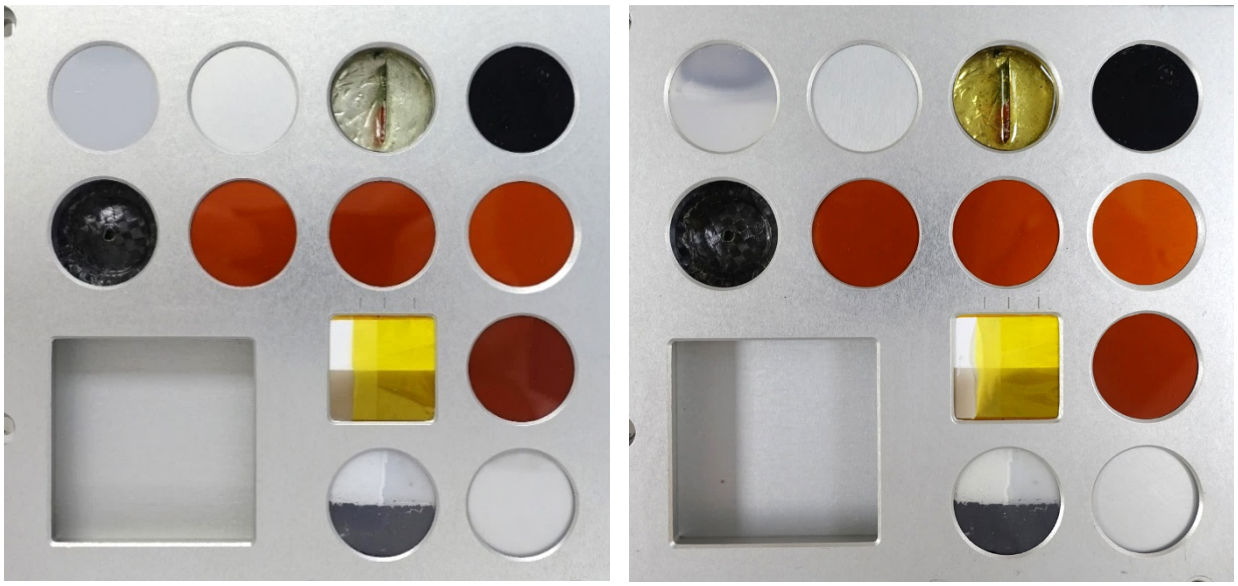

a. b.

Figure 36. Photographs of the MISSE-10 PCE-2 nadir MS deck (N3 MSC 13): a). Pre-flight with the PCE-2 nadir samples, and b). Post-flight showing minimal visual changes.

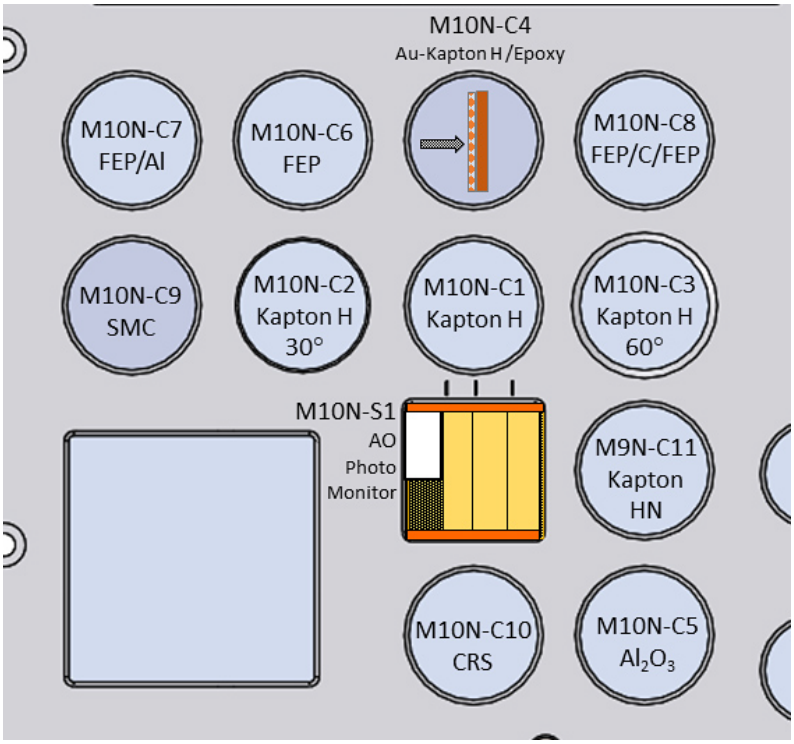

Figure 37. The MISSE-10 PCE-2 Z2 zenith sample map.

The MISSE-10 nadir AO fluence was determined to be 6.94×10^{18} atoms/cm^2 based on dehydrated mass loss of the nadir Kapton H AO fluence witness sample (M10N-C1 F).[23] This AO fluence is slightly higher than the MISSE-10 zenith AO fluence even though the nadir direct space exposure (0.48 years) was less than the MISSE-10 zenith exposure (0.69 years). This is attributed to the MISSE-FF off-set angle, which points the nadir face 8° into ram and the zenith face 8° away from ram. A 1-inch square multi-layered Photographic AO Fluence Monitor sample (M10N-S1 F) was flown along with a MISSE-10 nadir samples.[23] This sample can be seen in the photographs in Figure 36. Post-flight visible erosion of the carbon layer (and lack of erosion of the Kapton layers) indicated an AO fluence of $<1.73\times10^{19}$ atoms/cm^2, which is consistent with the AO fluence determined based on dehydrated mass loss of the Kapton H sample (M10N-C1 F).[23]

Table 9 provides the MISSE-10 LEO AO E_y values for the PEC-2 nadir samples. Included in Table 9 is the MISSE-10 nadir sample ID, material, material abbreviation, sample layer thickness, dehydrated mass loss, exposed surface area, density, and the MISSE-10 nadir AO fluence. All the AO E_y samples were 1-inch (2.54 cm) circular in size and only one sample layer was flown. The AO fluence, and corresponding AO E_y values, are based on Kapton H mass loss of 0.106 mg.

Three Kapton H samples were flown as part of the PCE-2 MISSE-10 nadir samples to determine the effect of the sample holder chamfer angle on the AO E_y with grazing AO exposure. The MISSE-10 nadir samples included Kapton H flown in MSC decks with 30° (M10N-C2 F), 45° (M10N-C1 F), and 60° (M10N-C3 F) chamfer angles (θ). As mentioned previously, the standard MISSE sample holder has a 45° chamfer. Once again, the AO E_y of the Kapton H in the standard 45° chamfer holder was assumed to be 3.00×10^{-24} cm^3/atom, as this sample was used as the Kapton H AO fluence witness sample.[23] The AO E_y of the Kapton H samples in the 30° and 60° chamfer holders were 2.31×10^{-24} cm^3/atom and 2.93×10^{-24} cm^3/atom, respectively. Thus, there was not a significant difference in the AO E_y for the 45° and 60° chamfer holders. However, the 30° chamfer angled holder had a lower mass loss and thus lower AO E_y, possibly due to AO scattering away from the sample surface instead of towards the sample surface. A Kapton HN sample (M10N-C11 F) was also flown. The AO E_y for the nadir Kapton HN was 1.21×10^{-24} cm^3/atom, which is substantially lower than for the Kapton H samples. The reason for this is currently unknown.

An alumina sample (M10N-C5 F) was flown in the nadir direction for contamination analyses and had a very small mass loss (0.013 mg). XPS analyses of the sample indicated the presence of 8.1 at.% Si, as listed in Table 2, similar to the nadir alumina sample. Detailed contamination results for M10N-C5 F are provided in Reference 27.

Samples of clear Teflon FEP, back-surface metallized FEP, and back-surface carbon painted-FEP were flown in the nadir direction of MISSE-10. As can be seen in Table 9, the mass loss and thus corresponding AO E_y for the MISSE-10 nadir FEP (M10N-C6 F) and FEP/Al (M10N-C7 F) samples were similar at 7.34×10^{-25} and 6.86×10^{-25} cm^3/atom, respectively. However, the carbon back-surface painted Teflon FEP sample (M10N-C8 F) had ≈39X higher mass loss with an AO E_y of 2.87×10^{-23} cm^3/atom. It is not clear why the nadir carbon back-surface painted Teflon FEP sample has such a significantly higher AO E_y. Once again, the clear and back-surface metallized Teflon FEP samples exhibited UV fluorescence in the space exposure area.

Table 9. Erosion Data for the MISSE-10 PCE-2 Nadir Flight Samples.

MISSE-10 Nadir ID	Material	Abbreviation	Thickness (mils)	Mass Loss (g)	Exposed Surface Area (cm^2)	Density (g/cm^3)[15]	MISSE-10 Nadir AO Fluence ($atoms/cm^2$) [23]	MISSE-10 Nadir AO E_y ($cm^3/atom$)
M10N-C1 F	Polyimide (PMDA) (Kapton H) - 45° chamfer (Standard)	Kapton H	5	0.000106	3.567	1.4273	**6.94E+18**	***3.00E-24***
M10N-C2 F	Polyimide (PMDA) (Kapton H) - 30° chamfer edge	Kapton H	5	0.000082	3.576	1.4273	6.94E+18	2.31E-24
M10N-C3 F	Polyimide (PMDA) (Kapton H) - 60° chamfer edge	Kapton H	5	0.000103	3.545	1.4273	6.94E+18	2.93E-24
M10N-C5 F	Alumina slide	Al_2O_3	63	0.000013	3.618	3.987^	6.94E+18	1.33E-25
M10N-C6 F	Fluorinated ethylene propylene (Teflon FEP)	FEP	5	0.000039	3.570	2.1443	6.94E+18	7.34E-25
M10N-C7 F	Aluminized-Teflon (FEP/Al)*	FEP/Al	5	0.000036	3.559	2.1443	6.94E+18	6.86E-25
M10N-C8 F	Teflon FEP clad carbon paint (India Ink) (FEP/C/FEP)*	FEP/C/FEP	14	0.001523	3.570	2.1443	6.94E+18	2.87E-23
M10N-C9 F	Shape memory composite	SMC	275	-0.000202	3.519	1.18**	6.94E+18	N/A
M10N-C10 F	Low density polyethylene for cosmic ray shielding	CRS (LD)	22	0.000183	3.620	0.907**	6.94E+18	8.05E-24
M10N-C11 F	Polyimide (PMDA) (Kapton HN)	Kapton HN	5	0.000043	3.583	1.4346	6.94E+18	1.21E-24

*Teflon FEP is space facing
^https://www.matweb.com/index.aspx
**Sample Collaborator[21]

An Au-Kapton H/Epoxy sample (M10N-C4 F) was flown in the nadir direction to study the AO fluence and undercutting at 90° to ram, similar to the zenith sample. The Au-Kapton H/Epoxy flight sample, shown in Figure 38, has not been analyzed yet. However, the epoxy substrate did not darken, as shown in Figure 38b, like the zenith sample did. Thus, it appears either the direct solar radiation exposure (only albedo radiation is present in the nadir direction), or the higher radiation dose caused the epoxy to darken.

a. b.

Figure 38. Post-flight photographs of the Au-Kapton H/Epoxy sample (M10N-C4 F): a). Image of the flight sample showing the ½ scratched Au coated surface and the ½ NaCl sprayed surface, and b). Visible light image of the flight (F) and control (B) samples.

A SMC sample (M10N-C9 F) was flown in the MISSE-10 nadir direction and experienced mass gain. Thus, an AO E_y value of "N/A" is listed for this.

Additional post-flight analyses can be found for the following PCE-2 nadir flight samples:

- SMC (M10N-C9 F): References 45 and 47
- CRS-Low Density (M10N-C10 F): References 45 and 46

MISSE-12 and MISSE-15 Polymers and Composites Experiment-3 (PCE-3)

MISSE-12 PCE-3 Ram Samples

Figure 39 shows pre- and post-flight photographs of the MISSE-12 ram MS deck (R2 MSC 4) section containing the 30 PCE-3 ram samples. Figure 40 provides a sample map showing the specific location of the PCE-3 ram samples. As can be seen by comparing the images in Figure 39, the 0.89 year LEO ram space exposure resulted in significant discoloration of the anodized MSC deck and of several PCE-3 samples. The white line in the post-flight photo of the M12R-C6 F (FEP/C) sample is a reflection and is not discoloration of the sample. The coating got smeared on the right side of the lower right sample M12R-C19 F (S383-70 silicone ½ coated with sunscreen and ½ coated with ZnO in Braycote, with an Al separator) sometime between integration of the sample into the flight hardware and de-integration.

a.

b.

Figure 39. Photographs of the MISSE-12 PCE-3 ram SS deck (R2 MSC 4): a). Pre-flight with the PCE-3 ram samples, and b). Post-flight showing discoloration of the MSC deck and numerous samples.

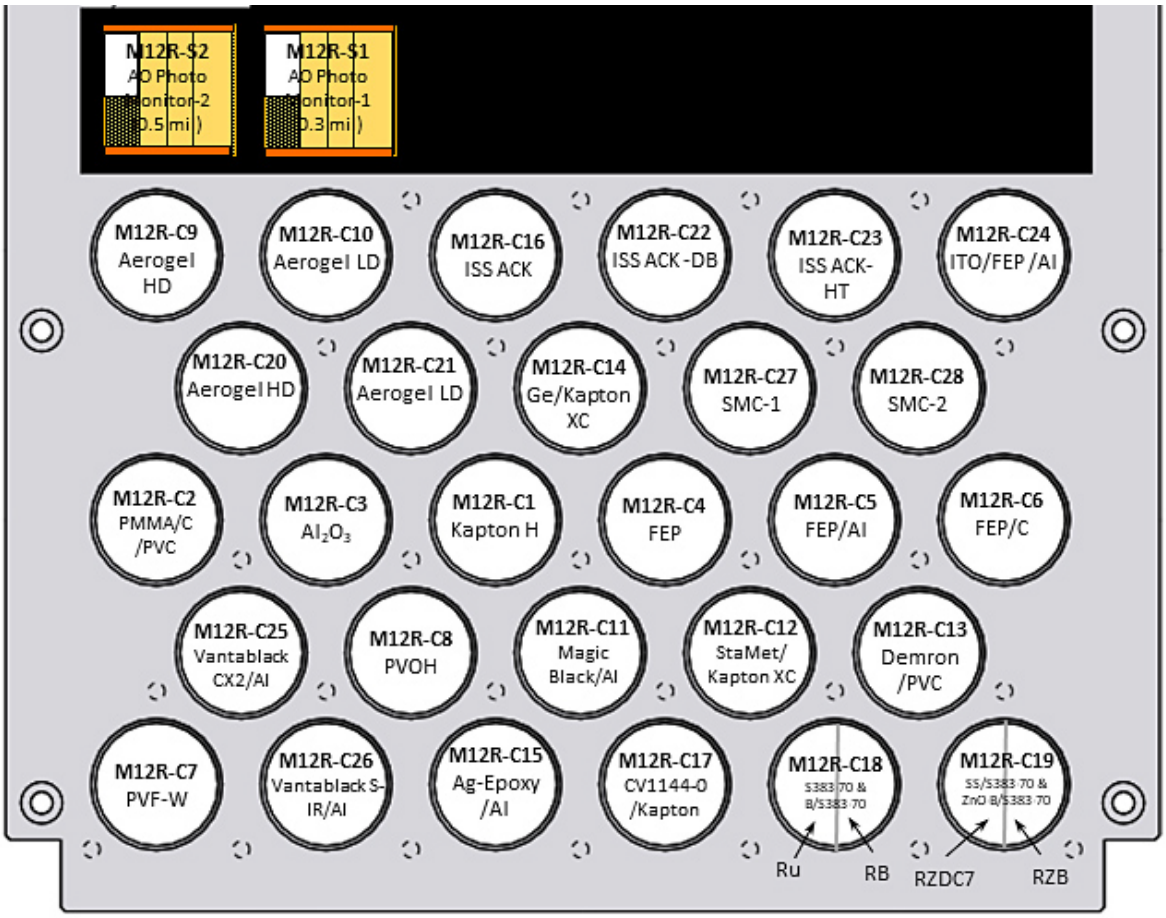

Figure 40. The MISSE-12 PCE-3 R2 ram sample map.

The MISSE-12 ram AO fluence was determined to be 2.97×10^{20} atoms/cm^2 based on dehydrated mass loss of the ram Kapton H AO fluence witness sample (M12R-C1 F).[23] Table 10 provides the MISSE-12 LEO AO E_y values for the PEC-3 ram samples. Included in Table 10 is the MISSE-12 ram sample ID, material, material abbreviation, sample layer thickness, number of sample layers flown, dehydrated mass loss, exposed surface area, density, and the MISSE-12 ram AO fluence. All samples for AO E_y were 1-inch (2.54 cm) circles with the exception of M12R-C18 F and M12R-C19 F (described above). Sample M12R-C18 F contained two semicircular S383-70 silicone docking seal samples: 1) uncoated S383-70 silicone (RU), and 2) Braycote coated S383-70 silicone (RB). The AO E_y was only determined for the uncoated S383-70 silicone (RU) sample. The AO E_y was not determined for M12R-C19 F, as noted below. The majority of the ram erosion samples were single layer samples. Only two multilayered ram samples were flown: 1) the M12R-C1 F AO fluence monitor, and 2) M12R-C8 F polyvinyl alcohol (PVOH). For M12R-C1 F, only the top layer was eroded and hence only Part A was weighed post-flight and compared with the Part A pre-flight mass for determining sample mass loss. For M12R-C8 F, the three layers were wavy (pre-flight) and stuck together post-flight. Hence, the mass loss for the PVOH sample was based on the pre- and post-flight mass of all three sample layers.

Table 10. Erosion Data for the MISSE-12 PCE-3 Ram Flight Samples.

MISSE-12 Ram ID	Material	Abbreviation	Thickness (mils) (# Layers Flown)	Mass Loss (g)	Exposed Surface Area (cm^2)	Density (g/cm^3)[15]	MISSE-12 Ram AO Fluence ($atoms/cm^2$)[23]	MISSE-12 Ram AO E_y ($cm^3/atom$)
M12R-C1 F	Polyimide (PMDA) (Kapton H)	Kapton H	5 (2)	0.004451	3.499	1.4273	**2.97E+20**	***3.00E-24***
M12R-C3 F	Alumina slide	Al_2O_3	63 (1)	*0.000005*+	3.495	3.987^	2.97E+20	*1.13E-27*
M12R-C4 F	Fluorinated ethylene propylene (Teflon FEP)	FEP	5 (1)	0.001449	3.497	2.1443	2.97E+20	6.50E-25
M12R-C5 F	Aluminized-Teflon (FEP/Al)*	FEP/Al	5 (1)	0.001416	3.496	2.1443	2.97E+20	6.36E-25
M12R-C6 F	Teflon FEP back-surface spray painted with BBQ black (carbon) paint*	FEP/C	14 (1)	0.002509	3.497	2.1443	2.97E+20	1.13E-24
M12R-C7 F	Crystalline polyvinyl fluoride w/white pigment (white Tedlar)	PVF-W	2 (1)	0.001256	3.499	1.6241	2.97E+20	7.44E-25
M12R-C8 F	Polyvinyl alcohol (MonoSol M1000)	PVOH	**1.5 (3)**	0.005872	3.497	1.28^^	2.97E+20	4.41E-24
M12R-C9 F	Polyimide aerogel (High density)	Aerogel HD	118 (1)	-0.001467	3.496	0.153**	2.97E+20	N/A
M12R-C10 F	Polyimide aerogel (Low density)	Aerogel LD	118 (1)	0.002089	3.498	0.087**	2.97E+20	2.31E-23
M12R-C11 F	Magic Black (Acktar Ltd.) coated aluminum	Magic Black/Al	135 (1)	-0.000015	3.498	1.9**	2.97E+20	N/A
M12R-C12 F	StaMet coated Kapton XC	StaMet/Kapton XC	1 (1)	0.000064	3.485#	2.5**	2.97E+20	2.46E-26
M12R-C13 F	Demron (black polyester/polymer+metal blend/clear embossed polyethylene)/PVC	Demron/PVC	28 (1)	0.006155	3.496	3.8**	2.97E+20	1.56E-24
M12R-C14 F	Ge coated Kapton XC	Ge/Kapton XC	2.75 (1)	-0.000038	3.496	1.41**	2.97E+20	N/A
M12R-C15 F	Silver filled epoxy (ECCOBOND 56C)/Al	Ag Epoxy/Al	135 (1)	0.000177	3.499	3.45	2.97E+20	4.94E-26
M12R-C17 F	CV1144-0 coated Kapton	CV1144-0/Kapton	3 (1)	0.000692	3.500	1.0^^	2.97E+20	6.66E-25
M12R-C18 F (RU)	Uncoated S383-70 silicone (semicircular sample)	S383-70 (RU)	90 (1)	0.000234	1.750	1.27^^	2.97E+20	3.55E-25
M12R-C20 F	Polyimide aerogel (High density, AO etched)	Aerogel HD-AO	118 (1)	0.002416	3.497	0.153**	2.97E+20	1.52E-23
M12R-C21 F	Polyimide aerogel (Low density, AO etched)	Aerogel LD-AO	118 (1)	0.004008	3.498	0.087**	2.97E+20	4.43E-23
M12R-C25 F	Vantablack CX2/aluminum (6061-T651)	Vantablack CX2/Al	135 (1)	0.002201	3.493	0.430**	2.97E+20	4.93E-24
M12R-C26 F	Vantablack (S-IR)/aluminum (6061-T651)	Vantablack (S-IR)/Al	135 (1)	0.001783	3.500	0.370**	2.97E+20	4.63E-24
M12R-C27 F	Shape memory composite-1	SMC-1	275 (1)	0.004242	3.331	1.18**	2.97E+20	3.63E-24
M12R-C28 F	Shape memory composite-2	SMC-2	275 (1)	0.004359	3.334	1.18**	2.97E+20	3.73E-24

*Teflon FEP is space facing
^https://www.matweb.com/index.aspx
^^Manufacturer's Data Sheet (NuSil CV-1144-0 Data Sheet; Parker S383-70 Data Sheet; MonoSol M1030 Data Sheet)
**Sample Collaborator[21]
#Exposed surface area adjusted for impact site
+*Within balance error*

Two square AO Photo Monitors (M12R-S1 F with three 0.3 mil Kapton layers, and M12R-S2 F with three 0.5 mil Kapton layers) were flown as part of the sample set. The AO fluence was determined to be ≈3.0×10^{20} atoms/cm^2 and 3.13×10^{20} atoms/cm^2 for M12R-S1 F and M12R-S2 F, respectively. The M12R-S1 F AO fluence is based on visual erosion and the M12R-S2 F AO fluence is based on Zygo optical profile scans. These values are close to the AO fluence determined based on dehydrated mass of M12R-C1 F. Detailed post-flight analyses of these samples are reported by de Groh in Reference 23. Field emission scanning electron microscope (FESEM) images were taken showing the ram erosion texture of Kapton H from AO Photo Monitor M12R-S2 F. A post-flight photograph of the AO Photo Monitor (M12R-S2 F) is provided in Figure 41.[23] Two erosion morphology images from M12R-S2 F are shown in Figure 42.[23]

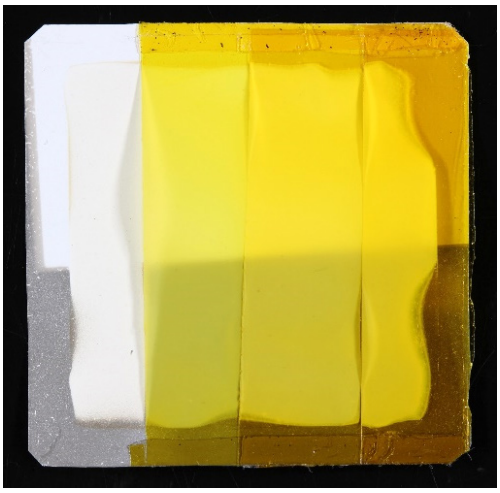

Figure 41. Post-flight photograph of AO Photo Monitor M12R-S2 F.

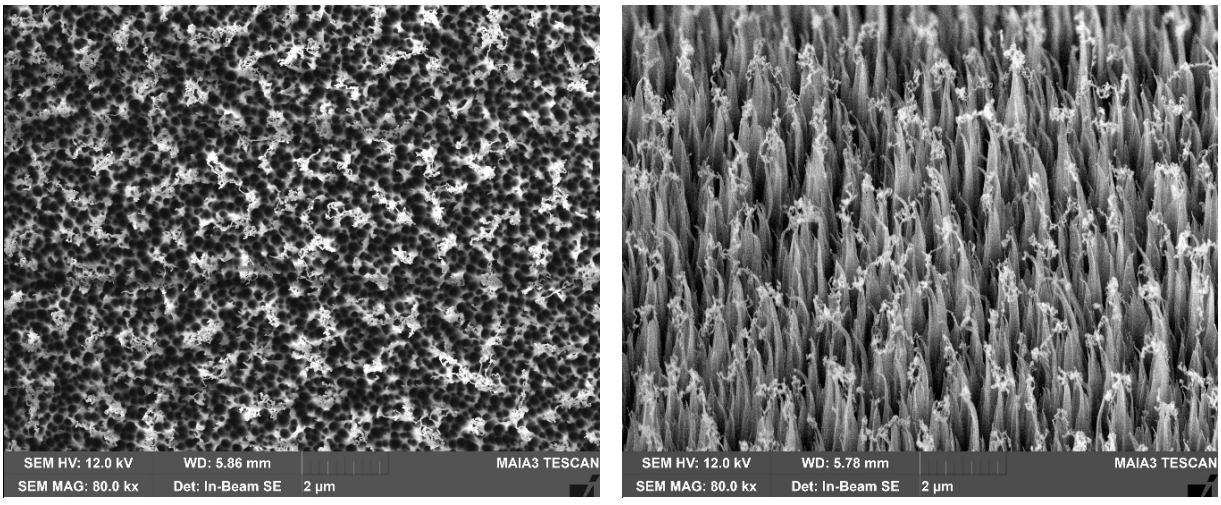

a. b.

Figure 42. Post-flight SEM images showing the ram erosion texture of Kapton H on AO Photo Monitor (M12R-S2 F): a). Image taken at 0° tilt angle, and b). Image taken at 45° tilt angle showing the fine typical LEO AO ram cone-like texture.

An alumina sample was flown in the ram direction (M12R-C3 F) for contamination analyses and had mass loss within error of the balance (0.005 mg). XPS analyses of the sample indicated the presence of 15.1 at.% Si, as listed in Table 2. This is a significant amount of Si contamination, which could impact AO fluence and AO E_y data. Detailed contamination results for M12R-C3 F are provided in Reference 27.

Samples of clear Teflon FEP, back-surface metallized FEP, and back-surface carbon coated-FEP were flown in the ram direction of MISSE-12. The back-surface carbon coated FEP sample was spray painted with BBQ black (carbon) paint (FEP/C). As can be seen in Table 10, the mass loss and thus corresponding AO E_y for the MISSE-12 ram FEP (M12R-C4 F) and FEP/Al (M12R-C5 F) samples were similar at 6.50×10^{-25} and 6.36×10^{-25} cm^3/atom, respectively. The back-surface carbon coated Teflon FEP sample (M12R-C6 F) had ≈1.7X higher mass loss with an AO E_y of 1.13×10^{-24} cm^3/atom, attributed to the higher on-orbit passive heating. Once again, Teflon FEP samples exhibited UV fluorescence in the space exposure area.

A White Tedlar sample (M12R-C7 R) had a significantly lower AO E_y (7.44×10^{-25} cm^3/atom) than Kapton, as expected, due to the AO durable TiO_2 particles. The flight sample was found to have discolored to a light brown color, as shown in Figure 43a. The space exposed area of the flight sample had a brownish color when imaged with a UV light, as shown in Figure 43b.

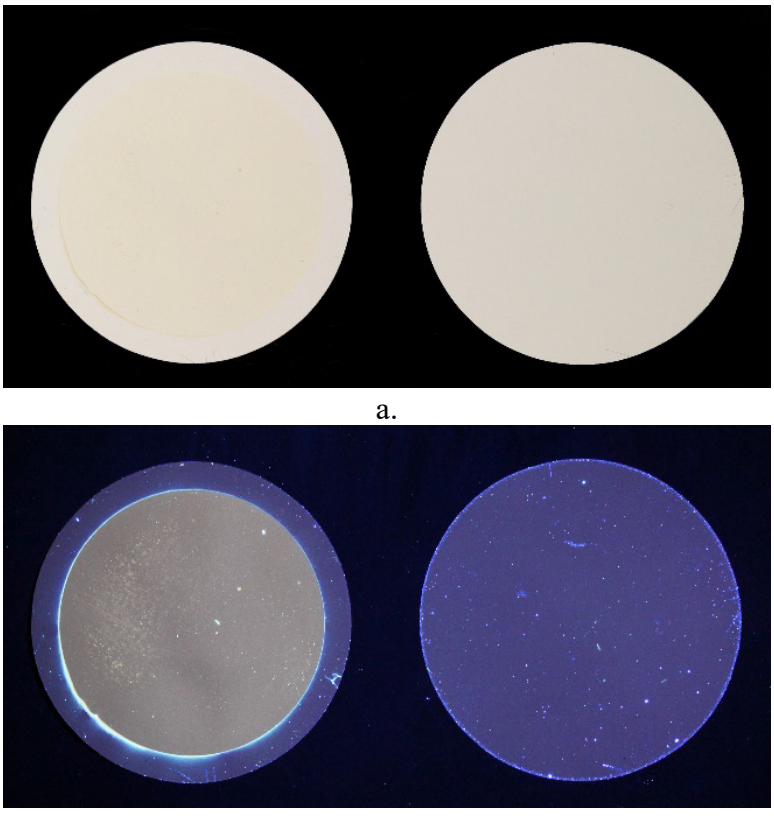

a.

b.

Figure 43. Post-flight photographs of White Tedlar flight (M12R-C7 F, left) and control (M12R-C7 B, right) samples: a). Visible light image, and b). UV light (365 nm) image.

Sample M12R-C8 F has three layers of 1.5 mil thick polyvinyl alcohol (PVOH). The top, space exposed, layer (Part A) became textured and yellowed as can be seen in Figure 44a. As seen in Table 10, the AO E_y was 4.41×10^{-25} cm^3/atom. Under UV light, the top layer has a strong UV fluorescence. But, interestingly, the underlying layers (Part B) also fluoresce more than the control sample layers, with decreasing intensity with layer depth as can be seen in Figure 44b.

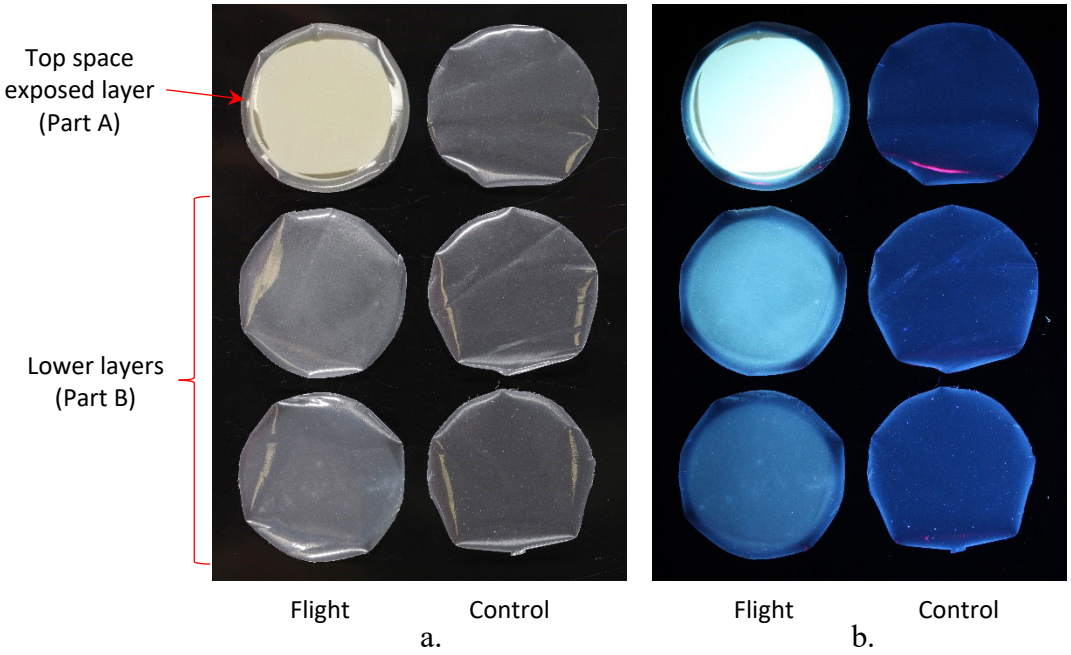

Figure 44. Post-flight photographs of PVOH flight (M12R-C8 F, left) and control (M12R-C8 B, right) samples: a). Visible light image, and b). UV light (365 nm) image.

A StaMet coated Kapton XC sample (M12R-C12 F) was flown. The 1-inch circular flight sample had a fairly large impact site, as shown in Figure 45. The impact penetrated the StaMet coated Kapton XC layer and also through the Al backing disc, which is shown in Figure 45b. A close-up of the impact site taken with a Keyence VHX-7000 Digital Optical Microscope is shown in Figure 45c. The area of the impact was determined to be 0.008 cm^2 based on Keyence image analyses (i.e. the black area shown in Figure 45d). Thus, the exposed surface area for the StaMet coated Kapton XC was determined to be 3.485 cm^2 (3.493 cm^2 – 0.008 cm^2) and the corresponding AO E_y is 2.46×10^{-26} cm^3/atom based on a mass loss of 0.064 mg.

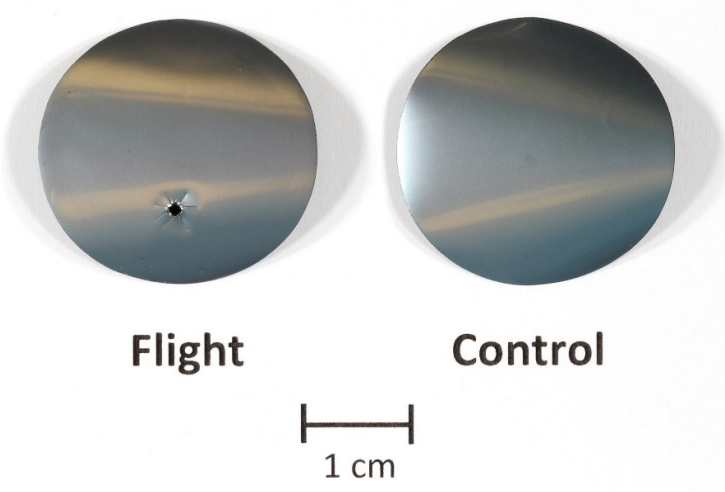

a.

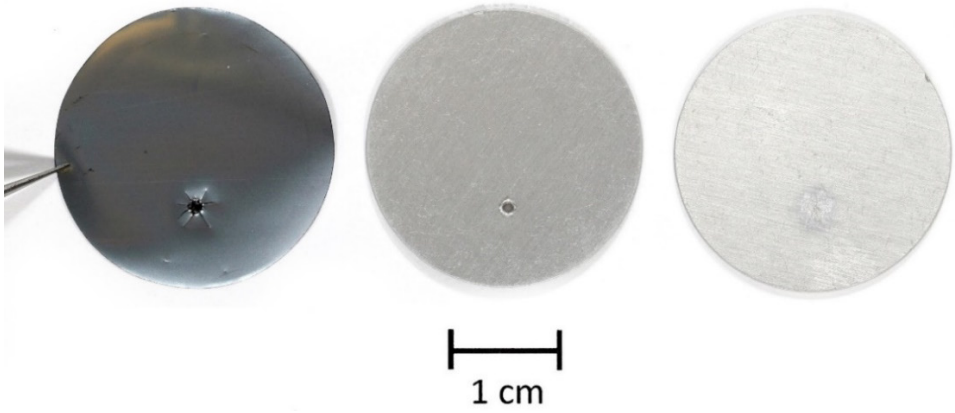

b.

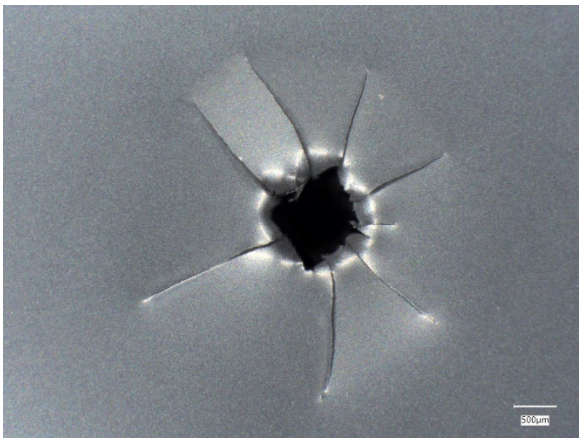

c.

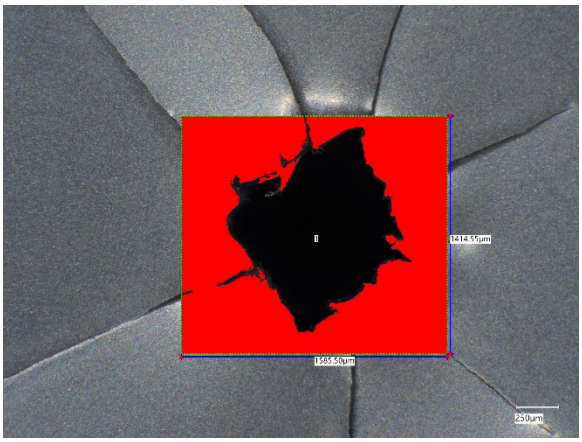

d.

Figure 45. Post-flight photographs of StaMet coated Kapton XC flight (M12R-C12 F) sample: a). Flight and control samples, and b). Flight sample with two backing Al spacers (center, spacer directly behind flight sample, right 2nd spacer), c). Keyence image of the impact site, and d). Keyence analysis area (black area is 0.008 cm^2).

There was also a small impact site in a CV1144-0 coated Kapton flight sample (M12R-C17 F). Visible light and UV light photographs of the flight (left) and control (right) samples are provided in Figure 46a and 46b, respectively. A close-up image of the impact site taken with the Keyence optical microscope is shown in Figure 46c. The area of the impact was determined to be 0.001 cm^2 and the corresponding AO E_y is 6.66×10^{-25} cm^3/atom based on a mass loss of 0.692 mg. The impact appears have occurred later in the mission as there is some "silicate" cracking which can be seen in Figure 46c below the impact hole. The smoother area in the upper left corner of the image in Figure 46c is the MSC deck holder protected area. As can be seen in Figure 46b, the exposed area of the flight sample fluoresces under UV (365 nm) light.

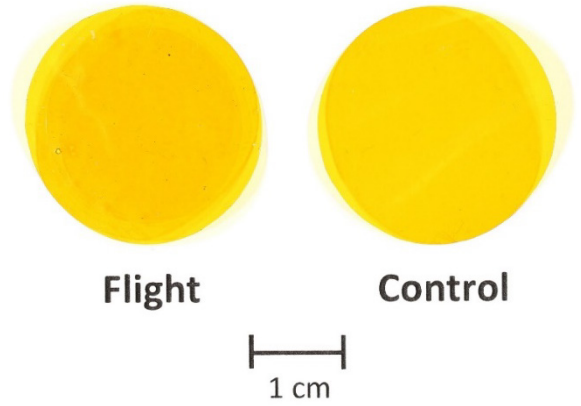

a.

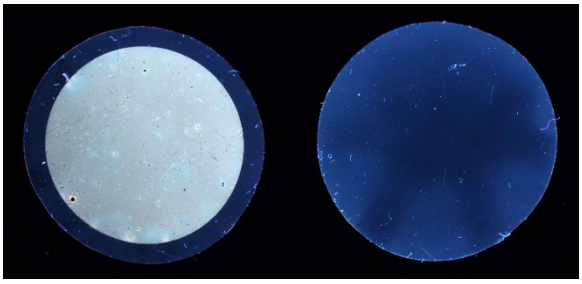

b.

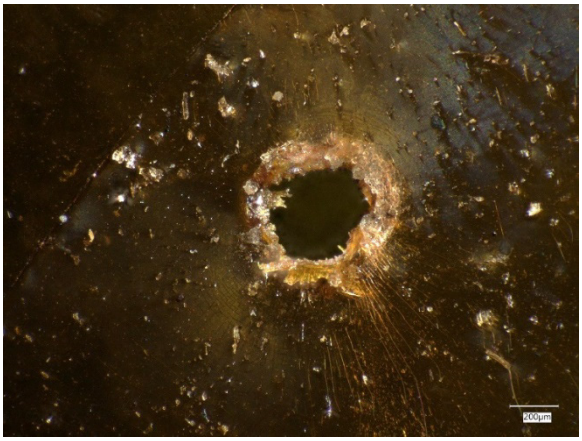

c.

Figure 46. Post-flight photographs of CV1144-0 coated Kapton flight (M12R-C17 F) sample: a). Visible light image of the flight and control samples, b). UV light image of the flight (left) and control (right) samples, and c). Keyence image of the impact site.

A few other samples that changed color or darkened included Demron fabric (M12R-C13 F), Ge coated Kapton XC (M12R-C14 F), and silver filled epoxy coated Al (M12R-C15 F), as shown in Figure 47. As can be seen in Figure 47a, the black surface of the Demron radiation resistant fabric was completely eroded away. The Demron fabric AO E_y is 1.54×10^{-24} cm^3/atom based on a mass loss of 6.155 mg. The Ge coated Kapton XC (M12R-C14 F) darkened a little, as seen in Figure 47b. This sample did not erode but gained a small amount of mass (0.038 mg), possibly due to contamination. As expected, the silver filled epoxy darkened significantly with AO oxidation, as shown in Figure 47c. The silver filled epoxy sample AO E_y is low (4.94×10^{-26} cm^3/atom) based on a mass loss of 0.177 mg.

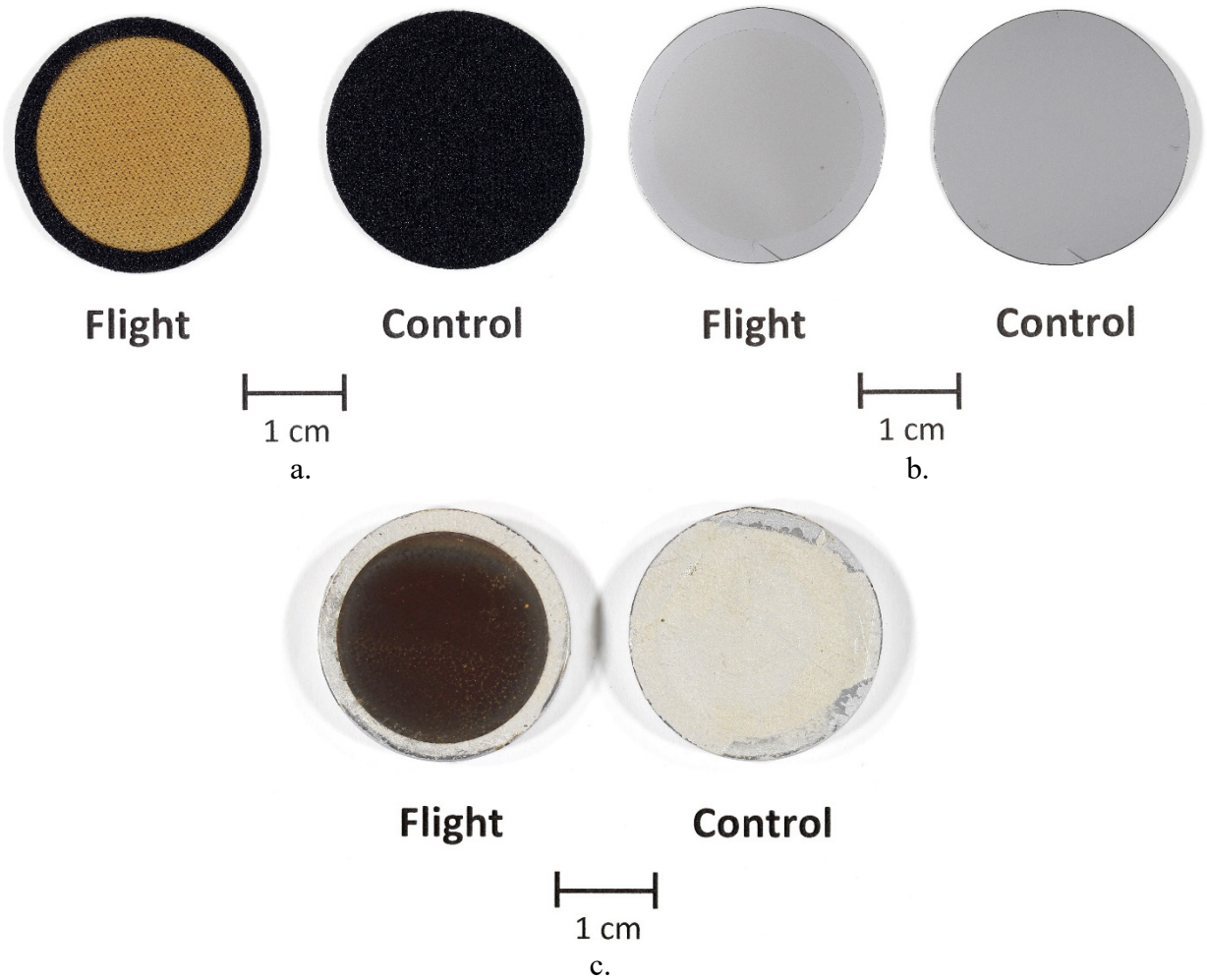

Figure 47. Post-flight photographs of MISSE-12 ram flight and control samples: a). Demron fabric (M12R-C13 F and B), b). Ge coated Kapton XC (M12R-C14 F and B), and c). Silver filled epoxy coated Al (M12R-C15 F and B).

The AO E_y for the PCE-3 ram flight samples listed in Table 11 either have not been analyzed yet, or the sample was not flown for AO E_y characterization.

Table 11. MISSE-12 PCE-3 Ram Flight Samples with No Erosion Data.

MISSE-12 Ram ID	Material	Abbreviation	Thickness (mils)
M12R-C2 F	Early mission AO F photographic detector (drops of PMMA/carbon soot/white vinyl siding (polyvinyl chloride (PVC) resin))	PMMA/C/PVC	42
M12R-C16 F	ISS Array Coated Kapton (SiO2/Kapton)	ISS ACK	1
M12R-C19 F	S383-70 silicone (1/2 coated with sunscreen and 1/2 coated with ZnO in Braycote) flown with an Al separator	SS/S383-70 (RZDC7) & ZnO-B/S383-70 (RZB)	90
M12R-C22 F	ISS Array Coated Kapton (SiO2/Kapton), Directed beam	ISS ACK-DB	1
M12R-C23 F	ISS Array Coated Kapton (SiO2/Kapton), Hyperthermal	ISS ACK-HT	1
M12R-C24 F	ITO/Teflon/aluminum	ITO-FEP	5

Additional post-flight analyses can be found for the following PCE-3 ram flight samples:

- Polyimide aerogel (M12R-C9 F, M12R-C10 F, M12R-C20 F and M12R-C21 F): References 41 and 42
- Vantablack (S-IR) coated Al (M12R-C26 F): Reference 43
- SMC (M12R-C27 F and M12R-C28 F): References 45 and 47
- S383-70 silicone (M12R-C18 F and M12R-C19 F): Reference 50

MISSE-12/MISSE-15 PCE-3 Wake Samples

Figure 48 shows pre- and post-flight photographs of the MISSE-12 wake MS deck (W3 MSC 6) with the 42 PCE-3 wake samples. Because the wake samples were not exposed to the space environment during the MISSE-12 mission, the samples were re-flown in the same MSC sample holders during the MISSE-15 mission. It should be noted that any visual difference between Figure 48a and 48b are due to differences in image lighting and not actual sample changes caused by mission exposures. Figure 49 shows pre- and post-flight photographs of the MISSE-15 wake MS deck (W1 MSC 10) with the 42 PCE-3 wake samples. Figure 50 provides a sample map showing the specific location of the PCE-3 wake samples. As can be seen by comparing the images in Figure 49, the MISSE-15 0.44 year LEO ram space exposure resulted in discoloration of the anodized MSC deck and numerous PCE-3 samples.

a. b.

Figure 48. Photographs of the MISSE-12 PCE-3 wake MS deck (W3 MSC 6): a). Pre-flight with the PCE-3 wake samples, and b). Post-flight (with no direct space exposure during MISSE-12 mission).

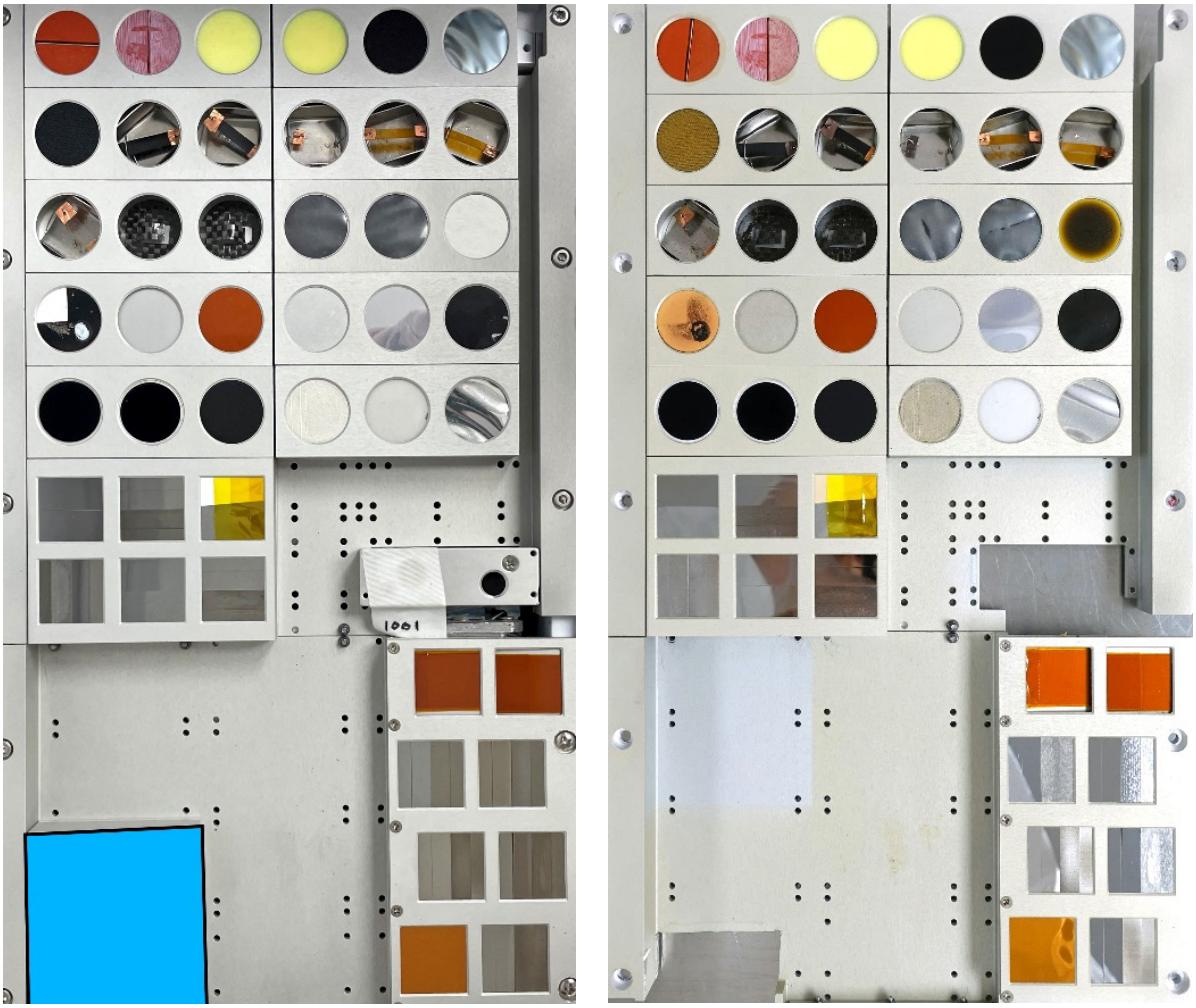

a. b.

Figure 49. Photographs of the MISSE-15 PCE-3 wake MS deck (W1 MSC 10): a). Pre-flight with the PCE-3 wake samples, and b). Post-flight showing discoloration of the MSC deck and numerous samples.

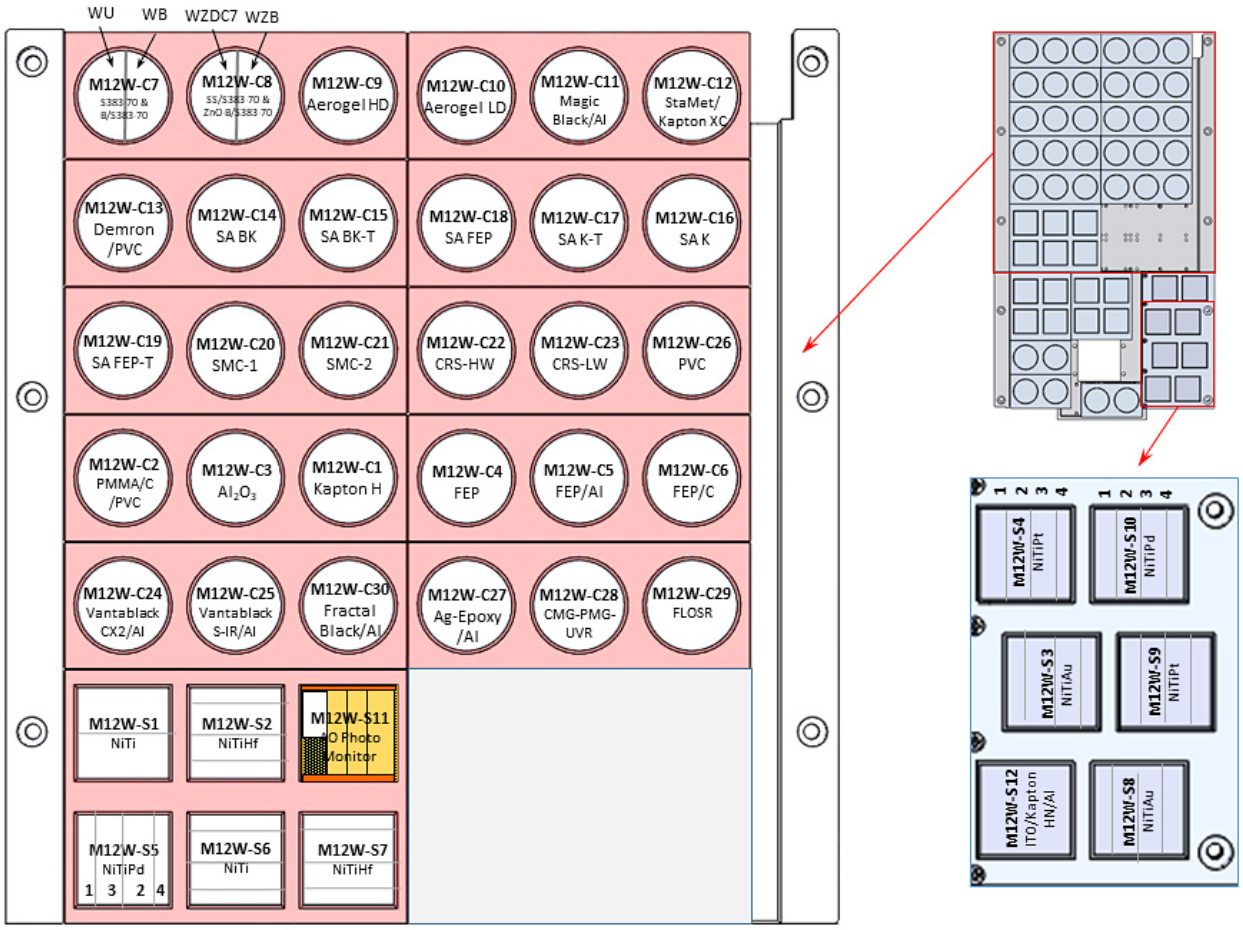

Figure 50. The MISSE-12 and MISSE-15 PCE-3 wake sample map.

The MISSE-15 wake AO fluence was determined to be 4.77×10^{18} atoms/cm^2 based on dehydrated mass loss of the ram Kapton H AO fluence witness sample (M12W-C1 F).[23] Table 12 provides the MISSE-15 LEO AO E_y values for the PEC-3 wake samples. Included in Table 12 is the MISSE-12/MISSE-15 wake sample ID, material, material abbreviation, sample layer thickness, dehydrated mass loss, exposed surface area, density, and the MISSE-15 wake AO fluence. All samples for AO E_y were single layer 1-inch (2.54 cm) circular or square with the exception of M12W-C7 F. Sample M12W-C18 F contained two semicircular S383-70 silicone docking seal samples: 1) uncoated S383-70 silicone (WU), and 2) Braycote coated S383-70 silicone (WB). The AO E_y was only determined for the uncoated S383-70 silicone (WU) sample. The back-up/control (B) samples for the following materials were flown instead of the "flight (F)" sample: Low density polyimide aerogel (M12W-C10 B), StaMet coated Kapton XC (M12W-C12 B), Vantablack CX2 coated aluminum (M12W-C24 B) and Flexible Optical Solar Reflector (M12W-C29 B). The density for the Flexible Optical Solar Reflector (FLOSR, M12W-C29 B) is an estimate based on the rule of mixtures (1.5 g/cm^3). The AO fluence, and corresponding AO E_y values, are based on Kapton H mass loss of 0.073 mg.

Table 12. Erosion Data for the MISSE-12/MISSE-15 PCE-3 Wake Flight Samples.

MISSE-12/ MISSE-15 Wake ID	Material	Abbreviation	Thickness (mils)	Mass Loss (g)	Exposed Surface Area (cm^2)	Density (g/cm^3)[15]	MISSE-15 Wake AO Fluence ($atoms/cm^2$)[23]	MISSE-15 Wake AO E_y ($cm^3/atom$)
M12W-C1 F	Polyimide (PMDA) (Kapton H)	Kapton H	5	0.000073	3.573	1.4273	**4.77E+18**	***3.00E-24***
M12W-C3	Alumina slide	Al_2O_3	63	*0.000003*+	3.578	3.987	4.77E+18	4.90E-26
M12W-C4 F	Fluorinated ethylene propylene (Teflon FEP)	FEP	5	0.000118	3.554	2.1443	4.77E+18	3.25E-24
M12W-C5 F	Aluminized-Teflon (FEP/Al)*	FEP/Al	5	0.000134	3.557	2.1443	4.77E+18	3.68E-24
M12W-C6 F	Teflon FEP back-surface spray painted with BBQ black (carbon) paint*	FEP/C	14	0.000702	3.573	2.1443	4.77E+18	1.92E-23
M12W-C7 F (WU)	Uncoated S383-70 silicone (semicircular sample)	S383-70 (WU)	90	-0.000670	1.776	1.27^^	4.77E+18	N/A
M12W-C9 F	Polyimide aerogel (High density)	Aerogel HD	118	-0.010941	3.574	0.153	4.77E+18	N/A
M12W-C10 B	Polyimide aerogel (Low density)	Aerogel LD	118	-0.007450	3.582	0.087	4.77E+18	N/A
M12W-C11 F	Magic Black (Acktar Ltd.) coated aluminum	Magic Black/Al	135	-0.000091	3.583	1.9	4.77E+18	N.A
M12W-C12 B	StaMet coated Kapton XC	StaMet/Kapton XC	1	0.000056	3.600	2.50**	4.77E+18	1.30E-24
M12W-C13 F	Demron (black polyester/polymer+metal blend/clear embossed polyethylene)/PVC	Demron/PVC	28	0.000825	3.574	3.8**	4.77E+18	1.27E-23
M12W-C20 F	Shape memory composite-1	SMC-1	275	0.000293	3.402	1.18**	4.77E+18	1.53E-23
M12W-C21 F	Shape memory composite-2	SMC-2	275	0.000301	3.423	1.18**	4.77E+18	1.56E-23
M12W-C22 F	Cosmic ray shielding (High weight shielding layer)	CRS-HW	39	0.001162	3.549	0.907**	4.77E+18	7.56E-23
M12W-C23 F	Cosmic ray shielding(Low weight shielding layer)	CRS-LW	39	0.001392	3.569	0.907**	4.77E+18	9.01E-23
M12W-C24 B	Vantablack CX2/aluminum (6061-T651)	Vantablack CX2/Al	135	-0.000168	3.586	0.43**	4.77E+18	N/A
M12W-C25 F	Vantablack (S-IR)/aluminum (6061-T651)	Vantablack (S-IR)/Al	135	-0.000088	3.582	0.37**	4.77E+18	N./A
M12W-C26 F	Polyvinyl chloride	PVC	5	0.000649	3.554	1.34^^	4.77E+18	2.86E-23
M12W-C27 F	Silver filled epoxy (ECCOBOND 56C)/Al	Ag-Epoxy/Al	135	-0.000317	3.542	3.45^^	4.77E+18	N/A
M12W-C28 F	CMG (ceria doped borosilicate glass) Pseudo-morphic Glass with UVR (UV reject. coating)	CMG-PMG-UVR	7.5	0.000340	3.542	2.54^^	4.77E+18	7.93E-24
M12W-C29 B	Flexible Optical Solar Reflector (OSR)	FLOSR	7.5	0.000073	3.537	1.5**	4.77E+18	2.88E-24
M12W-C30 F	Fractal Black (Acktar Ltd.) coated aluminum	Fractal Black/Al	135	-0.000057	3.578	1.9**	4.77E+18	N/A
M12W-S12 F	Indium tin oxide coated Kapton HN/Al	ITO/Kapton HN/Al	2	0.000149	4.726	6.8#	4.77E+18	9.74E-25

*Teflon FEP is space facing
^https://www.matweb.com/index.aspx
^^Manufacturer's Data Sheet (Parker S383-70 Data Sheet; ECCOBOND 56C Data Sheet; Clear-Lay Rigid PVC Data Sheet)
J Vac Sci Tech A 19:5(2043-7); 2001
**Sample Collaborator[21]
+*Within balance error*

An alumina sample was flown in the wake direction (M12W-C3) for contamination analyses and had mass loss within error of the balance (0.003 mg). XPS analyses of the sample indicated the presence of 15.1 at.% Si, as listed in Table 2. This is the same level of Si contamination as the MISSE-12 ram alumina sample (M12R-C3 F). Once, again it is worth pointing out that this is a significant amount of Si contamination, which could impact AO fluence and AO E_y data. Detailed contamination results for M12W-C3 are provided in Reference 27.

Samples of clear Teflon FEP, back-surface metallized FEP, and back-surface carbon coated-FEP were flown in the wake direction of MISSE-12/MISSE-15. Like the MISSE-12 ram sample, the back-surface carbon coated FEP sample was spray painted with BBQ black (carbon) paint (FEP/C). As can be seen in Table 12, the mass loss and thus corresponding AO E_y for the MISSE-12 wake FEP (M12W-C4 F) and FEP/Al (M12W-C5 F) samples were similar at 3.25×10^{-24} and 3.68×10^{-24} cm^3/atom, respectively. The back-surface carbon coated Teflon FEP sample (M12W-C6 F) had ≈6X higher mass loss with an AO E_y of 1.92×10^{-23} cm^3/atom, attributed to the higher on-orbit passive heating. Once again, Teflon FEP samples exhibited UV fluorescence in the space exposure area.

A few samples that changed color or darkened included Demron fabric (M12W-C13 F), silver filled epoxy coated Al (M12W-C27 F), and polyvinyl chloride (PVC, M12W-C26 F) as shown in Figure 51. As can be seen in Figure 51a, the black surface of the Demron radiation resistant fabric was completely eroded away with the small amount of AO exposure or faded due to other LEO environmental factors. The Demron fabric AO E_y is 1.27×10^{-23} cm^3/atom based on a mass loss of 0.825 mg. The silver filled epoxy darkened significantly in the wake direction, as shown in Figure 51b, but it is not as dark as the ram sample (see Figure 47c). The sample gained mass (0.317 mg), thus the AO E_y is N/A. The PVC sample (M12W-C26 F) darkened significantly in the wake direction and the surface is cracked, as shown in Figure 51c. This is similar to the darkening of the MISSE-9 wake PVC sample (M9W-C8 F) shown in Figure 27. The MISSE-15 wake PVC AO E_y is 2.86×10^{-23} cm^3/atom based on a mass loss of 0.649 mg.

Because of the low AO fluence, and likely also due to the Si contamination, a number of samples had mass gain and thus the AO E_y is listed as N/A. These samples are: Uncoated S383-70 silicone (M12W-C7 F -WU), Polyimide aerogel - high density (M12W-C9 F), Polyimide aerogel - low density (M12W-C10 B), Magic Black coated Al (M12W-C11 F), Vantablack CX2 coated Al (M12W-C24 B), Vantablack (S-IR) coated Al (M12\W-C25 F), Silver filled epoxy (M12W-C27 F) and Fractal Black coated Al (M12W-C30 F). In addition, the AO E_y for the PCE-3 wake flight samples listed in Table 13 either have not been analyzed yet, or the sample was not flown for AO E_y characterization.

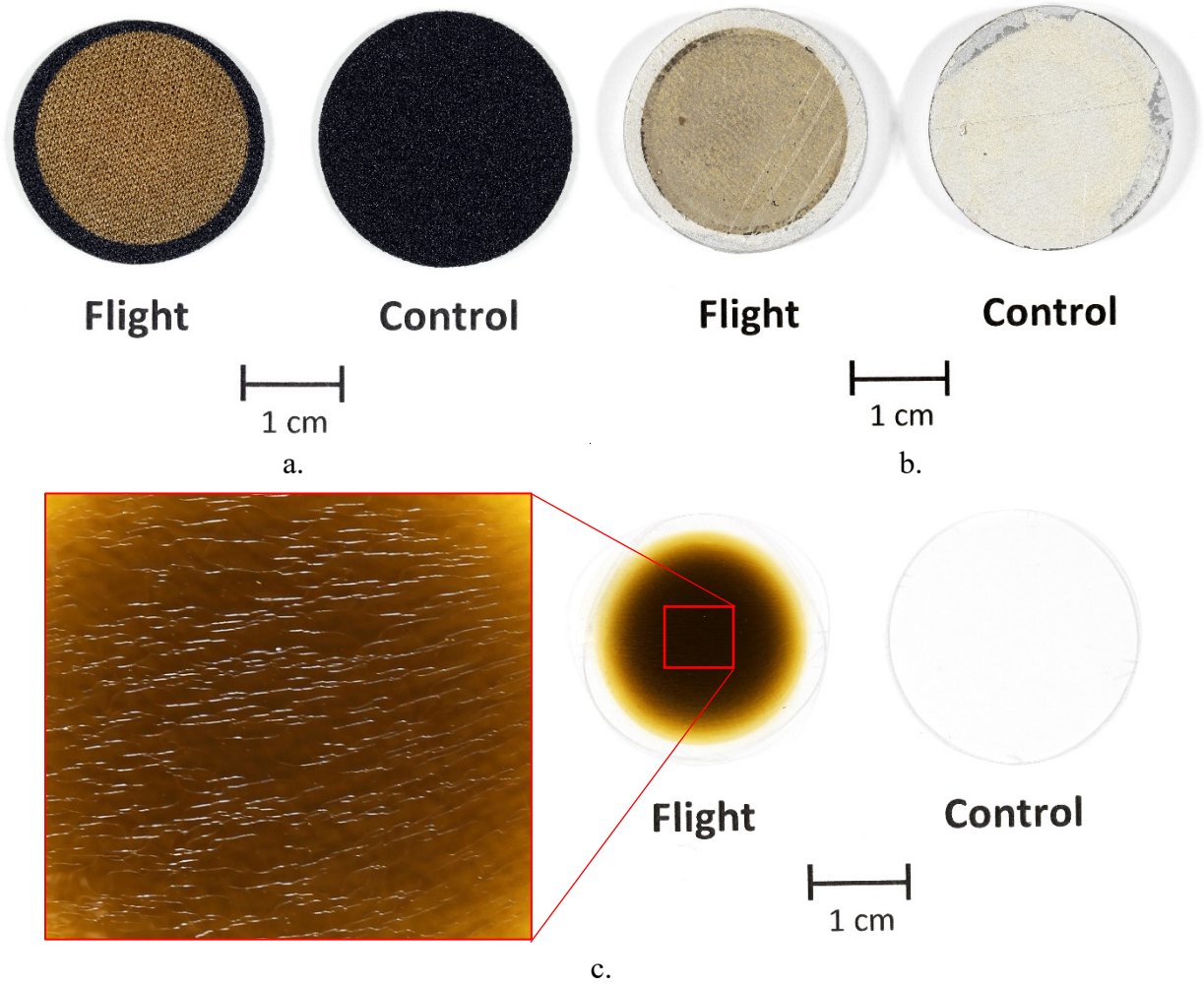

Figure 51. Post-flight photographs of MISSE-12/MISSE-15 wake flight and control samples: a). Demron fabric (M12W-C13 F and B), b). Silver filled epoxy coated Al (M12W-C27 F and B), and c). PVC (M12W-C26 F and B) with a close-up image showing cracking.

Additional post-flight analyses can be found for the following PCE-3 wake flight samples:

- S383-70 silicone (M12W-C7 F and M12W-C8 F): Reference 50
- Polyimide aerogel (M12W-C9 F and M12W-C10 B): References 41 and 42
- Vantablack (S-IR) coated Al (M12W-C25 F): Reference 43
- SMC (M12W-C20 F and M12W-C21 F): Reference 47

Table 13. MISSE-12/MISSE-15 PCE-3 Wake Flight Samples with No Erosion Data.

MISSE-12/ MISSE-15 Wake ID	Material	Abbreviation	Thickness (mils)
M12W-C2	Early mission AO F photographic detector (white vinyl siding (polyvinyl chloride (PVC) resin) - carbon soot - drops of PMMA)	PMMA/C/PVC	56
M12W-C8	S383-70 silicone (1/2 coated with sunscreen and 1/2 coated with ZnO in Braycote) flown with an Al separator	SS/S383-70 (WZDC7) & ZnO-B/S383-70 (WZB)	90
M12W-C14 F	Solar Array Black Kapton	SA BK	380
M12W-C15 F	Solar Array Black Kapton (tension)	SA BK-T	380
M12W-C16 F	Solar Array Kapton	SA K	380
M12W-C17 F	Solar Array Kapton (tension)	SA K-T	380
M12W-C18 F	Solar Array FEP	SA FEP	380
M12W-C19 F	Solar Array FEP (tension)	SA FEP-T	380
M12W-S1	Shape Memory Alloy (Bianary NiTi)	SMA NiTi	20
M12W-S2	Shape Memory Alloy (NiTiHf)	SMA NiTiHf	78
M12W-S3	Shape Memory Alloy (NiTiAu)	SMA NiTiAu	78
M12W-S4	Shape Memory Alloy (NiTiPt)	SMA NiTiPt	78
M12W-S5	Shape Memory Alloy (NiTiPd)	SMA NiTiPd	78
M12W-S6	Shape Memory Alloy (Bianary NiTi)	SMA NiTi	20
M12W-S7	Shape Memory Alloy (NiTiHf)	SMA NiTiHf	78
M12W-S8	Shape Memory Alloy (NiTiAu)	SMA NiTiAu	78
M12W-S9	Shape Memory Alloy (NiTiPt)	SMA NiTiPt	78
M12W-S10	Shape Memory Alloy (NiTiPd)	SMA NiTiPd	78

MISSE-12 PCE-3 Zenith Samples

Figure 52 shows pre- and post-flight photographs of the MISSE-12 zenith MS deck (Z1 MSC 18) sections containing the 14 PCE-3 zenith samples. Figure 53 provides a sample map showing the specific location of the PCE-3 zenith samples. As can be seen by comparing the images in Figure 52, the 0.45 year LEO zenith space exposure resulted in discoloration of the anodized MSC deck and a couple PCE-3 samples (M12Z-C2 F and M12Z-S1 F).

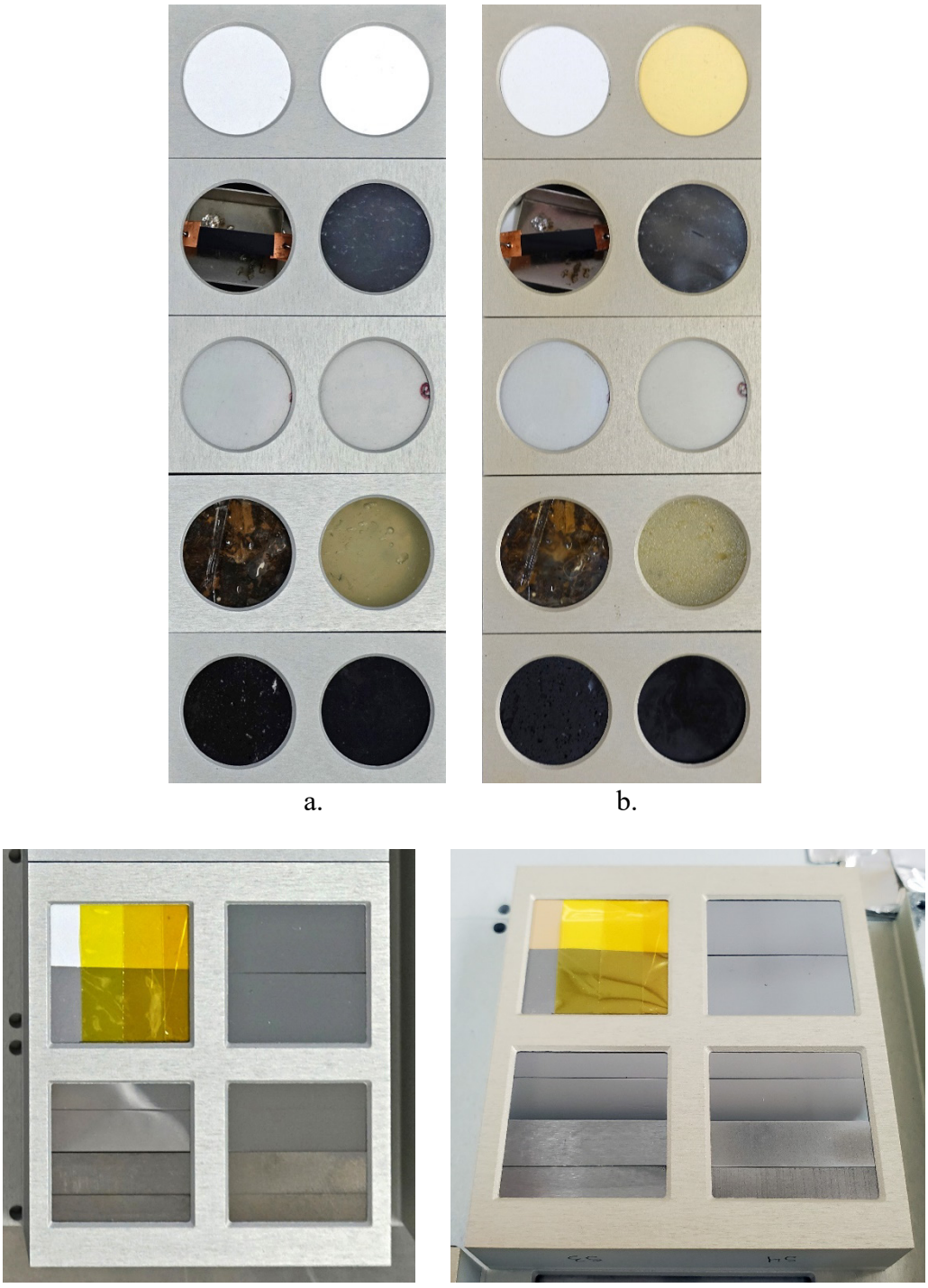

Figure 52. Photographs of the MISSE-12 PCE-3 zenith MS deck (Z1 MSC 18): a). Pre-flight of the 1-inch circular samples, b). Post-flight of the 1-inch circular samples showing discoloration of the MSC deck and M12Z-C2, c). Pre-flight of the 1-inch square samples, and d). Post-flight of the 1-inch square samples showing discoloration of the MSC deck and the M12Z-S1 AO Photo Monitor sample.

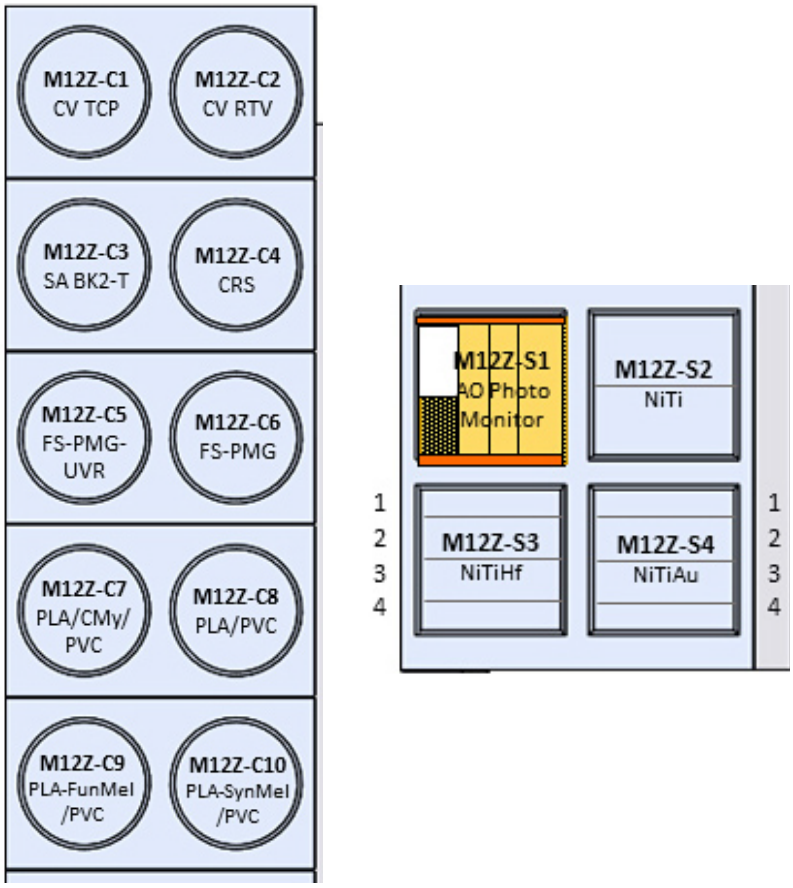

Figure 53. The MISSE-12 zenith PCE-3 zenith sample maps.

The MISSE-12 zenith AO fluence was determined to be ≈1.67×10^{18} atoms/cm^2 based on erosion texture of the Photographic AO Fluence Monitor (M12Z-S1 F) as described by de Groh in Reference 23. Table 14 provides the MISSE-12 LEO AO E_y values for the PCE-3 zenith samples. Included in Table 14 is the MISSE-12 zenith sample ID, material, material abbreviation, sample layer thickness, dehydrated mass loss, exposed surface area, density, and the MISSE-12 zenith AO fluence. All samples for AO E_y were single layer 1-inch (2.54 cm) circular or square.

The PCE-3 zenith samples did not include an alumina sample for contamination analyses, therefore one of the NiTi SMA samples (M12Z-S2 F) was used to analyze the molecular contamination as that material was not expected to erode with AO exposure. XPS analyses of the NiTi sample indicated the presence of 6.2 at.% Si, as listed in Table 2. This is less than half of the amount of Si contamination that the MISSE-12 ram and wake alumina samples experienced (15.1 at.%). Detailed contamination results for M12Z-S2 are provided in Reference 25.

A cosmic ray shielding - high weight shielding layer (CRS-HW) sample (M12Z-C4 F) had mass gain (0.049 mg), and so the AO E_y is listed as N/A. A unique set of samples flown as part of the PCE-3 in the zenith direction are melanin-based and compressed fungal mycelium samples. These samples (M12Z-C7 F to M12Z-C10 F) were flown for radiation protection assessment. Additional post-flight analyses of these melanin-based and compressed fungal mycelium samples are provided in References 51 and 52.

Table 14. Erosion Data for the MISSE-12 PCE-3 Zenith Flight Samples.

MISSE-12 Zenith ID	Material	Abbreviation	Thickness (mils)	Mass Loss (g)	Exposed Surface Area (cm^2)	Density (g/cm^3)[15]	MISSE-12 Zenith AO Fluence ($atoms/cm^2$)[23]	MISSE-12 Zenith AO E_y ($cm^3/atom$)
M12Z-S1 F	Photographic AO Fluence Monitor (0.3 mil layers)	AO Photo Monitor	10	N/A	N/A	1.4273	***≈1.67E+18***	***3.00E-24***
M12Z-C4 F	Cosmic ray shielding - High weight shielding layer	CRS-HW	39	-0.000049	3.597	0.907**	1.67E+18	N/A
M12Z-C5 F	Fused Silica Pseudomorphic Glass with UVR	FS-PMG-UVR	7	0.000201	3.596	1.602**	1.67E+18	2.09E-23
M12Z-C6 F	Fused Silica Pseudomorphic Glass	FS-PMG	8.5	0.000326	3.588	1.356**	1.67E+18	4.01E-23
M12Z-C7 F	Compressed mycelium with thin polylactic acid (PLA) coating on the space exposure side with a polyvinyl chloride backing layer	PLA/CMy/PVC	250	0.011487	3.566	1.18**	1.67E+18	1.63E-21
M12Z-C8 F	PLA with PVC backing layer	PLA/PVC	12	0.004067	3.583	1.18**	1.67E+18	5.76E-22
M12Z-C9 F	Fungal melanin powders infused into PLA with polyvinyl chloride (PVC) backing layer	PLA-FunMel/PVC	380	0.000544	3.551	1.05**	1.67E+18	8.74E-23
M12Z-C10 F	Synthetic melanin powders infused into PLA with polyvinyl chloride (PVC) backing layer	PLA-SynMel/PVC	380	0.001694	3.555	1.14**	1.67E+18	2.50E-22

**Sample Collaborator[21]

Two photovoltaic materials were flown in the zenith direction, one was a Fused Silica Pseudomorphic Glass sample with UVR coating (FS-PMG-UVR, M12Z-C5 F) shown in Figure 54, and the second was Fused Silica Pseudomorphic Glass without the UVR coating (FS-PMG, M12Z-C6 F) shown in Figure 55. Both samples experience some mass loss (0.201 mg for FS-PMG-UVR and 0.326 mg for FS-PMG). The FS-PMG-UVR (M12Z-C5 F) sample developed surface cracks, as can be seen in Figure 54b. The space exposed area also fluoresces under UV light, as can be seen in Figure 54c. The Fused Silica Pseudomorphic Glass without the UVR coating did not crack, but the space exposed area does fluoresce under UV light, as can be seen in Figure 55c.

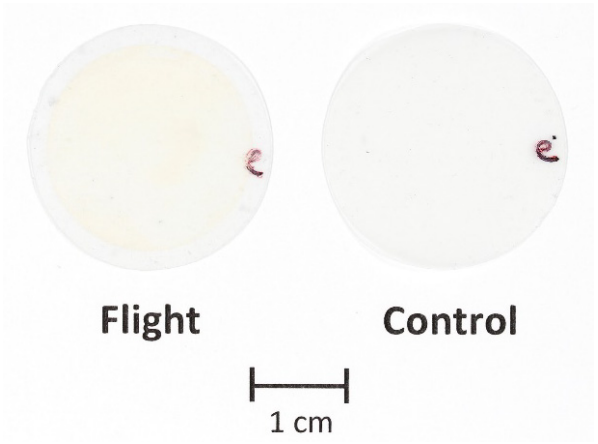

a.

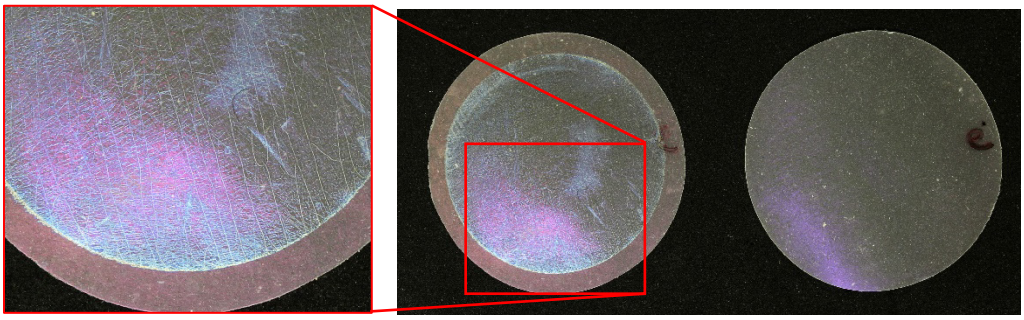

b.

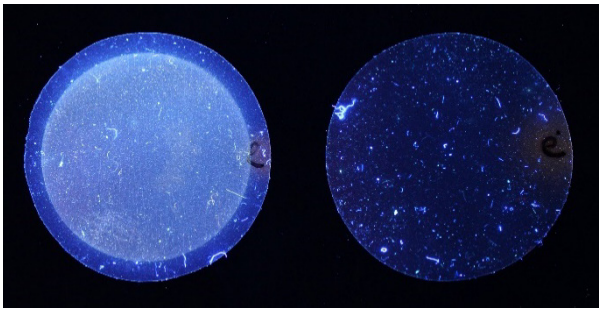

c.

Figure 54. Post-flight photographs of the Fused Silica Pseudomorphic Glass with UVR coating (FS-PMG-UVR) flight (M12Z-C5 F) and control (M12Z-C5 B) samples: a). Visible light image, b). Visible light image of the flight (left) and control (right) samples on black paper, and c). UV light image of the flight (left) and control (right) samples.

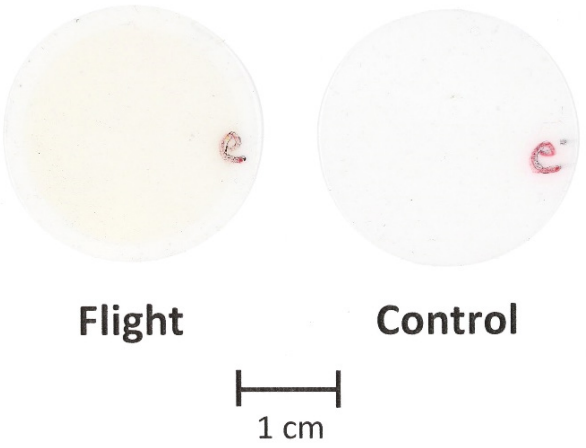

a.

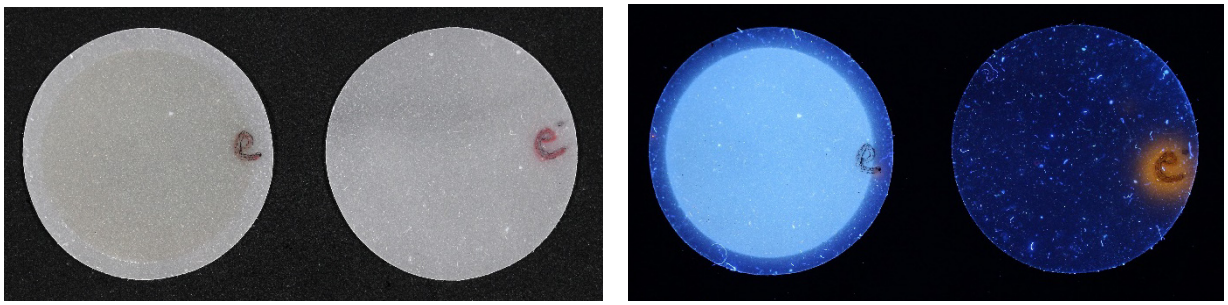

b. c.

Figure 55. Post-flight photographs of the Fused Silica Pseudomorphic Glass (FS-PMG) flight (M12Z-C6 F) and control (M12Z-C6 B) samples: a). Visible light image, b). Visible light image of the flight (left) and control (right) samples on black paper, and c). UV light image of the flight (left) and control (right) samples.

The AO E_y for the PCE-3 zenith flight samples listed in Table 15 either have not been analyzed yet, or the sample was not flown for AO E_y characterization.

Table 15. MISSE-12 Zenith Flight Samples with No Erosion Data.

MISSE-12 Zenith ID	Material	Abbreviation	Thickness (mils)
M12Z-C1 F	Crew Vehicle modified thermal control paint (S13NT: 6N/LO-1)	CV TCP	62.5
M12Z-C2 F	Crew Vehicle RTV (low outgassing) (RTV577-LV)	CV RTV	62.5
M12Z-C3 F	Solar Array Black Kapton (tension)	SA BK2-T	275
M12Z-S2 F	Shape Memory Alloy (Binary NiTi)	SMA NiTi	20
M12Z-S3 F	Shape Memory Alloy (NiTiHf)	SMA NiTiHf	78
M12Z-S4 F	Shape Memory Alloy (NiTiAu)	SMA NiTiAu	78

MISSE-13 Polymers and Composites Experiment-4 (PCE-4)

MISSE-13 PCE-4 Wake Samples

Figure 56 shows pre- and post-flight photographs of the MISSE-13 wake MS deck (W1 MSC 5) with the 26 PCE-4 wake MS samples. Figure 57 provides a sample map showing the specific location of the PCE-4 wake MS samples. As can be seen by comparing the images in Figure 56, the MISSE-13 0.44 year LEO wake space exposure resulted in discoloration of a few PCE-4 samples. The PCE-4 also included 24 tensile, two stressed solar sail and 13 shape memory alloy (SMA) samples that were not characterized for AO E_y.

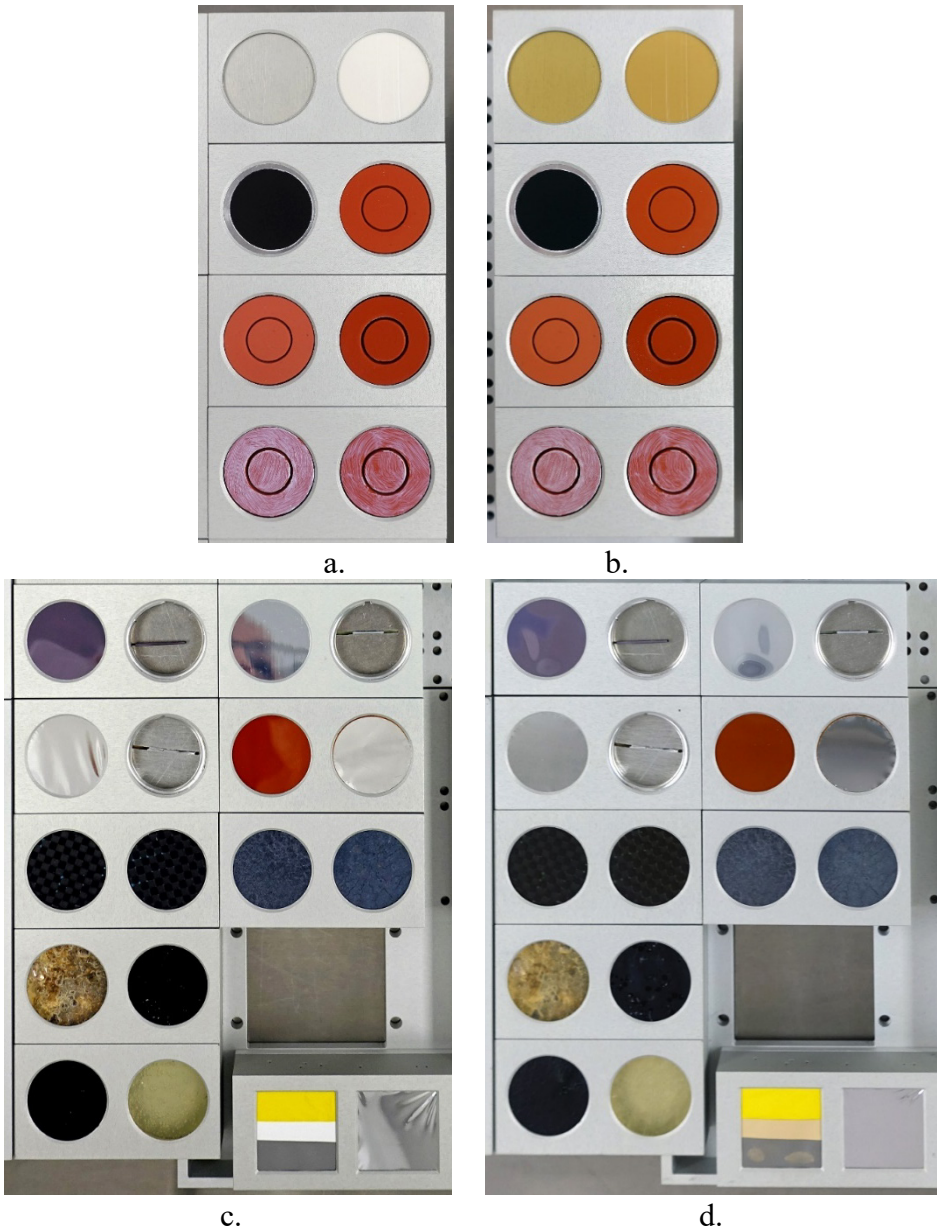

Figure 56. Photographs of the MISSE-13 PCE-4 wake MS deck (W1 MSC 5): a). Pre-flight of the upper deck samples, b). Post-flight of the upper deck samples, c). Pre-flight of the lower deck samples, and d). Post-flight of the lower deck samples.

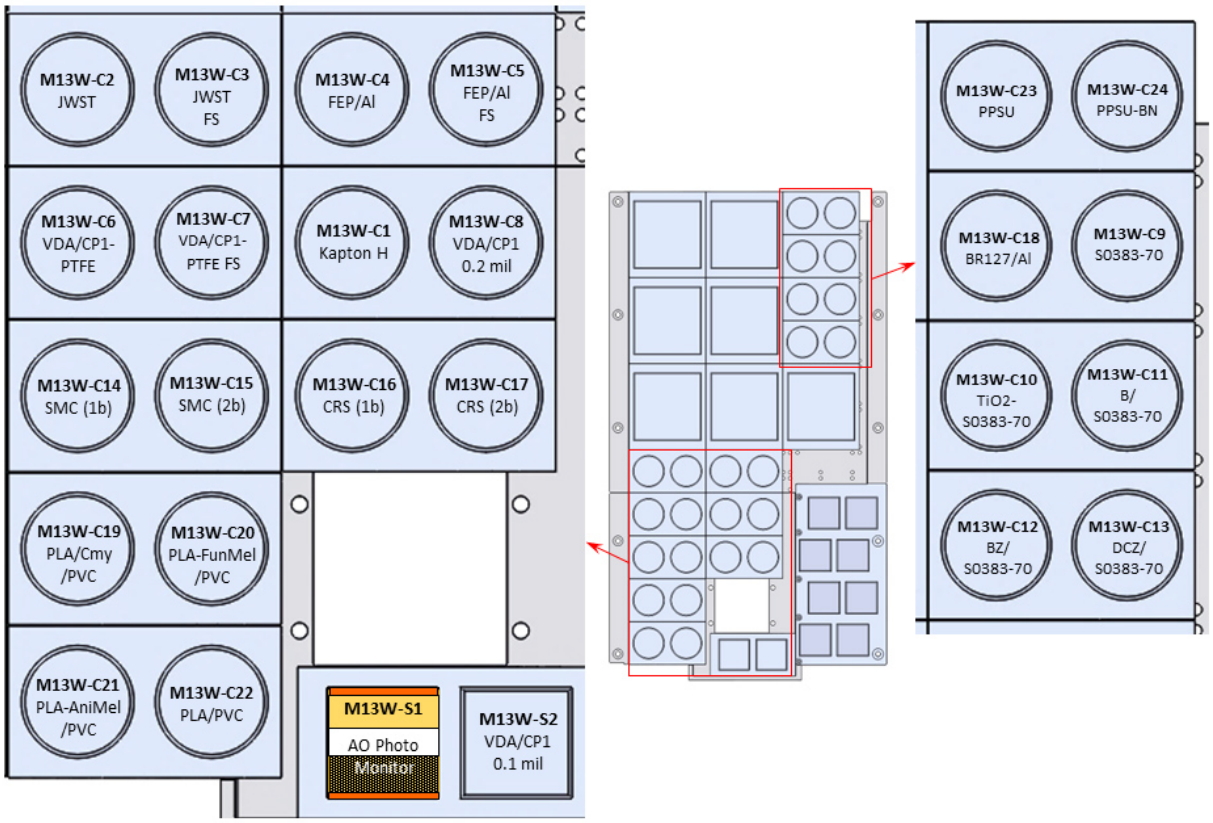

Figure 57. The MISSE-13 PCE-4 wake MS sample map.

The MISSE-13 wake AO fluence was determined to be 2.65×10^{18} atoms/cm^2 based on dehydrated mass loss of the wake Kapton H AO fluence witness sample (M13W-C1 F).[23] The AO fluence for the AO Photographic Monitor (M13W-S1 F) was $<<1.73\times10^{19}$ atoms/cm^2 based on visible erosion, which was consistent with the AO fluence for M13W-C1 F.[23] Table 16 provides the MISSE-13 LEO AO E_y values for the PEC-4 wake samples. Included in Table 16 is the MISSE-13 wake sample ID, material, material abbreviation, sample layer thickness, dehydrated mass loss, exposed surface area, density, and the MISSE-13 wake AO fluence. All samples for AO E_y were single layer 1-inch (2.54 cm) circular or square. The density for the James Webb Space Telescope (JWST) Sun shield sample (Si/2 mil Kapton E/VDA, M13W-C2 F) is for the Kapton E film layer. The AO fluence, and corresponding AO E_y values, are based on Kapton H mass loss of 0.040 mg.

Table 16. Erosion Data for the MISSE-13 PCE-4 Wake Flight Samples.

MISSE-13 Wake ID	Material	Abbreviation	Thickness (mils)	Mass Loss (g)	Exposed Surface Area (cm^2)	Density (g/cm^3)[15]	MISSE-13 Wake AO Fluence ($atoms/cm^2$)[23]	MISSE 13 Wake AO E_y ($cm^3/atom$)
M13W-C1 F	Polyimide (PMDA) (Kapton H)	Kapton H	5	0.000040	3.528	1.4273	**2.65E+18**	***3.00E-24***
M13W-C2 F	James Webb Space Telescope (JWST) Sun shield (Si/2 mil Kapton E/VDA)	JWST	2	0.000120	3.518	1.4617	2.65E+18	8.84E-24
M13W-C4 F	Aluminized-Teflon FEP*	FEP/Al	5	0.000121	3.558	2.1443	2.65E+18	6.01E-24
M13W-C6 F	VDA/CP1-PTFE composite solar sail material (Kapton HN frame/966 acrylic adhesive on back)	VDA/CP1-PTFE	0.3	0.000024	3.583	1.87**	2.65E+18	1.37E-24
M13W-C8 F	VDA/CP1 solar sail material (Kapton HN frame adhered with 3M 966 acrylic adhesive on front)	VDA/CP1	0.2	0.000119	3.517	1.54**	2.65E+18	8.28E-24
M13W-C14 F	Shape memory composite sample (1b)	SMC (1b)	47	0.000447	3.579	1.18**	2.65E+18	3.99E-23
M13W-C15 F	Shape memory composite (2b)	SMC (2b)	47	0.000508	3.577	1.18**	2.65E+18	4.54E-23
M13W-C16 F	Cosmic ray shielding (1b)	CRS (1b)	12	0.000362	3.519	0.907**	2.65E+18	4.28E-23
M13W-C17 F	Cosmic ray shielding (2b)	CRS (2b)	12	0.000368	3.520	0.907**	2.65E+18	4.35E-23
M13W-C18 F	BR-127 NC ESD/Al ^	BR-127 NC ESD/Al	136	0.000092	3.562	0.0875**	2.65E+18	1.12E-22
M13W-C19 F	Compressed mycelium with thin polylactic acid (PLA) coating on the space exposure side with a polyvinyl chloride (PVC) backing layer	PLA/CMy/PVC	250	0.010065	3.641	1.18**	2.65E+18	8.85E-22
M13W-C20 F	Fungal melanin powders infused into PLA with PVC backing layer	PLA-FunMel/PVC	380	0.002080	3.618	1.05**	2.65E+18	2.07E-22
M13W-C21 F	Animal melanin (octopus ink) infused into PLA with PVC backing layer	PLA-AniMel/PVC	380	0.002681	3.561	1.14**	2.65E+18	2.49E-22
M13W-C22 F	PLA with PVC backing layer	PLA/PVC	12	0.004618	3.576	1.18**	2.65E+18	4.13E-22
M13W-C23 F	Polyphenylsulfone (Radel 5500)	PPSU	12.5	0.000079	3.601	1.256**	2.65E+18	6.57E-24
M13W-C24 F	Polyphenylsulfone (Radel 5500) with hexagonal boron nitride platelets	PPSU-hBN	8.5	0.000102	3.614	1.267**	2.65E+18	8.38E-24
M13W-S2 F	VDA/CP1 NEA Scout solar sail material (with Kapton HN frame/966 acrylic adhesive on front)	VDA/CP1	0.1	0.000076	4.388	1.54**	2.65E+18	4.23E-24

*Teflon FEP is space facing
**Sample Collaborator[21]
^Solvay BR-127 non-chromated (NC) electric static dissipative (ESD) Modified Phenolic Primer (Black) on an Al substrate

The PCE-4 wake samples did not include an alumina sample for contamination analyses, therefore the back surface aluminized-Teflon FEP (FEP/Al) samples (M13W-C4 F) was used to analyze the molecular contamination. XPS analyses of the FEP/Al sample indicated the presence of 1.6 at.% Si, as listed in Table 2. Detailed contamination results for M13W-C4 F are provided in Reference 27.

The PCE-4 included a set of melanin-based and compressed fungal mycelium samples flown in the wake direction for radiation protection assessment. These samples (M12W-C19 F to M12W-C22 F) are very similar to the melanin and compressed fungal mycelium samples flown as part of the PCE-3 in the zenith direction (M12Z-C7 F to M12Z-C10 F). Additional post-flight analyses of these samples are provided in References 51 and 52.

The PCE-4 also included samples of polyphenylsulfone (M13W-C23 F) and polyphenyl-sulfone with hexagonal boron nitride (hBN) platelets (M13W-C24 F) to understand the aging behavior and durability of PPSU and the role of hBN filler after long-term exposure in a space environment. The PPSU-hBN flight sample lost a little more mass (0.079 mg) than the PPSU-hBN flight sample (0.012 mg). Post-flight photographs of the flight and control samples are provided in Figure 58. As can be seen in Figure 58a, both flight samples darkened with the wake space exposure. And, as can be seen in Figure 58b, the wake space exposure changed the UV fluorescence of both samples. Additional post-flight analyses of the PPSU and PPSU-hBN samples are provided by Williams et.al in Reference 53.

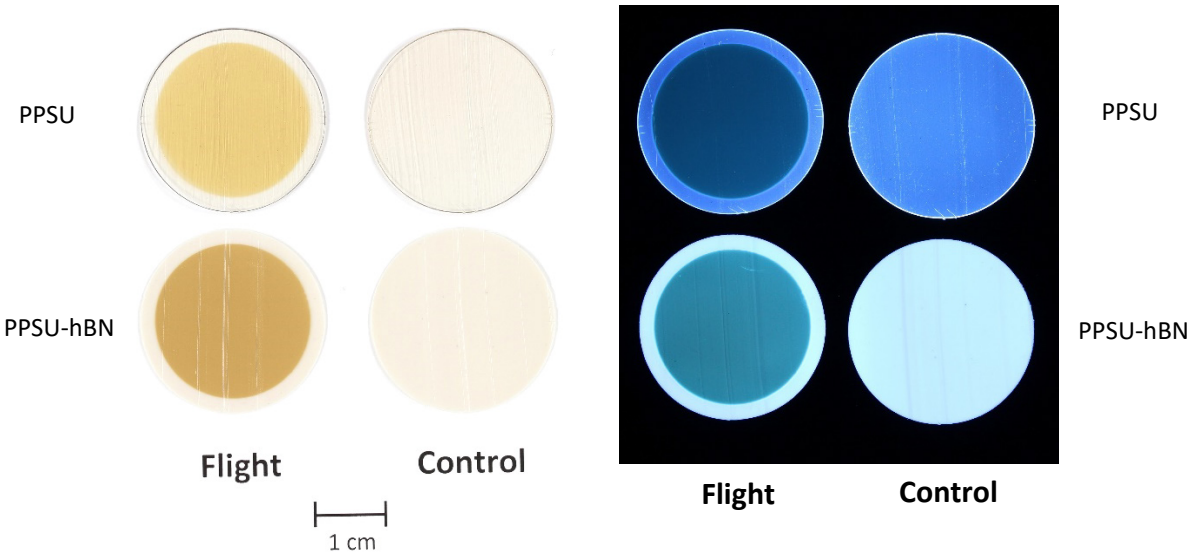

a. b.

Figure 58. Post-flight photographs of the PPSU and PPSU-hBN flight (M13W-C23 F and M13W-C24 F, respectively) and control (M13W-C23 B and M13W-C24 B, respectively) samples: a). Visible light image, and b). UV light image of the flight (left) and control (right) samples.

Various other PCE-4 wake samples such as cosmic ray shielding (CRS) samples (M13W-C16 F and M13W-C17 F) and various solar sail materials (M13W-C6 F, M13W-C8 F and M13W-S2 F) are currently being analyzed. One of the CRS samples (M13W-C16 F) is shown in Figure 59. The flight sample's fluorescence changed after the wake space exposure, as seen in Figure 59b. The PCE-4 included wake samples under folding stress, coated and uncoated docking seal samples, and 13 shape memory alloy (SMA) samples that were not characterized for AO E_y. These samples are listed in Table 17. The 24 tensile samples and two stressed solar sail samples, shown in Figure 60, were also not characterized for AO E_y. A list of the tensile and stressed solar sail samples are provided by de Groh in Reference 21.

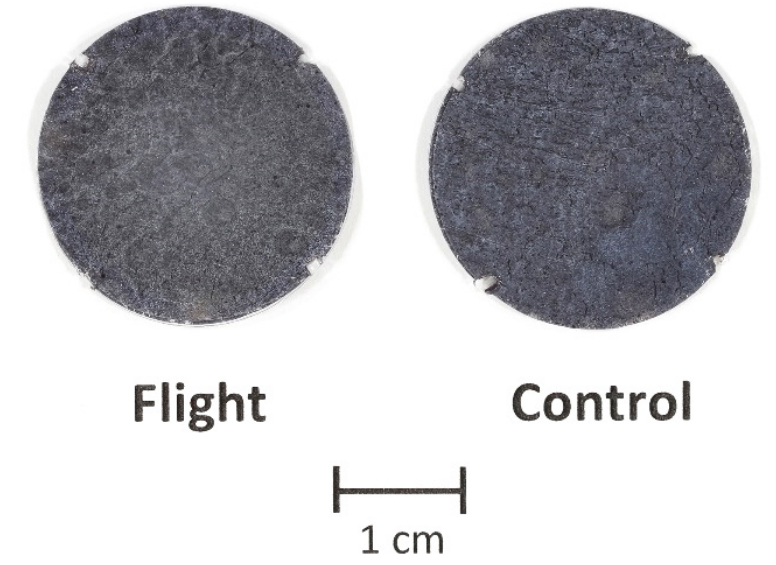

a.

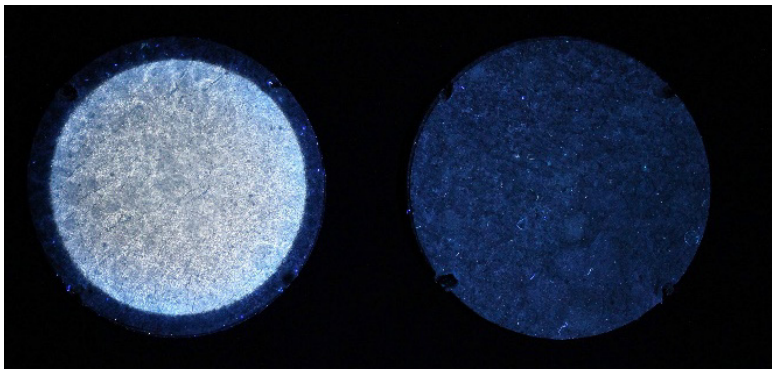

b.

Figure 59. Post-flight photographs of the CRS flight (M13W-C16 F) and control (M13W-C16 B) samples: a). Visible light image, and b). UV light image of the flight (left) and control (right) samples.

Figure 60. Post-flight photograph of the PCE-4 wake SMA, stressed solar sail and tensile samples.

Table 17. MISSE-13 Wake Flight Samples with No Erosion Data.

MISSE-13 Wake ID	Material	Abbreviation	Thickness (mils)
M13W-C3 F	JWST Sun shield material under folding stress	JWST FS	2
M13W-C5 F	Aluminized-Teflon FEP under folding stress*	FEP/Al FS	5
M13W-C7 F	VDA/CP1-PTFE composite solar sail material under folding stress	VDA/CP1-PTFE FS	0.3
M13W-C9 F	S0383-70 silicone (1"dia. seal)	S0383-70	210
M13W-C10 F	S0383-70 silicone with 1.5% titanium dioxide additive (1"dia. seal)	TiO2-S0383-70	210
M13W-C11 F	S0383-70 silicone coated with Braycote 601EF grease (1"dia. seal)	B/S0383-70	210
M13W-C12 F	S0383-70 silicone coated with Braycote 601EF grease plus ZnO (BZ) sunscreen (1"dia. seal)	BZ/S0383-70	210
M13W-C13 F	S0383-70 silicone coated Dow Corning 7 + ZnO (DCZ) sunscreen (1"dia. seal)	DCZ/S0383-70	210
M13W-R1 F	Shape Memory Alloys (13 samples: 2 - 0.5" x 1" + 12 - 0.25" x 1" pieces)	SMA	20

*Teflon FEP is space facing

Additional post-flight analyses can be found for the following PCE-4 wake flight samples:

- SMC (M13W-C14 F and M13W-C15 F): Reference 47
- Silicone elastomer docking seal materials (M13W-C9 F to M13W-C13 F): Reference 50

MISSE-13 PCE-4 Zenith Samples

Figure 61 shows pre- and post-flight photographs of the MISSE-13 zenith MS deck (Z2 MSC 19) with the 33 PCE-4 wake samples. Figure 62 provides a sample map showing the specific location of the PCE-4 zenith MS samples. As can be seen by comparing the images in Figure 61, the MISSE-13 0.44 year LEO zenith space exposure resulted in discoloration of the M13Z-S1 AO Photographic Monitor sample. The variation in appearance of the M13Z-R1 SMA samples are due to differences in reflections of the shiny samples during imaging, not changes due to space exposure.

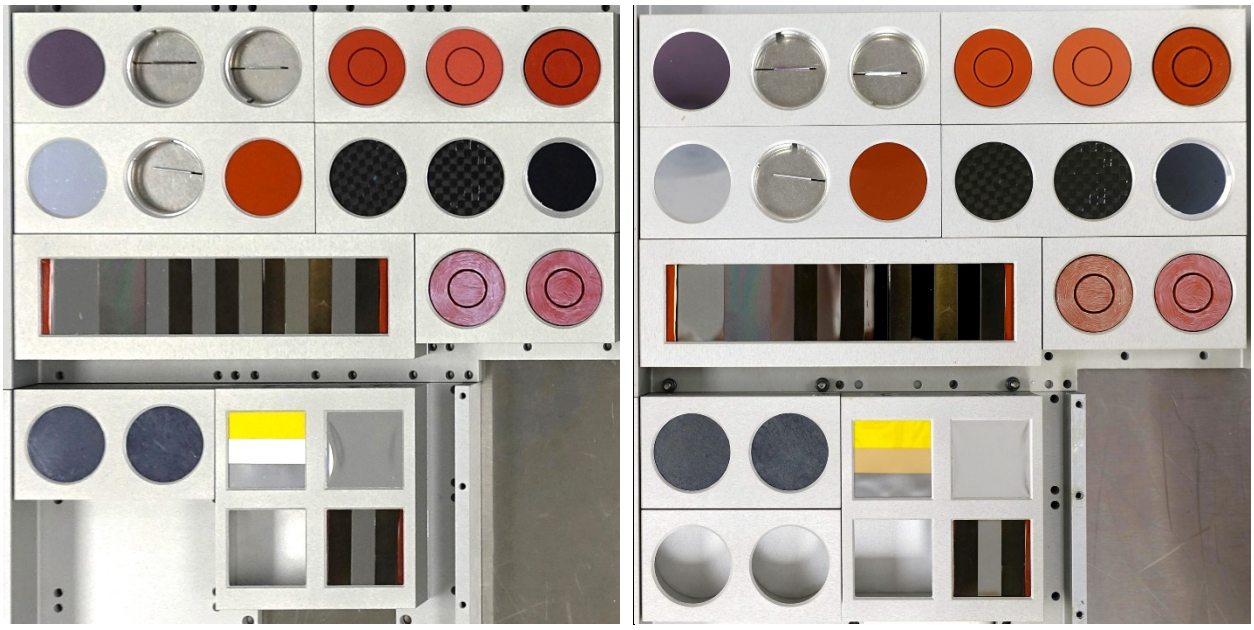

a. b.

Figure 61. Photographs of the MISSE-13 PCE-4 zenith MS deck (Z2 MSC 19): a). Pre-flight of the PCE-4 zenith samples, and b). Post-flight (with reflections in the SMA samples).

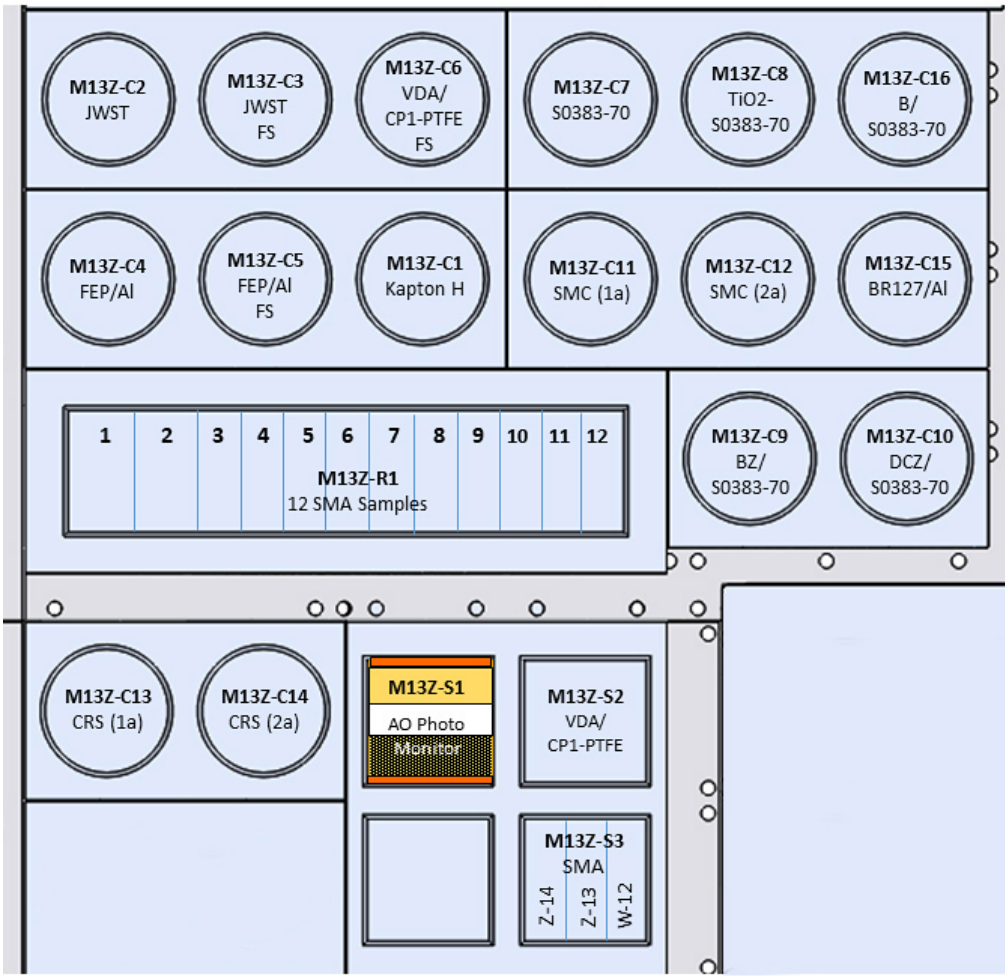

Figure 62. The MISSE-13 PCE-4 zenith MS sample map.

The MISSE-13 zenith AO fluence was determined to be 2.24×10^{18} atoms/cm^2 based on dehydrated mass loss of the zenith Kapton H AO fluence witness sample (M13Z-C1 F).[23] The AO fluence for the AO Photographic Monitor (M13Z-S1 F) was $<<1.73\times10^{19}$ atoms/cm^2 based on visible erosion, which was consistent.[23] Table 18 provides the MISSE-13 LEO AO E_y values for the PEC-3 zenith samples. Included in Table 18 is the MISSE-13 zenith sample ID, material, material abbreviation, sample layer thickness, dehydrated mass loss, exposed surface area, density, and the MISSE-13 zenith AO fluence. All samples for AO E_y were single layer 1-inch (2.54 cm) circular or square. The density for the James Webb Space Telescope (JWST) Sun shield sample (Si/2 mil Kapton E/VDA, M13Z-C2 F) is for the Kapton E film layer. The AO fluence, and corresponding AO E_y values, are based on Kapton H mass loss of only 0.034 mg.

The PCE-4 zenith samples did not include an alumina sample for contamination analyses, therefore the FEP/Al sample (M13Z-C4 F) was used to analyze any molecular contamination. XPS analyses of the FEP/Al sample indicated the presence of 2.2 at.% Si, as listed in Table 2. This is significantly less than the MISSE-12 ram and MISSE-12/MISSE-15 wake samples received. Detailed contamination results for M13Z-C4 F are provided in Reference 27.

Table 18. Erosion Data for the MISSE-13 PCE-4 Zenith Flight Samples.

MISSE-13 Zenith ID	Material	Abbreviation	Thickness (mils)	Mass Loss (g)	Exposed Surface Area (cm^2)	Density (g/cm^3)[15]	MISSE-13 Zenith AO Fluence ($atoms/cm^2$) [23]	MISSE 13 Zenith AO E_y ($cm^3/atom$)
M13Z-C1 F	Polyimide (PMDA) (Kapton H)	Kapton H	5	0.000034	3.538	1.4273	**2.24E+18**	***3.00E-24***
M13Z-C2 F	James Webb Space Telescope (JWST) Sun shield (Si/2 mil Kapton E/VDA)	JWST	2	0.000138	3.532	1.4617	2.24E+18	1.19E-23
M13Z-C4 F	Aluminized-Teflon FEP*	FEP/Al	5	0.000209	3.536	2.1443	2.24E+18	1.23E-23
M13Z-C11 F	Shape memory composite (1a)	SMC (1a)	47	0.000558	3.549	1.18**	2.24E+18	5.94E-23
M13Z-C12 F	Shape memory composite (2a)	SMC (2a)	47	0.000499	3.549	1.18**	2.24E+18	5.31E-23
M13Z-C13 F	Cosmic ray shielding (1a)	CRS (1a)	12	0.000594	3.521	0.907**	2.24E+18	8.29E-23
M13Z-C14 F	Cosmic ray shielding (1b)	CRS (2a)	12	0.000547	3.530	0.907**	2.24E+18	7.61E-23
M13Z-C15 F	BR-127 NC ESD/Al (Solvay BR-127 non-chromated (NC) electric static dissipative (ESD) Modified Phenolic Primer (Black) on an Al substrate)	BR-127 NC ESD/Al	137	0.000053	3.550	0.0875**	2.24E+18	7.60E-23
M13Z-S2 F	VDA/CP1-PTFE composite solar sail material (with Kapton HN frame/966 acrylic adhesive on back surface)	VDA/CP1-PTFE	0.3	0.000013	4.419	1.87**	2.24E+18	7.01E-25

*Teflon FEP is space facing
**Sample Collaborator[21]

The PCE-4 included silicone elastomer docking seal samples which were flown in the wake (M13W-C9 F to M13W-C13 F) and zenith (M13Z-C7 F to M13W-C10 F, and M13W-C16 F) directions. The samples included baseline (S0383-70 silicone), modified baseline (S0383-70 silicone with 1.5% titanium dioxide additive) and S0383-70 silicone with AO and UV protective coatings to evaluate the protection of silicone seals from the space environment. The coated samples were not analyzed for AO E_y. Post-flight photographs of the PCE-4 zenith samples are provided in Figure 63. As can be seen in Figure 63b, the S0383-70 silicone fluoresces after space exposure, while the control sample does not fluoresce. The samples with ZnO fluoresce a yellowish green color as shown in Figures 63f and 63h. A detailed report on the PCE-4 silicone elastomer docking seal samples, along with the PCE-3 silicone elastomer docking seal samples (M12R-C18 F, M12R-C19 F, M12W-C7 F and M12W-C8 F), is provided by Mathers in Reference 50.

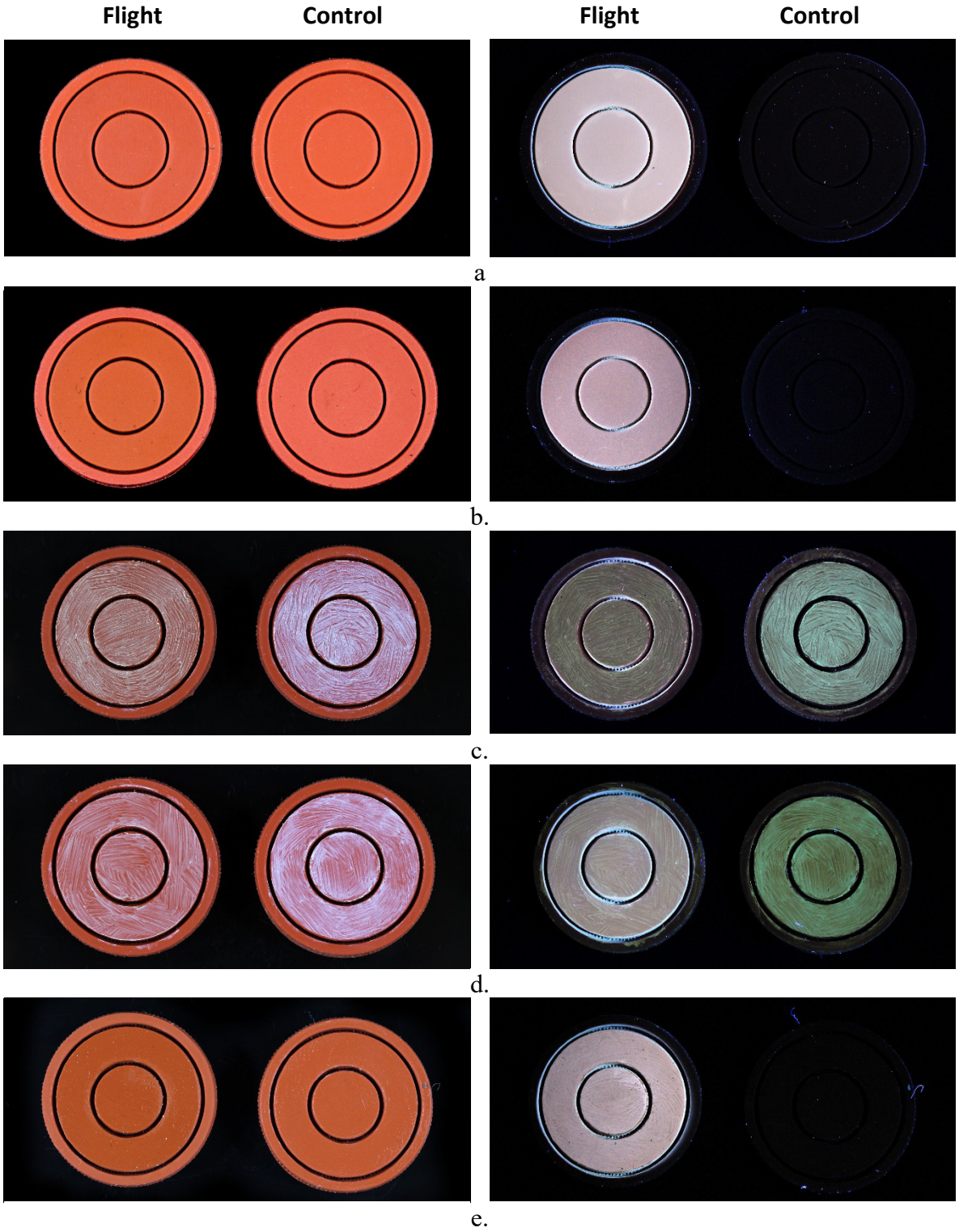

Figure 63. Post-flight photographs of the PCE-4 zenith silicone elastomer docking seal samples under visible light (left) and UV light (right): a). M13Z-C7 F and B, b). M13Z-C8 F and B, c). M13Z-C9 F and B, d). M13Z-C10 F and B, and e). M13Z-C16 F and B.

Various other PCE-4 zenith samples are still being analyzed, including the CRS samples (M13Z-C13 F and M13Z-C14 F), the solar sail samples (M13Z-S2 F and M13Z-C6 F), the PCE-4 zenith samples under folding stress, and SMA samples (M13Z-S3 F and M13Z-R1 F) that were not characterized for AO E_y. These samples, along with the silicone elastomer docking seal samples, are listed in Table 19. Additional post-flight analyses can be found in Reference 45 for the PCE-4 zenith SMC flight samples (M13Z-C11 F and M13Z-C12 F).

Table 19. MISSE-13 Zenith Flight Samples with No Erosion Data.

MISSE-13 Zenith ID	Material	Abbreviation	Thickness (mils)
M13Z-C3 F	JWST Sun shield material under folding stress	JWST FS	2
M13Z-C5 F	Aluminized-Teflon FEP under folding stress*	FEP/Al FS	5
M13Z-C6 F	VDA/CP1-PTFE composite solar sail material under folding stress	VDA/CP1-PTFE FS	0.3
M13Z-C7 F	S0383-70 silicone (for 1"dia. seal)	S0383-70	210
M13Z-C8 F	S0383-70 silicone with 1.5% titanium dioxide additive (1"dia. seal)	TiO2/S0383-70	210
M13Z-C9 F	S0383-70 silicone coated with Braycote 601EF grease plus ZnO (BZ) sunscreen (1"dia. seal)	BZ/S0383-70	210
M13Z-C10 F	S0383-70 silicone coated Dow Corning 7 + ZnO (DCZ) sunscreen (1"dia. seal)	DCZ/S0383-70	210
M13Z-C16 F	S0383-70 silicone coated with Braycote 601EF grease (1"dia. seal)	B/S0383-70	210
M13Z-S3 F	Shape Memory Alloys: W12, Z13, Z14 (1/4" x 1" pieces)	SMA	20
M13Z-R1 F	Shape Memory Alloys (12 samples (Z1-Z12): 2 - 0.5" x 1" + 12 - 0.25" x 1" pieces (Binary NiTi, etc.))	SMA	20

*Teflon FEP is space facing

Summary and Conclusions

NASA Glenn has flown four spaceflight experiments with 365 flight samples on ISS's MISSE-Flight Facility (MISSE-FF) to study space environmental durability of various polymers, composites, protective coatings, and other spacecraft materials. These experiments are the Polymers and Composites Experiment-1 (PCE-1) flown as part of the MISSE-9 mission, the PCE-2 flown as part of the MISSE-10 mission, the PCE-3 flown as part of the MISSE-12 and MISSE-15 missions, and the PCE-4 flown as part of the MISSE-13 mission. Although each experiment had numerous sample objectives, the primary objective was to determine the LEO AO E_y of spacecraft materials as a function of solar irradiation and AO fluence.

The PCE 1-4 experiments were successfully flown from April 2018 (launch on SpaceX-14) to August 2022 (returned on SpaceX-25). The PCE-1 included samples flown in ram, wake and zenith directions. The PCE-2 included samples flown in ram, zenith and nadir directions. The PCE-3 included samples flown in ram, wake and zenith directions. Finally, the PCE-4 included samples flown in wake and zenith directions. Due to closure of the MSCs to protect against on-orbit contamination during numerous visiting vehicles, the direct space exposure duration varied from 0.44 years (MISSE-13 and MISSE-15 wake) to 1.17 years (MISSE-10 ram). The AO ram fluence varied from 2.97×10^{20} atoms/cm^2 after 0.89 years of direct space exposure (with relatively high levels of Si contamination) on MISSE 12 to 3.93×10^{20} atoms/cm^2 after 1.17 years of direct space exposure on MISSE-10.

The LEO AO E_y for 150 samples flown in the LEO ram, wake, zenith or nadir directions have been determined. The majority of AO E_y values were determined based on dehydrated mass loss. The ram AO E_y values for uncoated polymers were found to range from 3.81×10^{-25} cm^3/atom for polytetrafluoroethylene (M9R-C20 F) exposed to an AO fluence of 3.44×10^{20} atoms/cm^2 on MISSE-9 to 4.43×10^{-23} cm^3/atom for AO etched low density polyimide aerogel (M12R-C21 F) exposed to an AO fluence of 2.97×10^{21} atoms/cm^2 on MISSE-12. Because of the low AO fluence and relatively high Si contamination, a number of MISSE-12 ram and MISSE-12/MISSE-15 wake samples experienced mass gain. Thus, AO E_y values are not provided for these samples.

Although there are calculated AO E_y values for the zenith, wake and nadir samples, the ram AO E_y for a particular material is a more reliable value in terms of AO exposure because the zenith, wake and nadir directions were exposed to either no, or very little, AO and thus other space environmental factors (i.e. vacuum, thermal extremes and thermal cycling, and/or various types of radiation) could be responsible for the mass loss. Because the AO E_y is computed based on the mass loss divided by the AO fluence, the AO E_y is greatly magnified for any mass loss for very low AO fluence exposures.

In addition to providing LEO AO E_y values, other space induced effects are discussed for a variety of the PCE 1-4 flight samples such as changes in sample appearance and color, and changes in UV fluorescence as compared to control samples. The erosion morphology texture of a Kapton AO fluence sample was provided, along with images of a MMOD impact sites. References for additional post-flight analyses for numerous PCE 1-4 samples are also provided.

References

1. Dickerson, R.E., Gray, H.B., and Haight, G P., *Chemical Principles 3rd Edition*. Menlo Park, CA, Benjamin Cummings Publishing Co. Inc. p. 457, 1979.
2. de Groh, K.K., Banks, B.A. and McCarthy, C.E., Spacecraft Polymers Atomic Oxygen Durability Handbook, NASA–HDBK–6024, 2017.
3. National Aeronautics and Space Administration: U.S. Standard Atmosphere, 1976. NASA TM–X–74335, 1976.
4. Gregory, J.C., "Interaction of Hyperthermal Atoms on Surfaces in Orbit: The University of Alabama Experiment," David E. Brinza, Ed., *Proceedings of the NASA Workshop on Atomic Oxygen Effects*, *Nov. 10–11*, *1986*. JPL 87–14, pp. 29–30.
5. Dever, J.A., "Low Earth Orbital Atomic Oxygen and Ultraviolet Radiation Effects on Polymers," NASA TM 103711, February 1991.
6. de Groh, K.K., Banks, B.A., Miller, S.K.R., and Dever, J.A., Degradation of Spacecraft Materials (Chapter 28), Handbook of Environmental Degradation of Materials, Myer Kutz (editor), William Andrew Publishing, pp. 601–645, 2018.
7. O'Neal, R.L., Levine, A.S. and Kiser, C.C., *Photographic Survey of the LDEF Mission*. NASA SP-531. NASA LaRC: Hampton, VA (1996).
8. de Groh, Kim K., and Banks, Bruce A., "Atomic Oxygen Undercutting of Long Duration Exposure Facility Aluminized-Kapton Multilayer Insulation, "*Journal of Spacecraft and Rockets*, Vol. 31, No. 4, 1994, pp. 656–664.
9. de Groh, K. K., Banks, B. A., Dever, J. A., Jaworske, D. J., Miller, S. K., Sechkar, E. A. and Panko, S. R., "NASA Glenn Research Center's Materials International Space Station Experiments (MISSE 1-7)," Proceedings of the International Symposium on

"SM/MPAC&SEED Experiment," Tsukuba, Japan, March 10-11, 2008, JAXA-SP-08-015E, March 2009, pp. 91 – 119; also NASA TM-2008-215482, December 2008.
10. Banks, B. A., de Groh, K. K. and Miller, S.K., "Low Earth Orbital Atomic Oxygen Interactions With Spacecraft Materials," MRS Symposium Proceedings, Vol. 851, NN8.1; also NASA/TM–2004-213400, 2004.
11. Banks, B. A., Simmons, J. C., de Groh, K. K. and Miller, S. K., "The Effect of Ash and Inorganic Pigment Fill on the Atomic Oxygen Erosion of Polymers and Paints," Proceedings of the 12th International Symposium on Materials in the Space Environment (ISMSE 12), ESA SP–705, Noordwijk, The Netherlands, 2013.
12. American Society for Testing and Materials: 2000 ASTM Standard Extraterrestrial Spectrum Reference E–490–00, 2000. (https://www.nrel.gov/grid/solar-resource/spectra-astm-e490.html)
13. de Groh, K. K., "Materials Spaceflight Experiments," Encyclopedia of Aerospace Engineering, R. Blockley and W. Shyy (eds). John Wiley & Sons Ltd, Chichester, UK, pp. 2535–2552 (2010).
14. de Groh, K. K., Jaworske, D. A., Kinard, W. H., Pippin, H. G., Jenkins, P. P, "Tough Enough for Space: Testing Spacecraft Materials on the ISS," *Technology Innovation*, Vol. 15, No. 4, 2011, pp.50-53.
15. de Groh, K. K., Banks, B. A., McCarthy, C. E., Rucker, R. N., Roberts L. M. and Berger, L. A., "MISSE 2 PEACE Polymers Atomic Oxygen Erosion Experiment on the International Space Station," *High Performance Polymers*, 20 (2008) 388–409.
16. de Groh, K. K. and Banks, B. A., "Atomic Oxygen Erosion Data from the MISSE 2-8 Missions," NASA/TM-2019-219982, May 2019.
17. de Groh, K. K., Banks, B. B., Mitchell, G. G., Yi, G. T., Guo, A., Ashmead, C. C., Roberts, L. M., McCarthy, C. E. and Sechkar, E. A., "MISSE 6 Stressed Polymers Experiment Atomic Oxygen Erosion Data," Proceedings of the '12th International Symposium on Materials in the Space Environment (ISMSE 12)', Noordwijk, The Netherlands (ESA SP-705, February 2013); also NASA TM-2013-217847.
18. de Groh, K. K., Banks, B. A., Yi, G. T., Haloua, A., Imka, E. C., Mitchell, G. G., Asmar, O. C., Leneghan, H.A. and Sechkar, E. A., "Erosion Results of the MISSE 7 Polymers Experiment and Zenith Polymers Experiment After 1.5 Years of Space Exposure," NASA/TM-2016-219167, December 2016 (Corrected Copy March 2017).
19. de Groh, K. K. and Banks, B.A., "The Erosion of Diamond and Highly Oriented Pyrolytic Graphite After 1.5 Years of Space Exposure," NASA TM-2018-219756, February 2018.
20. de Groh, K. K., Banks, B.A., Asmar, O. C., Yi, G. T., Mitchell, G. G., Guo, A. and Sechkar, E. A., "Erosion Results of the MISSE 8 Polymers Experiment After 2 Years of Space Exposure on the International Space Station," NASA-TM-2017-219445, February 2017.
21. de Groh, K. K. and Banks, B. A., "MISSE-Flight Facility Polymers and Composites Experiment 1-4 (PCE 1-4)," NASA TM-20205008863, February 2021.
22. Aegis Aerospace - Commercial Space (2023): https://aegisaero.com/commercial-space-services/.
23. de Groh, K. K. and Banks, B. A., "Space Environmental Exposure of the MISSE 9-15 Polymers and Composites Experiment 1-4 (PCE 1-4)," NASA/TM-20240000755/REV1, 2025.
24. Aegis Aerospace "MISSE MSC UV Equivalent Sun Hours Calculation" Report (A. Goode, MEMO-MISSE-0004 Rev C03, August 17, 2022)
25. de Groh, K. K., Whitt, A. and Banks, B.A., "Effect of Space Exposure on the Tensile Properties of MISSE Teflon Flight Samples," NASA/TM-20250003725.

26. Personal Communication with Jeffrey Buell, Aegis Aerospace (May 2023)
27. de Groh, K. K., Lukco, D., Crowell, S. F., Gregor, S. J. and Banks, B.A., "Analyses of the MISSE 9-15 Polymers and Composites Experiment 1-4 (PCE 1-4) Contamination Samples," NASA TM/20240000941, February 2024.
28. de Groh, K. K., McCarthy, C. E., Girish, K. M., Banks, B. A., Kaminski, C., Youngstrom, E. E., Lillis, M., Youngstrom, C. A., Hammerstrom, A. M., Hope, S. and Marx, L. M., "Rehydration Data for the Materials International Space Station Experiment (MISSE) Polymer Films," NASA TM-2019-220063, February 2019.
29. Banks, B. A., Mirtich, M. J., Rutledge, S. K., and Swec, D. M., "Sputtered Coatings for Protection of Spacecraft Polymers," Thin Solid Films, vol. 127, 1985, pp. 107–114; also NASA TM–83706, 1984.
30. Visentine, J. T., Leger, L. J., Kuminecz, J. F. and Spiker, I. K., "STS–8 Atomic Oxygen Effects Experiment," AIAA-85-0415, 1985.
31. Koontz, S. L., Lubert, J. L., Visentine, J. T., Hunton, D. E., Cross, J. B. and Hakes, C. L., "EOIM–III Mass Spectrometry and Polymer Chemistry: STS 46, July–August 1992," Journal of Spacecraft and Rockets, Vol. 32, No. 3, 1995, pp. 483–495.
32. Gregory, J. C., "On the Linearity of Fast Atomic Oxygen Effects," NASA CP 3257, 1994, 193-198.
33. Young, P. R., St. Claire, A. K., and Slemp, W. S., "Response of Selected High Performance Polymers Films to LEO Exposure," Technical Proceedings of the 38th International SAMPE Symposium, May 1993, 664-678.
34. Silverman, E. M., "Space Environmental Effects on Spacecraft: LEO Materials Selection Guide," NASA CR–4661, Part 1, August 1995.
35. Bourassa, R. J. and Gillis, J. R., "Atomic Oxygen Exposure of LDEF Experiment Trays," NASA CR 189627, May 1992
36. de Groh, K. K., Banks, B. A. and Demko, R., "Techniques for Measuring Low Earth Orbital Atomic Oxygen Erosion of Polymers," Proceedings of the SAMPE 2002 Conference, Long Beach, CA May 6-10, 2002, pp. 1279-1292; also NASA TM-2002-211479, March 2002.
37. de Groh, K. K. Banks, B. A. Clark, G. W. Hammerstrom, A. M. Youngstrom, E. E. Kaminski, C. Fine E. S. and Marx, L. M., "A Sensitive Technique Using Atomic Force Microscopy to Measure the Low Earth Orbit Atomic Oxygen Erosion of Polymers," NASA/TM-2001-211346, December 2001.
38. Banks, B. A., de Groh, K. K., Miller, S. K. and D. K. Waters, "Lessons Learned from Atomic Oxygen Interaction with Spacecraft Materials in Low Earth Orbit," Proceedings of the 9th International Conference "Protection of Materials and Structures from Space Environment," (May 19–23, 2008 in Toronto, Canada) Ed. J.I. Kleiman, AIP Conference Proceedings 1087, pp. 312–328, 2009; also NASA/TM-2008-215264, July 2008.
39. J. A. Townsend, P. A. Hansen, J. A. Dever, K. K. de Groh, B. A. Banks, L. Wang and C. He, "Hubble Space Telescope Metallized Teflon FEP Thermal Control Materials: On-Orbit Degradation and Post-Retrieval Analysis," *High Performance Polymers 11 (1999) 81-99.*
40. de Groh, K. K, Perry, B. A., Mohammed, J. A. and Banks, B.A., "Analyses of Hubble Space Telescope Aluminized-Teflon Multilayer Insulation Blankets Retrieved After 19 Years of Space Exposure," NASA TM-2015-218476, February 2015.
41. Malakooti, S., Vivod, S. L. and de Groh, K. K., "Durability of Polyimide Aerogels in The Space Environment," Presented at the 2024 SEM Annual Conference and Exposition on Experimental and Applied Mechanics, June 3-6, 2024, Vancouver, WA. *(Presentation format)*

42. Malakooti, S., Vivod, S. L., de Groh, K. K., Cashman, J. L., Meador, MA. B., Scheiman, D. A., Salem, J. A., Crowell, S.F. and McCorkle, L. S., "Space Environment Exposure Effects on Polyimide Aerogels," *Polymer Degradation and Stability*, Vol. 239, 2025, ISSN 0141-3910, (https://doi.org/10.1016/j.polymdegradstab.2025.111398).
43. Deyanova, J. E., Torres, D., Fleming, J., Devaud, G. and de Groh, K. K., "Effect of the MISSE Space Environment on Specialized Materials," Presented at the 2024 NSMMS & CRASTE Joint Symposium, June 24-27, 2024, Madison, WI. *(Presentation format)*
44. de Groh III, H. C., de Groh, K. K., Gregor, S. J. and Banks, B.A. "Space Exposure of Indium Tin Oxide Coatings," NASA/TM-20240002413, March 2024.
45. Santo, L., Quadrini, F., Bellisario, D., de Groh, K. and Banks, B., "Shape Memory Polymer Composites and Cosmic Ray Shielding Materials in Open Space," Extended Abstract of the Applied Space Environments Conference (ASEC), May 13-17, 2019, Los Angeles, CA.
46. Santo, L, Quadrini, F. and de Groh, K. K., "Space Application of Polyethylene for Cosmic Ray Shielding." Invited presentation given at the Society of Plastics Engineering (SPE) International Polyolefins Conference, Feb. 18-21, 2024, Galveston, TX. *(Presentation format)*
47. Santo, L., Quadrini, F., Bellisario, D., Iorio, L. and de Groh, K. K., "Shape Memory Polymer Composites After Long-term Exposure in Space Environment by the MISSE Facility," presented at the ISSRDC 2022 Conference, July 25-28, 2022, Washington D.C. *(Presentation format)*
48. Santo, L., Quadrini, F., Bellisario, D., Iorio, L., Proietti, A. and de Groh, K. K., "Effect of the LEO Space Environment on the Functional Performances of Shape Memory Polymer Composites," *Composites Communication*, 48 (2024) 101913.
49. Kang, J. H., Gordon, K., Bryant, R., Wilkie, W. K., de Groh, K., Stohlman, O. Fernandez, J., Warren, J., Dean, G., Schneider, N., Denkins, T., Stark, A., Brown, P. and Chamberlain, M., "Space Environmental Damage Assessment on Sail/Deorbit Materials in Low Earth Orbit," presented at the 6th International Symposium on Space Sailing, June 5-9, 2023, New York, NY. *(Presentation format)*
50. Mather, J. L., de Groh, K. K. and de Groh III, H. C., "Testing of Sunscreen-Protected Silicone Seals from MISSE-12 and MISSE-13 On-Orbit Flights," NASA/TM-20250004725, May 2025.
51. Benyo T., Casadevall, A., Cordero, R. JB, de Groh, K. K., Dhinojwala, A., Dragotakes, Q., Maurer, C., Singla, S. and Trunek, A., "Melanin-based biomaterials for radiation shielding and harvesting applications in space," presented at the ISSRDC 2022 Conference, July 25-28, 2022, Washington D.C. *(Presentation format)*
52. Cordero, R. J. B., de Groh, K. K., Dragotakes, Q., Singla, S., Maurer, C., Trunek, A., Chiu, A., Hwang, J., Crowell, S., Benyo, T., Thon, S. M., Rothschild, L. J., Dhinojwala, A. and Casadevall, A., "Radiation Protection and Structural Stability of Fungal Melanin Polylactic Acid Biocomposites in Low Earth Orbit," *Proc. Natl. Acad. Sci*. U.S.A. 122 (18) e2427118122, https://doi.org/10.1073/pnas.2427118122 (2025).
53. Williams, T. S., Fuchs, W. K., Nguyen, B. N., de Groh K. K., and Santiago, D., "Exposure of Polyphenylsulfone and Polyphenylsulfone-Hexagonal Boron Nitride Composite Films in LEO Wake Environment," *MRS Advances* (January 2024).